

University of Kentucky

UKnowledge

Theses and Dissertations--Physiology

Physiology

2020

STRIATED MUSCLE SPECIFIC RIBOSOMAL PROTEIN L3-LIKE: EFFECT OF KNOCKOUT ON CARDIAC FUNCTION AND PROTEIN TRANSLATION

Laura P. Brown

University of Kentucky, laura.peterson@uky.edu

Author ORCID Identifier:

 <https://orcid.org/0000-0001-5683-2074>

Digital Object Identifier: <https://doi.org/10.13023/etd.2020.320>

[Right click to open a feedback form in a new tab to let us know how this document benefits you.](#)

Recommended Citation

Brown, Laura P., "STRIATED MUSCLE SPECIFIC RIBOSOMAL PROTEIN L3-LIKE: EFFECT OF KNOCKOUT ON CARDIAC FUNCTION AND PROTEIN TRANSLATION" (2020). *Theses and Dissertations--Physiology*. 46.

https://uknowledge.uky.edu/physiology_etds/46

This Doctoral Dissertation is brought to you for free and open access by the Physiology at UKnowledge. It has been accepted for inclusion in Theses and Dissertations--Physiology by an authorized administrator of UKnowledge. For more information, please contact UKnowledge@lsv.uky.edu.

STUDENT AGREEMENT:

I represent that my thesis or dissertation and abstract are my original work. Proper attribution has been given to all outside sources. I understand that I am solely responsible for obtaining any needed copyright permissions. I have obtained needed written permission statement(s) from the owner(s) of each third-party copyrighted matter to be included in my work, allowing electronic distribution (if such use is not permitted by the fair use doctrine) which will be submitted to UKnowledge as Additional File.

I hereby grant to The University of Kentucky and its agents the irrevocable, non-exclusive, and royalty-free license to archive and make accessible my work in whole or in part in all forms of media, now or hereafter known. I agree that the document mentioned above may be made available immediately for worldwide access unless an embargo applies.

I retain all other ownership rights to the copyright of my work. I also retain the right to use in future works (such as articles or books) all or part of my work. I understand that I am free to register the copyright to my work.

REVIEW, APPROVAL AND ACCEPTANCE

The document mentioned above has been reviewed and accepted by the student's advisor, on behalf of the advisory committee, and by the Director of Graduate Studies (DGS), on behalf of the program; we verify that this is the final, approved version of the student's thesis including all changes required by the advisory committee. The undersigned agree to abide by the statements above.

Laura P. Brown, Student

Dr. John J. McCarthy, Major Professor

Dr. Kenneth S. Campbell, Director of Graduate Studies

STRIATED MUSCLE SPECIFIC RIBOSOMAL PROTEIN L3-LIKE: EFFECT OF
KNOCKOUT ON CARDIAC FUNCTION AND PROTEIN TRANSLATION

DISSERTATION

A dissertation submitted in partial fulfillment of the
requirements for the degree of Doctor of Philosophy in the
College of Medicine
at the University of Kentucky

By
Laura Peterson Brown
Lexington, Kentucky
Director: Dr. John J. McCarthy, Professor of Physiology
Lexington, Kentucky
2020

Copyright © Laura Peterson Brown 2020
<https://orcid.org/0000-0001-5683-2074>

ABSTRACT OF DISSERTATION

STRIATED MUSCLE SPECIFIC RIBOSOMAL PROTEIN L3-LIKE: EFFECT OF KNOCKOUT ON CARDIAC FUNCTION AND PROTEIN TRANSLATION

Ribosomes are the molecular machinery of the cell that catalyzes synthesis of peptides from amino acids. The eukaryotic ribosome is made up of four strands of ribosomal RNA (rRNA) and ~80 ribosomal proteins. While many tissues routinely exhibit variations of ribosomal protein stoichiometry, tissue specific ribosomal proteins are rare. The ribosomal protein with the highest tissue specificity of any ribosomal protein is found in striated muscle, ribosomal protein L3-like (RPL3L). Other than its tissue specificity, association with atrial fibrillation, and chromosomal location, there is little known about the function of RPL3L. However, its ubiquitously expressed paralog, RPL3, has been well documented to be essential for ribosome biogenesis, aid in peptidyl transfer, and increase translational fidelity.

This thesis, therefore, seeks to address the critical gap in knowledge on the function of RPL3L in striated muscle and specifically, the effect of RPL3L knockout (KO) on cardiac function and protein translation *in vivo*. To that end, a RPL3L KO mouse was generated that, instead of striated muscle-specific RPL3L, expresses the ubiquitous RPL3 in striated muscles.

The first aim of this dissertation was to test the hypothesis that RPL3L KO would induce cardiac arrhythmias by expression in the atria. First the expression pattern of RPL3 and RPL3L in the wild-type (WT) heart were established by both RT-PCR and Western blot. Both indicated that while the ventricle has high expression of RPL3L, RPL3 is found at much lower levels (~10% that of RPL3L). The atria however, had the opposite expression pattern with RPL3 being high and RPL3L not expressed. In order to determine if the RPL3L KO mice recapitulated the fibrillation phenotype seen in humans with *Rpl3l* variants, we performed echocardiography and electrocardiography on WT and KO mice. No changes were observed in heart rate, ejection fraction, wall thickness during systole or diastole, fractional shortening or stroke volume under resting conditions. When telemetry fitted mice were treated with the β_2 adrenergic receptor agonist, isoproterenol, both WT and KO mice showed a significant increase in heart rate after treatment ($p=0.02$ and 0.0007 respectively) but the rate of response was significantly more rapid in KO mice ($p= < 0.0001$). Due to the increase in rate of response to isoproterenol in the KO, we

hypothesized that loss of expression of RPL3L in the pace-making center of the heart, the sinoatrial node, was responsible for the rapid increase in heart rate. To that end, single-cell RNA sequencing data from nuclei of the sinoatrial node, and proteomic data from the sinoatrial node were queried. Analysis revealed that RPL3L is expressed at a very low level at the mRNA level in the sinoatrial node but that it is not detected at the protein level. These results do not support the hypothesis that loss of RPL3L in the atria causes atrial fibrillation, rather this evidence suggests that if RPL3L plays a role in atrial fibrillation, it is likely secondary to a ventricular pathology.

The second aim of this dissertation was to test the hypothesis that RPL3L plays a functionally specialized role in the ribosome causing enhanced translation of a subset of mRNAs, thereby conferring preferential recruitment to mRNAs which are specific to striated muscle. Actively translating ribosomes of cardiac tissue were isolated via polysome fractionation and were subsequently subjected to RNA sequencing (RNA-seq). Analysis revealed that there were 216 mRNAs that were differentially translated (but not differentially transcribed). Of these mRNAs, 68 were more highly translated in WT (RPL3L-ribosomes) whereas 148 were more highly translated in the KO (RPL3-conatining ribosomes). Gene ontology of differentially translated mRNAs showed highest enrichment for genes involved in RNA binding and splicing. These results support the hypothesis that there is differential translation of a subset of mRNAs

This study demonstrates that KO of RPL3L is not lethal, and while it does cause changes in cardiac response to isoproterenol, its loss is not sufficient to induce atrial fibrillation in mice. This study also demonstrates that RPL3L expression is robust and highly specific to the ventricles of the heart but that its expression exhibits only minor alterations on the cardiac translome. The findings here help to further our understanding of translation in the heart and its effects on cardiac physiology.

KEYWORDS: Ribosome, Protein Translation, Heart, Sinoatrial Node, Atrial Fibrillation

Laura Peterson Brown

06/02/2020

Date

STRIATED MUSCLE SPECIFIC RIBOSOMAL PROTEIN L3-LIKE: EFFECT OF
KNOCKOUT ON CARDIAC FUNCTION AND PROTEIN TRANSLATION

By
Laura Peterson Brown

John J. McCarthy
Director of Dissertation

Kenneth Campbell
Director of Graduate Studies

06/02/2020

Date

ACKNOWLEDGMENTS

The following thesis, while an individual work, benefited from the insights and direction of several people. First, my Thesis Chair, John J. McCarthy who was a constant source of encouragement, who challenged me and helped me develop into a scientist. I would also like to thank my committee, Charlotte Peterson, Seven Estus, Timothy Butterfield, Brian Delisle, and my outside examiner, Douglas Harrison.

I would also like to thank those who helped mold me into a scientist on a daily basis – my lab mates: Yuan Wen, Ivan Vechetti, Alexander Alimov, Taylor Valentino, Vandre Casagrande-Figueiredo and Brooks Mobely. I would also like to thank Ivan Vechetti Jr. for his patience with me, his unending willingness to help, hear my ideas, and give feedback. I would like to thank Yuan Wen for always listening to my constantly new hypotheses, challenging my thinking, and his constant, encouraging support. I could not have done it without you two. I would also like to thank Shelby Meier for years of emotional and scientific support, as well as help preparing for my defense.

I never intended my educational journey to go this far, nor did I think I was even capable of it, but I would like to thank all the people who always believed in me. Firstly, my family, my parents Celeste and David Peterson, my parents in law, Jane and Ron Brown, and all my siblings, especially my brother Joshua Peterson who was always unabashedly proud of me from start to finish. I would like to thank my husband, Christopher Brown who has supported me in every way possible and has always believed in me even when I did not believe in myself. When challenges arose, he was always the one to assure me that I could overcome it. When experiments would fail, his was the

shoulder that I cried on. I cannot thank him enough for putting up with me, helping me, and encouraging me through this journey.

Lastly, I would like to thank United States taxpayers. Without their support this research would have never been possible. I was supported both by a National Institute of Health grant as well as a National Science Foundation Graduate Research Fellowship. The NIH grant kick-started this whole project, and the NSF grant gave me the liberty to study what I felt were the most important things to know about the beguiling protein, RPL3L. Thank you to each and every taxpayer. Your support of basic research does not go unnoticed or unappreciated.

TABLE OF CONTENTS

ACKNOWLEDGMENTS.....	iii
LIST OF TABLES	viii
LIST OF FIGURES	ix
CHAPTER 1. Introduction	1
1.1 <i>The History of the Ribosome.....</i>	<i>1</i>
1.2 <i>Ribosome Biogenesis.....</i>	<i>4</i>
1.3 <i>Ribosome Function</i>	<i>7</i>
1.4 <i>5' Untranslated Region</i>	<i>8</i>
1.4.1 <i>Internal Ribosomal Entry Site</i>	<i>8</i>
1.4.2 <i>Upstream Open Reading Frame</i>	<i>10</i>
1.4.3 <i>Terminal Oligopyrimidine Tract</i>	<i>11</i>
1.5 <i>Ribosomal Protein Stoichiometry and Paralog Substitution.....</i>	<i>12</i>
1.5.1 <i>Ribosome Stoichiometry</i>	<i>12</i>
1.5.2 <i>Ribosomal Paralogs.....</i>	<i>13</i>
1.5.3 <i>Striated Muscle Specific RPL3-like</i>	<i>16</i>
1.5.4 <i>Transcriptional Regulation</i>	<i>17</i>
1.5.5 <i>C-terminus of RPL3L</i>	<i>18</i>
1.5.6 <i>Ribosome Localization.....</i>	<i>18</i>
1.6 <i>Knowledge Gap.....</i>	<i>20</i>
CHAPTER 2. Loss of cardiac specific ribosomal protein L3-like has modest effects on the cardiac translato	21
2.1 <i>Introduction.....</i>	<i>21</i>
2.2 <i>Methods.....</i>	<i>23</i>
2.2.1 <i>Animals</i>	<i>23</i>
2.2.2 <i>RNA Isolation.....</i>	<i>24</i>
2.2.3 <i>RT-PCR.....</i>	<i>24</i>
2.2.4 <i>Western Blot.....</i>	<i>25</i>
2.2.5 <i>Polysome Fractionation.....</i>	<i>26</i>
2.2.6 <i>RNA-sequencing and Bioinformatics.....</i>	<i>26</i>
2.2.7 <i>Cardiomyocyte dispersal</i>	<i>27</i>
2.2.8 <i>Transverse Tubules.....</i>	<i>29</i>
2.2.9 <i>Calcium Tolerance.....</i>	<i>29</i>
2.2.10 <i>Gene Ontology.....</i>	<i>29</i>
2.2.11 <i>Statistics.....</i>	<i>30</i>
2.3 <i>Results.....</i>	<i>30</i>
2.3.1 <i>RPL3 and RPL3L Expression During Post-natal Development</i>	<i>30</i>
2.3.2 <i>RPL3L KO Strategy</i>	<i>31</i>

2.3.3	Translational Enrichment	33
2.3.4	Differential Splicing	38
2.3.5	Calcium Handling.....	40
2.3.6	Transverse Tubules.....	42
2.4	<i>Discussion</i>	43
2.4.1	Summary of Findings	43
2.4.2	Ribosome Specialization	43
2.4.3	Translational Enrichment	44
2.4.4	Calcium Homeostasis	44
2.4.5	Possible Roles of RPL3L and Future Directions	45
CHAPTER 3. Loss of ventricular- specific ribosomal protein rpl3l enhances response to acute adrenergic stimulation		47
3.1	<i>Introduction</i>	47
3.1.1	Atrial Fibrillation.....	47
3.1.2	RPL3L Tissue Specificity.....	47
3.1.3	Knowledge Gap.....	48
3.2	<i>Materials and Methods</i>	49
3.2.1	Animals	49
3.2.2	RNA Isolation.....	49
3.2.3	RT-PCR Analysis	50
3.2.4	Western Blot Analysis.....	50
3.2.5	Single-cell RNA-Sequencing Analysis.....	51
3.2.6	Quantitative Proteomics	52
3.2.7	Echocardiography.....	53
3.2.8	Electrocardiography	53
3.2.9	Statistics.....	54
3.3	<i>Results</i>	55
3.3.1	Atria and Ventricular Expression of RPL3L	55
3.3.2	Echocardiography and Electrocardiography.....	56
3.3.3	Single Cell RNA Sequencing of the SAN	60
3.3.4	Quantitative Proteomics	61
3.4	<i>Discussion</i>	63
3.4.1	Summary of Findings	63
3.4.2	Tissue Specificity	63
3.4.3	Possible Roles of RPL3L.....	64
3.4.4	Phenotype of RPL3L KO Mice	65
3.4.5	Possible Roles of RPL3L in Atrial Fibrillation	66
3.4.6	Genome Wide Association Studies	68
CHAPTER 4. Reflections and looking ahead to future studies		69
4.1	<i>Reflections</i>	69
4.1.1	The Translatome.....	70
4.1.2	Calcium Handling and Cardiac Function	71
4.1.3	Atrial Fibrillation.....	72
4.2	<i>Future Directions</i>	73
4.2.1	Ribo-seq.....	73
4.2.1.1	Initiation.....	73

4.2.1.2	Elongation	74
4.2.1.3	Processivity	74
4.2.2	Muscle Function	75
4.2.3	Sinoatrial Node Subpopulations	75
APPENDICES		77
REFERENCES		97
VITA.....		108

LIST OF TABLES

Table 1: Echocardiography	58
---------------------------------	----

LIST OF FIGURES

Figure 1: Up-regulation of <i>Rpl3l</i> in the heart during post-natal development.....	31
Figure 2: Effective knockdown of RPL3 expression in the heart.	33
Figure 3 Modest differences in heart polysome composition between RPL3L KO and WT.	35
Figure 4: Transcript abundance is primary determinant of translation.	37
Figure 5: Gene ontology of differentially spliced mRNAs.	39
Figure 6: KO cardiomyocytes show an increase in calcium sensitivity.	41
Figure 7: T-tubules of RPL3L mice show a decrease in regularity.	42
Figure 8. Ventricular specific expression of RPL3L.	56
Figure 9: Loss of RPL3L does not affect cardiac function.	58
Figure 10: Electrical activity of the heart in WT and KO mice.	59
Figure 11: Low expression of <i>Rpl3l</i> in sinoatrial node.	61
Figure 12: RPL3L barely detectable in sinoatrial node.	62

CHAPTER 1. INTRODUCTION

1.1 The History of the Ribosome

The theory that a virus could cause cancer was a hotly debated topic in the 1920's. Despite the rudimentary knowledge of viruses, the theory that a virus could cause cancer was ridiculed (Rheinberger 1995). The nay-sayers reasoned that because cancer arose randomly in the body it must be an endogenous chemical mutagen. A young medical doctor and scientist, who wished to make his mark by disproving the theory that a virus could cause cancer, boarded a ship in Belgium and sailed to New York to work with James B. Murphy at Rockefeller Institute in 1929 (Rheinberger 1995). Six years later while searching for the amorphous chemical that he hypothesized was causing a particular tumor in chicken, the young doctor, Albert Claude, found a small but active tumor producing fraction that was unexpected. He described a "particulate matter of uniform size" in the microsome fraction which he believed to be in some way associated with mitochondria and play a role in cell differentiation (Claude 1940). After much analysis he noted that these particles were made up of "nucleoprotein of the ribose type," and lipid, and when centrifuged it separated in a stepwise fashion. This was the newest suspect for causing cancer and Claude threw himself into this research for the next decade. But much to Claude's dismay, when using a non-cancerous chick embryo as a negative control, he also found large quantities of these particles. Claude was rightfully dismayed, his theory that this active fraction was causing cancer appeared to be fatally flawed because it was also in non-cancerous cells. He concluded that these particles must not be the source of cancer, rather, they were "particulate components of the cytoplasm"

(Claude 1940). Not dissuaded, Claude continued studying the ribonucleoprotein particles of the microsomal fraction and had many theories about their function - a favorite of which was that they were immature mitochondria. Despite his efforts, little headway was made in discerning the role of these mysterious particles.

Meanwhile, George Palade, a Romanian scientist was attempting to map the enzymatic landscape of the cell. Frustrated with salt gradients causing mitochondrial rupture, he employed sucrose centrifugation and found that this produced a robust microsome fraction. Coincidentally Palade combined both biochemistry and electron microscopy to image cellular fractions and noted that there was a “small, granular component” of the cell that was found on much of the endoplasmic reticulum but their connection to the ribonucleolar microsomes remained elusive (Palade 1955). Over the next decade research on these particles found in the microsomal fraction expanded (Rheinberger 1995). While their role in the cell was hotly debated, everyone agreed that the name “ribonucleoprotein particles of the microsome fraction” was too long. When R.B. Roberts suggested the abbreviation “ribosome” the rest of the community embraced the name (Roberts 1958). Thus, the beginning of ribosome research was born.

In 1955, John Littlefield demonstrated that the ribosome was responsible for amino acid incorporation (Littlefield, Keller et al. 1955). By adding radiolabeled amino acids into the ribosomal fraction, Dr. Littlefield showed that although proteins were being labeled, the ribosome itself was rarely labeled - indicating that the ribosome was involved in translation but not being highly translated itself (Littlefield, Keller et al. 1955). Scientists hypothesized that the RNA in a ribosome was for informational use and that the RNA was simply being wrapped around ribosomal proteins in order to be decoded.

Some even went as far as proposing a one gene, one ribosome, one protein hypothesis (Brenner, Jacob et al. 1961). However this was hotly debated because if this were true, there should be ribosomes of varying sizes due to variation in gene length; but because ribosomal weight was highly consistent between tissues and between many organisms, all the RNA within a ribosome had to be made of the same or similar RNA. In the spring of 1961, Sydney Brenner and colleagues published an article called "An unstable intermediate carrying information from genes to ribosomes for protein synthesis" that outlined what is now known as messenger RNA (Brenner, Jacob et al. 1961). Within a matter of a few years, the remaining mysteries of transfer RNA (tRNA), ribosomal RNA (rRNA), ribosomal proteins and the fundamental enzymatic reactions they collectively underwent, were elucidated and research shifted from functional analysis of the ribosome to structural inquiries of the ribosome and the specifics of ribosome biogenesis.

Initially naming of ribosomal proteins did not follow any structured conventions, and each lab would often have their own naming conventions which lead to publications between labs to be confusing and almost impossible to use due to lack of consistent identifiers for any given protein (Wittmann, Stofflet et al. 1971). In 1971, a naming convention was implemented that solved many of these issues. The proposed ribosomal protein nomenclature dictated that the ribosomal proteins be first named denoting their association with the ribosome (ribosomal protein, RP) and then their association with either the large or small subunit (L or S respectively), followed by a number. A variation of this naming convention is used to denote paralogs. Paralogs are given the same name as the protein from which they arose but with a suffix of Like (L) or denoted with a letter (A/B) to differentiate the proteins (Williams and Sussex 1995, Chaillou, Zhang et al.

2016). Additionally, ribosomal proteins that are found on sex chromosomes contain X or Y to indicate the chromosome (Lopes, Miguel et al. 2010). Although new naming conventions have been proposed, this model is the most commonly used and will be used for the remainder of this dissertation (Ban, Beckmann et al. 2014).

1.2 Ribosome Biogenesis

Ribosome biogenesis requires a symphony of RNA polymerases I, II, and III, as well as assembly factors, chaperones, and protein synthesis of ribosomal proteins.

Transcription of ribosomal DNA (rDNA) requires selectivity factor 1 complex (SL-1, also known as TIF-1B), upstream binding factor (UBF), RNA Polymerase transcription factor 3 (TIF-1A, also known as Rrn3), and all 14 subunits of RNA polymerase I (Pol I) which together are known as the preinitiation complex (PIC) (Buttgereit, Pflugfelder et al. 1985, Kuhn and Grummt 1992, Yamamoto, Nogi et al. 1996, Voit, Hoffmann et al. 1999, Friedrich, Panov et al. 2005, Fernandez-Tornero, Moreno-Morcillo et al. 2013). UBF binds as a homodimer to both the core promoter and the upstream core element to create a DNA loop structure (O'Mahony, Smith et al. 1992, Reeder 1995). The SL-1 complex is recruited to the promoter where it then binds both UBF and the rDNA. The Pol I/TIF-1A complex is then recruited to the promoter to complete the PIC (Bell, Learned et al. 1988). rDNA transcription continues until Pol I encounters transcription termination factor 1. Termination proteins stall transcription and transcript release factors dissociate Pol I from the rDNA (Mason, Sander et al. 1997, Jansa and Grummt 1999, Sirri, Roussel et al. 1999). Transcription by Pol I produces a single 47S RNA that contains the mature 18S, 5.8S, and 28S rRNA with two internal transcribed spacers and flanked by external transcribed spacers at the 5' and 3' ends. The 47S RNA is then

processed by post-transcriptional cleavage into 28S, 5.8S and 18S rRNA (Lazdins, Delannoy et al. 1997). As the ribosome is maturing there are ~150 non-ribosomal proteins that associate to aid in biogenesis (Tschochner and Hurt 2003).

In contrast, 5S rRNA transcription is relatively simple with pol III transcribing 5S RNA, which then binds to RPL5. The 5S-RPL5 complex is then shuttled to the nucleolus and begins aiding in ribosome biogenesis of the large subunit (Michael and Dreyfuss 1996, Dechampesme, Koroleva et al. 1999).

Transcription of mRNAs required for ribosome assembly occurs by RNA polymerase II. This process happens rapidly and then the mRNAs are shuttled to the cytoplasm for translation. After translation, the proteins are shuttled to the nucleolus, via a nucleolar localization signal, for ribosome biogenesis (Moreland, Nam et al. 1985, Rosorius, Fries et al. 2000, Meyer, Hung et al. 2007). In the nucleolus the ribosomal proteins and rRNA are sequentially incorporated into the ribosome in the final stages of subunit biogenesis (Kruiswijk, Planta et al. 1978, Mitterer, Murat et al. 2016). Once the large and small subunits are fully formed, they are exported to the cytosol where they can then assemble on mRNA and begin translation.

Given that ribosome biogenesis is the most expensive metabolic process for cells, ribosome biogenesis is tightly regulated (Warner 1999, Raska, Koberna et al. 2004). Production of rRNA is negatively regulated by p53 (a tumor suppressor) and positively regulated by c-Myc (an oncogene). When c-Myc is activated by a growth stimulus it directly binds to consensus elements in rDNA and associates with the Pol I-specific SL1 which then causes transcription of rRNA (Grandori, Gomez-Roman et al. 2005). Conversely, high levels of ribosomal proteins in the cell (specifically RPL5 and RPL11)

will bind to Mdm2 which then activates p53, halting transcription of rDNA and consequently, ribosome biogenesis as a whole (Golomb, Volarevic et al. 2014). During times of cellular stress or differentiation, ribosome biogenesis is reduced via chromatin remodeling and inhibition of transcription (Leary and Huang 2001). These mechanisms together ensure that ribosome biogenesis occurs only when needed and that this costly cellular function ceases as soon as the cell's requirements are met.

While there are numerous proteins that target many areas of ribosome biogenesis, there is one master regulator: mammalian target of rapamycin (mTOR). mTOR is a serine/threonine protein kinase that when activated can modulate cell growth and protein synthesis through phosphorylation of targets including ribosomal protein S6 kinase (RPS6K) and 4E binding proteins (4EBP). After activation, RPS6Ks can then increase protein synthesis by enhancing RNA helicase activity to promote initiation, elongation factors to increase the speed of translation, and increase ribosome biogenesis (Wang, Li et al. 2001, Shahbazian, Roux et al. 2006, Jastrzebski, Hannan et al. 2007). During periods of cellular stress, 4EBPs interact with eIF4E, which inhibits formation of the initiation complex. When 4EBPs are phosphorylated by effectors of mTOR, eIF4E is released from 4EBPs and can bind to eIF4G to form the initiation complex (Beretta, Gingras et al. 1996). mTOR regulation and effects are far reaching and complex, but here we briefly discuss a few of its effects on translation; for a more comprehensive review of mTOR see Gringas et al and Drummond et al (Gingras, Kennedy et al. 1998, Drummond and Rasmussen 2008).

1.3 Ribosome Function

The function of the ribosome is to catalyze the synthesis of single amino acids into peptides. Ribosomal proteins stabilize the rRNA while it catalyzes the transfer of an amino acid from the charged tRNA, to a chain of amino acids. Although simple sounding, translation is a multi-step process that requires a host of protein factors and is energetically expensive.

There are three classical stages to translation: Initiation, Elongation and Termination. Initiation of translation in eukaryotic cells begins with the 40S (small) subunit, in complex with eukaryotic initiation factor 3 (eIF3) and eIF2-GTP/Met-tRNA, are recruited to the 5' cap of an mRNA (Merrick 1992, Hinnebusch 2006). The half-mer and its complex scan the mRNA from 5' to 3' until a start codon is encountered. Once the start codon (usually AUG) is positioned in the P-site of the 40S ribosome, eIF5 stimulates GTP hydrolysis which causes eIF2 to dissociate from the small subunit, eIF5B then associates allowing the 60S (large) subunit to join the 40S subunit and complete 80S ribosome assembly (Pestova, Lomakin et al. 2000). Elongation begins when eukaryotic elongation factor (eEF) 1A binds GTP and an aminoacylated tRNA at the A-site of the ribosome. tRNA codon recognition triggers GTP hydrolysis of eEF1A causing it to release from the ribosome which allows the tRNA to move into the A-site (Sasikumar, Perez et al. 2012). eEF1B will then catalyze eEF1A bound ADP back to ATP so that it is once again active. After peptide bond formation has occurred, eEF2 translocates the mRNA by one codon so that the next codon is in the A-site (Riis, Rattan et al. 1990). Translation termination begins when the ribosome encounters a stop codon (UAA, UGA or UAG) in the A-site. Eukaryotic release factor (eRF) 1 and 3 act in a collaborative fashion: eRF3 inserts a tRNA-like molecule into the A-site while eRF1 evaluates the stop

codon (Alkalaeva, Pisarev et al. 2006) eRF1 has been shown to have a high level of accuracy in codon discrimination, likely an evolutionary adaptation that prevents incorrect elongation termination (Salas-Marco and Bedwell 2005). Once termination has begun eRF3 increases the speed of termination by acting as a termination specific GTPase (Salas-Marco and Bedwell 2004).

1.4 5' Untranslated Region

Regulation of translation is typically carried out via the 5' untranslated region (5'-UTR) of mRNA. The 5'-UTR region can encode motifs that either recruit ribosomes, repress translation or both depending on cellular stimuli. Three of the more common motifs are internal ribosomal entry sites (IRES), upstream open reading frames (uORF), and 5' terminal oligopyrimidine tracts (5'TOP).

1.4.1 Internal Ribosomal Entry Site

While most translation initiation occurs on the 5' cap of mRNA, an IRES occurs within the 5'-UTR of mRNAs and preferentially recruits the ribosome for translation. This mechanism is commonly used by viruses to hijack the translational machinery of the cell so that viral mRNAs are preferentially translated over host mRNAs (Quade, Boehringer et al. 2015). Some viral IRESs can even begin translation in the absence of initiation factors, an ability that is further exploited by expression of a protease that cleaves eIF4G, a cap binding adaptor protein (Belsham, McInerney et al. 2000, Pestova and Hellen 2003, Schuler, Connell et al. 2006). In this way, the virus frees initiating

ribosomes from host mRNA, blocks further initiation via the 5' cap, and increases IRES mediated translation.

In eukaryotes, IRESs are used to enhance translation of required mRNAs even during times of translational suppression, but they can also recruit specific ribosomal proteins and perhaps act in a more specialized capacity.

In mammalian systems IRESs are commonly used to translate mRNAs that are specific to differentiated cells. For instance, in the neuronal system, dendrites require constant protein production to ensure lasting changes after synaptic activation, but the initiation machinery is found at relatively low concentrations. Pinkstaff et al demonstrated that there were key mRNAs that were translated independent of 5' cap after synaptic activation (Pinkstaff, Chappell et al. 2001). Upon investigation, they found the alpha subunit of calcium-calmodulin-dependent kinase II (CAMK2A), activity-regulated cytoskeletal associated protein (ARC), dendrin (DDN), microtubule associated protein 2 (MAP2) and neurogranin (NRGN) were all translated via IRESs. These types of mRNAs that are enriched in specific tissues are believed to have evolved IRESs so that even when global protein translation is decreased, key mRNAs can still be translated.

IRESs have also been reported to be involved in the preferential recruitment of ribosomes with specific ribosomal protein composition. Xue et al demonstrated that ribosomes containing RPL38 preferentially associated with the 5'UTR of HOX mRNAs (Xue, Tian et al. 2015). When RPL38 was mutated, there was no longer preferential translation which lead to abnormalities in eye, tail and skeletal development in mice (Kondrashov, Pusic et al. 2011).

Shi et al showed the association of different ribosomal proteins with the ribosome influenced the composition of the polysomes such RPS25-containing ribosomes were significantly more likely to translate mRNAs involved in organelle organization whereas RPL10A-containing ribosomes were more likely to translate mRNAs involved in embryonic development (Shi, Fujii et al. 2017). They confirmed that many of these mRNAs contained IRESs, while other mRNAs conferred 5'-UTR ribosome recruitment via an unknown mechanism.

1.4.2 Upstream Open Reading Frame

Upstream open reading frames (uORFs) are translational start sites that are in the 5'-UTR. This sequence causes ribosomes to prematurely initiate, begin translation, and then terminate due to an in-frame stop codon before the true start site at the beginning of exon 1. By allowing ribosomes to initiate and terminate before translation of the encoded protein, this 5' element can suppress protein expression.

uORFs can also decrease translation of mRNAs by increasing mRNA degradation (Matsui, Yachie et al. 2007). Non-sense mediated decay is a process that normally detects and degrades mRNAs that code for non-functional proteins or proteins that have harmful mutations. Non-sense mutations that lead to a premature stop codon, are preferentially degraded to ensure incorrectly made proteins do not remain in the cell. uORFs in mRNA can mimic aberrant stop codons to promote their own degradation (Oliveira and McCarthy 1995, Tanaka, Sotta et al. 2016). Additionally, some uORFs produce cis-acting peptides, or encode rare amino acids causing the ribosome to stall during translation,

therefore targeting the mRNA for degradation (Meijer and Thomas 2003, Oyama, Itagaki et al. 2004, Gaba, Jacobson et al. 2005).

Considering about half of all human and mouse genes contain uORFs in their UTRs it is remarkable that any of these transcripts are translated. However, the context in which an uORF appears can alter its ability to be translated. For instance, some uORF AUGs have “high visibility” (an A at the -3 position relative to the AUG) leading to almost exclusive translation of the uORF (Baim and Sherman 1988). On the other hand, if the 5'-UTR length leading up to the uORF is below 15 nucleotides, the uORF will likely not be translated, and the ribosome will have a much higher chance of beginning translation at the true start site (van den Heuvel, Bergkamp et al. 1989). Two factors can help determine ribosome re-initiation, the length of the uORF, and the context of the stop codon. Shorter uORFs allow for more efficient reinitiation likely due initiation factors still being in close proximity if elongation is quite short (Luukkonen, Tan et al. 1995, Hinnebusch 2006). If the uORF is longer than 35 codons, it is very unusual to have re-initiation (Luukkonen, Tan et al. 1995).

1.4.3 Terminal Oligopyrimidine Tract

Given the energetically costly nature of ribosome biogenesis, and protein translation, it seems intuitive that there would be a consensus sequence to up-regulate or suppress production of translational machinery in varying growth or starvation conditions. Five prime terminal oligopyrimidine tract (5'-TOP) motifs are just such a sequence. TOP-containing mRNAs encode proteins of the translational machinery and are subject to translational control via their oligopyrimidine motif; characterized by a

cysteine residue at the cap site of a 5'-UTR, followed by 4-15 pyrimidines (Mariottini, Bagni et al. 1988, Nakanishi, Kohno et al. 1988, Perry and Meyuhas 1990, Levy, Avni et al. 1991, Jefferies, Reinhard et al. 1994, Perry 2005). During times of growth, mTORC-1 phosphorylates the translational repressor 4E-BP1 causing it to dissociate from eIF4E; the freed eIF4E can then bind capped mRNAs and begin translation initiation. During cellular stress suppression, mTORC-1 inactivation causes 4E-BP to remain in the unphosphorylated state, bound to EIF4E which diminishes its ability to bind TOP motifs more than other mRNAs (Avni, Biberman et al. 1997, Hornstein, Git et al. 1999, Thoreen, Chantranupong et al. 2012, Miloslavski, Cohen et al. 2014).

1.5 Ribosomal Protein Stoichiometry and Paralog Substitution

1.5.1 Ribosome Stoichiometry

Eukaryotic ribosomes contain 79 ribosomal proteins, many of which are essential for biogenesis and function (Martin-Marcos, Hinnebusch et al. 2007, Rosado, Kressler et al. 2007, Russ 2007, Poll, Braun et al. 2009, Al-Hadid, Roy et al. 2016). Even haploinsufficiency of some ribosomal proteins can cause detrimental phenotypic changes or even death. For example, when a single copy of RPS6 was knocked out in the mouse it was embryonic lethal (Panic, Tamarut et al. 2006). Patients that are haploinsufficient for the ribosomal protein SA are born without spleens and are prone to life threatening infections (Bolze, Mahlaoui et al. 2013). However, not all ribosomal proteins are required, and in many cases the ribosome's requirements vary by organism, and tissue type (Chaillou, Zhang et al. 2016, Shi, Fujii et al. 2017). While minor differences in the

ribosome were observed from tissue to tissue, many believed this to be due to the challenges of ribosome isolation rather than actual, biologically relevant changes in ribosome composition. The notion of ribosome homogeneity was perpetuated by the fact that most research on the ribosome was, and still is, done in bacteria and yeast. While there are some changes in both bacterial and yeast ribosome composition under certain conditions, most laboratories studying ribosome heterogeneity are focused on changes in mammalian systems (Huang, Zhao et al. 2006, Shi, Fujii et al. 2017, Parks, Kurylo et al. 2018). Over the past few decades there has been ample evidence that ribosome protein composition is a fluid ebb and flow between various ribosomal proteins rather than static expression of 79 identical ribosomal proteins (Slavov, Semrau et al. 2015, Chaillou, Zhang et al. 2016, Guimaraes and Zavolan 2016). The first evidence of differential ribosome stoichiometry in a developing embryo was in the heart. Kirby et al demonstrated that RPL10 was increased in neural crest cells during septation of the outflow tract in the developing heart (Kirby, Cheng et al. 1995).

1.5.2 Ribosomal Paralogs

Seventy-nine ribosomal proteins and 4 strands of rRNA allows for many variations of ribosome composition but the introduction of paralogs further increase the possibilities (Kirby, Cheng et al. 1995, Ban, Nissen et al. 2000, Sugihara, Honda et al. 2010, Parks, Kurylo et al. 2018). A duplication event millions of years ago in eukaryotes lead to multiple copies of ribosomal genes; it is hypothesized that this duplication event increased fitness due to lower chances of disease caused by haploinsufficiency. Over the years, these duplicated ribosomal genes have accumulated mutations and given rise to paralogs, many of which exhibit high tissue specificity (Van Raay, Connors et al. 1996,

Wong, Li et al. 2014, Guimaraes and Zavolan 2016). *Arabidopsis* is believed to have gone through three duplication events leading to 80 ribosomal genes that are encoded by 249 genes (Lynch and Conery 2000, Simillion, Vandepoele et al. 2002). For years paralogs of ribosomal genes were believed to be functionally redundant until Rotenberg et al showed that the knockdown of RPL16 paralog caused phenotypic defects in *Saccharomyces cerevisiae*, indicating the paralog was functional (Rotenberg, Moritz et al. 1988). Since then, the functional significance of paralogs has come to the forefront of ribosomal studies and several of these duplicated genes have been shown to serve in a specialized capacity. In *Arabidopsis* RPL16A is specific to root stele and anthers and is thought to be important in pollen production; its paralog, RPL16B, is not tissue specific but is considered to be necessary for cell division in *Arabidopsis* (Williams and Sussex 1995).

Although the core RPL3 is a single gene in yeast, there are two variations in plants that are highly conserved (Fried and Warner 1981, Kim, Zhang et al. 1990, Nishi, Kidou et al. 1993, Barakat, Szick-Miranda et al. 2001). In rice, RPL3A and RPL3B only differ in 5 amino acids, 4 of which are very minor alterations (chemically similar amino acids). However, these small changes have led to functional diversity. Zheng et al. demonstrated that in rice RPL3A cannot compensate for the loss of RPL3B (Zheng, Wang et al. 2016). A mutation of RPL3B caused plants to be smaller, have retarded root growth, as well as vascular, and leaf defects; yet a mutation of RPL3A had no effect. Similar results were found when the same gene was knocked out in *N. tabacum* (Popescu and Tumer 2004). Phenotypic changes like these due to loss or mutation of a ribosomal

protein paralog are signs that particular ribosomal proteins may cause the ribosome to function in a specialized capacity.

Some ribosomal protein genes are found in sex chromosomes making a compelling argument that specific ribosomal proteins could play an important role in reproductive functions. For example, RPS4Y2 is expressed only in testes and prostate while its paralog, RPS4Y1, is expressed throughout the body, indicating that that RPS4Y2 carries out a function that is not met by the ubiquitous RPL4Y1. Men who underwent normal spermatogenesis showed 5 times more RPS4Y2 than men who were azoospermic. Although the sequences of these two homologs is 94% conserved, their C-termini are very different, which is believed to cause interactions with testes and prostate specific extra-ribosomal factors (Lopes, Miguel et al. 2010).

Kondrashov et al. demonstrated that there is differential translation of a subset of HOX genes when RPL38 is mutated, but not when RPS19, RPS20, RPL24, or RPL29 are mutated; indicating that not all ribosomal proteins confer a specialized function to the ribosome (Kondrashov, Pusic et al. 2011). After a similar study, Komili proposed a “ribosomal code” by which the variation of ribosome composition alters the type and frequency of transcripts that are translated providing for a level of gene regulation that has been, until recently, unrecognized (Komili, Farny et al. 2007). Not only do ribosomal proteins vary between tissue types but ribosome composition may affect whether or not the transcript accumulates in polysomes or remains a monosome (Slavov, Semrau et al. 2015). Ribosomes from mouse embryonic stem cells that were in the polysome fraction showed supra-stoichiometric quantities of RPL30, RPL27A, RPS18, and RPS17, while monosome fractions were enriched in RPS9, RPL5, RPS3 and RPS4X (Slavov, Semrau

et al. 2015). These findings provide evidence that ribosomal composition may alter the frequency of translation of some mRNAs.

1.5.3 Striated Muscle Specific RPL3-like

RPL3 is a ubiquitously expressed protein that is essential for ribosome assembly, interacts with three other ribosomal proteins, and touches the peptidyl transferase site within the ribosome (Ban, Nissen et al. 2000, Smith, Lee et al. 2008, Garcia-Gomez, Fernandez-Pevida et al. 2014). Interestingly, its paralog, RPL3L, is only expressed in striated muscle (Van Raay, Connors et al. 1996).

The expression of these ribosomal protein paralogs also shows a high degree of variation throughout the lifecycle. RPL3 expression during mouse post-natal development is highest at day one and then progressively decrease until day 21 where its expression remains low under resting conditions. The expression of its paralog, RPL3L, is the inverse of RPL3 (Chaillou, Zhang et al. 2016). Under normal conditions in mice during adulthood, RPL3 levels are low and its paralog, RPL3L, is relatively high (Komili, Farny et al. 2007). However, during skeletal muscle hypertrophy RPL3 is upregulated by 5-fold and RPL3L expression decreased by 82% (Chaillou, Zhang et al. 2016). Such differential expression of RPL3L and its paralog during hypertrophy suggests there are different classes of ribosomes in skeletal muscle under resting conditions and during growth.

The benefit of ribosomal transcript specificity in skeletal muscle is obvious - producing a ribosomal protein that has a high affinity for maintenance transcripts under

daily conditions, and a paralog that has an increased affinity for muscle sarcomeric transcripts would be a highly energy efficient mechanism to regulate a metabolically costly function - skeletal muscle growth.

1.5.4 Transcriptional Regulation

Commonly ribosomal protein regulation is seen as operating as one concerted regulatory pathway that responds to stimuli. However, differential expression of paralogs indicates that there is another level of complexity; there must be some secondary mechanism of modulating ribosomal protein expression that is dependent upon a particular stimulus. There has been almost no research on the regulation of ribosomal paralogs at the transcriptional level. The regulatory mechanism of RPL3L is completely unknown but some evidence suggests that ribosomal proteins may repress expression of their paralog. O'Leary et al reported that, in yeast, expression of RPL22 decreased the stability of its own paralog, RPL22-like1, by binding to a hairpin loop on the mRNA that encodes for RPL22-like1 (O'Leary, Schreiber et al. 2013). Alternatively, in human cells, RPS16 binds to the first intron of its mRNA to inhibit its own splicing (Ivanov, Parakhnevich et al. 2010). In yeast, RPS28b has been shown to uncap its own mRNA which prevents further translation, enhancing transcript degradation (Badis, Saveanu et al. 2004). Although it remains to be determined, one of these regulatory mechanisms could explain how the inverse pattern of expression for RPL3L and RL3 is achieved.

1.5.5 C-terminus of RPL3L

RPL3 and RPL3L are 74% identical in amino acid sequence indicating that some structural similarities are necessary to function. However, their inverse expression patterns, and tissue specificity of RPL3L, suggest that they are not functionally redundant. Aside from the few amino acid alterations in the body of the protein, RPL3L has 8 additional amino acids on the C-terminus, which could be the key to its functional differences. One possible mechanism by which RPL3L-containing the ribosome becomes specialized is by the C-terminus of RPL3L interacting with skeletal muscle specific transcripts to regulate their expression. Lopes et al hypothesized that C-terminal differences in ribosomal proteins might cause changes in the small and large subunit assembly, or alter the association of other proteins with the ribosome (Lopes, Miguel et al. 2010). Gamalinda and Woolford showed that C-terminal differences in ribosomal proteins could be the key to their function and that even minor variations of these C-termini could completely change their chemical associations with rRNA or other ribosomal proteins (Gamalinda and Woolford 2014). In yeast, a loss of the external globular tail of RPL4 significantly compromised ribosome function, stalling ribosome biogenesis at 27S and subsequently reducing the amount of ribosomes found in polysome fractions (Gamalinda and Woolford 2014).

1.5.6 Ribosome Localization

In most organs, mature ribosomes are found either free in the cytosol, or bound to the endoplasmic reticulum. Ribosomes freely floating in the cytosol translate water

soluble proteins (Palade 1955). In the event that the protein being translated is non-polar, a lipid localization signal is translated, the ribosome halts, and the ribosome translocates to the endoplasmic reticulum to complete translation (Fried and Warner 1981, Walter and Blobel 1981, Noriega, Chen et al. 2014). Interestingly, ribosomes in striated muscle have yet another location where they can be bound, Z-disk (Lewis, Moskovitz et al. 2018). A primary function of the Z-disk is to serve as a site for actin filament anchoring as part of the sarcomere but is also known to be a site where there is an enrichment of sarcomeric mRNA and ribosomes. Unlike translocation of ribosomes to the endoplasmic reticulum, ribosome localization to the Z-disk is not due to a translation of a peptide sequence that causes the ribosome to translocate. We know this because even in the presence of the translation inhibitor, cycloheximide, ribosomes and sarcomeric mRNAs remain enriched at the Z-disk (Lewis, Moskovitz et al. 2018). This mechanism for localized protein translation in striated muscle remains to be elucidated. Given striated muscle has some of the largest proteins within the cell, it is not surprising that it would be more energetically favorable to have translation occur near the site of use. Lewis et al noted that the pattern of ribosome localization, although present in post-natal mice, was a much less pronounced pattern than the prominent Z-disk localization observed in adult skeletal muscle (Lewis, Moskovitz et al. 2018). The muscle-specific expression of RPL3L, its increasing expression throughout post-natal development, and C-terminal differences – support the intriguing hypothesis that RPL3L C-termini contain the sequence by which these ribosomes assemble at the Z-disk.

1.6 Knowledge Gap

Ribosomes are an indispensable complex of rRNA, and proteins whose composition varies with cellular conditions such as disease state, cellular stress, developmental stage, and tissue type. Striated muscle has a unique ribosomal protein, RPL3L, that is differentially expressed during post-natal development and adult muscle hypertrophy. The extent of conservation of RPL3L indicates a specialized function that cannot be compensated for by the ubiquitous RPL3. There are currently no published studies on the physiological, or protein translation implications, on the role of RPL3L in cardiac function and translation. The purpose of the research described in this dissertation, is to address these gaps in knowledge with the hope of shedding light on the role of RPL3L in the heart.

CHAPTER 2. LOSS OF CARDIAC SPECIFIC RIBOSOMAL PROTEIN L3-LIKE HAS MODEST EFFECTS ON THE CARDIAC TRANSLATOME

2.1 Introduction

The function of the ribosome is to translate messenger RNA (mRNA) into protein making the ribosome indispensable for cellular proliferation, differentiation and maintenance. The eukaryotic ribosome is made up of two subunits that contain four strands of rRNA and 79 ribosomal proteins (RPs). The small subunit contains 18S rRNA and 33 RPs and the large subunit is comprised of 5S, 5.8S and 28S rRNAs and 46 RPs (Ben-Shem, Garreau de Loubresse et al. 2011).

Since the naming of the “ribosome” (ribonucleoprotein microsome) over 60 years ago, the ribosome has been viewed as functioning in a constitutive manner, in a “housekeeping” capacity without any real regulative properties (Roberts 1958, Hess and Oberhauser 1966). Komili and colleagues have challenged this long-standing dogma by proposing the concept of a “ribosome code” in which specialized classes of ribosomes preferentially translate select sets of mRNAs (Komili, Farny et al. 2007). The concept of ribosome specialization is a major paradigm shift for the field of gene regulation as it represents a completely new level of regulatory control – reminiscent of microRNAs almost two decades ago (Couzin 2002, Moss and Poethig 2002, Xue and Barna 2012).

The specialization of the ribosome has been proposed to occur through several possible mechanisms which include post-translational modifications of rRNA and/or proteins as well as the protein composition of the ribosome, RPs in particular (Al-Hadid,

Roy et al. 2016, Eralles, Marchand et al. 2017, Shi, Fujii et al. 2017, Genuth and Barna 2018, Magee and Ware 2019). The concept of ribosome specialization is supported by recent evidence showing ribosomal protein abundance and composition is more heterogeneous across different cell-types than was previously appreciated (Gupta and Warner 2014, Guimaraes and Zavolan 2016). Of particular interest was the muscle-specific expression of ribosomal protein L3-like (*Rpl3l*), a paralog of the ubiquitously expressed *Rpl3* (Van Raay, Connors et al. 1996, Gupta and Warner 2014, Guimaraes and Zavolan 2016). As the most ancient protein predicted to associate with the ancestral large ribosomal subunit, it is not surprising that RPL3 plays a fundamental role in the peptidyl transferase function of the ribosome; however, why striated muscle has evolved its own version of RPL3 remains an intriguing mystery (Kondrashov, Pusic et al. 2011, Caetano-Anolles and Caetano-Anolles 2015). Based on studies from the Barna laboratory, we have developed a working model proposing RPL3L-containing ribosomes have acquired a specialized function that is necessary for the maintenance of sarcomeric protein expression (Kondrashov, Pusic et al. 2011, Xue, Tian et al. 2015). Specifically, we hypothesize that RPL3-like containing ribosomes preferentially associate with sarcomeric mRNAs to ensure robust translation. To test this hypothesis, we used RNA-seq to determine mRNA composition of polyribosomes (polysomes) isolated from cardiac muscle of WT and *Rpl3l* KO mice. In contrast to our hypothesis, the results from this analysis revealed approximately 1% of the transcripts were significantly different between ribosomes with or without RPL3L suggesting RPL3L has a modest influence on the cardiac transcriptome.

2.2 Methods

2.2.1 Animals

All experimental procedures performed in this study were approved by the University of Kentucky Institutional Animal Care and Use Committee. The *Rpl3l*^{-/-} KO mouse (C57BL/6 background) was generated by Ingenious Targeting Laboratory (see Fig. 2A). A 9.3 kb genomic DNA fragment was used to construct the targeting vector which was subcloned from a positively identified C57BL/6 BAC clone (RP23-124B17). The region was designed such that the long homology arm (LA) extends ~5.64 kb from the 3' end of the FAST (Flexible Accelerated STOP Tetracycline Operator-Knockin) cassette with the short homology arm (SA) extending approximately 3.66 kb from 5' end of the FAST cassette (Tanaka, Ahmari et al. 2010). The FAST cassette was flanked by two loxP sites and consists of a PGK/EM7-Neo-pA sequence, a FRT-flanked stop cassette and a Tet operator combined with a CMV minimal promoter sequence. The FAST cassette was followed by the prototype Kozak sequence (GCCACC) which was placed immediately upstream of the endogenous ATG initiation site of *Rpl3l* gene. The targeting vector was confirmed by restriction analysis and sequencing after each modification. The boundaries of the two homology arms were confirmed by sequencing with P6 and T73 primers that read through both sides of the backbone vector into the genomic sequence. The FAST cassette insertion was confirmed by sequencing with BOSO SQ1, LAN1 and BOSO SQ2 primers. BOSO SQ1 and LAN1 sequencing confirmed the 5' genomic sequence/FAST cassette junction. BOSO SQ2 sequencing confirmed the 3' FAST/genomic sequence junction. Homologous recombination was used to insert the FAST cassette upstream of the *Rpl3l* transcription start site.

Heterozygous *Rpl3l*^{+/-} mice were bred to generate KO and WT littermates and housed in a humidity- and temperature-controlled facility, maintained on a 14:10 hour light-dark cycle with food and water *ad libitum*. Mice were euthanized using carbon dioxide followed by cervical dislocation.

2.2.2 RNA Isolation

Total RNA was isolated from the ventricles using Trizol reagent (ThermoFisher Scientific, Waltham, MA USA) and QuickRNA mini-prep kit plus (Zymo Research, Irvine, CA USA) according to the manufacturer's protocol. Immediately upon euthanasia, the heart was excised, and isolated ventricles were minced and then homogenized using a Bullet Blender (Next Advance, Troy, NY USA) and 1 mm zirconia beads (BioSpec Products, Bartlesville, OK USA). Total RNA concentration and purity was determined by measuring the optical density (230, 260, and 280 nm) with a Nanodrop 1000 spectrophotometer (ThermoFisher Scientific, Waltham, MA USA).

2.2.3 RT-PCR

Complementary DNA was generated from 500 ng of total RNA using the SuperScript IV Reverse Transcriptase (ThermoFisher Scientific, Waltham, MA USA). TaqMan Fast Advanced Master Mix and TaqMan probes (*Rpl3* Mm02342628_g1, *Rpl3l* Mm00481336_g1, and *Gapdh* Mm99999915_g1) were used for real-time PCR (Thermo Fisher Scientific, Waltham, MA USA). The $2^{(-\Delta\Delta CT)}$ was calculated using *Gapdh* to normalize mRNA expression.

2.2.4 Western Blot

Frozen heart samples were homogenized in RIPA buffer (50m Tris HCl pH 7.4, 1% Triton X100, 0.5% sodium deoxycholate, 0.1% SDS, 150 mM NaCl, 2 mM EDTA, 50 mM NaF) with Halt Protease Inhibitor Cocktail (ThermoFisher, Waltham, MA USA). Protein concentration was measured using DC Protein Assay (Bio-Rad, Hercules, CA USA). Thirty micrograms of whole-cell homogenate samples were prepared for SDS-PAGE by boiling for 5 min in SDS sample buffer (50mM Tris-HCl pH 6.8, 10% glycerol, 2% SDS, 0.02% bromophenol blue, 1% β -mercaptoethanol). Following SDS-PAGE, protein was transferred onto nitrocellulose membrane (Bio-Rad, Hercules, CA USA). Membranes were blocked with 5% milk in TBS-T (TBS, 0.1% Tween-20) for 1 hr and then incubated overnight at 4 °C with primary antibody. Primary antibody dilutions were as follows: RPL3 rabbit anti-mouse 1:2000 (Abcam ab228638, Cambridge, MA USA); RPS6 rabbit anti-mouse 1:5000 (Abcam ab40820, Cambridge, MA USA); RPL3L rabbit anti-mouse 1:2000 was generated by ThermoFisher Scientific using peptide sequence GPQKKHLEKEKPETLGNM. For analysis of knockout, membranes were washed in TBS-T and then incubated for 1 hr at room temperature with a goat anti-rabbit secondary antibody conjugated to 680nm fluorophore (ThermoFisher, Waltham, MA USA). Fluorescent intensity was measured using the Licor Odyssey instrument with band intensity quantified using ImageJ. For analysis of RPL3 and RPL3L expression during post-natal development membranes were blotted with 1:2,000 RPL3 (ab228638, Abcam, Cambridge, MA USA), 1:2,000 RPL3L (described above) and 1:5,000 RPS6 (Cat #2217, Cell Signaling, Danvers, MA USA) in 5% BSA with TBS-T overnight at 4 °C. Membranes were washed in TBS-T and then blotted for one hour with goat, anti-rabbit

horseradish peroxidase at a dilution of 1:10,000 (ThermoFisher Scientific, Waltham, MA USA). Luminol enhancer (ThermoFisher Scientific, Waltham, MA USA) was used to induce chemiluminescence which was detected using CL-X Posure™ film (ThermoFisher Scientific, Waltham, MA USA).

2.2.5 Polysome Fractionation

Polysome fractionation was performed as described by Garelick and colleagues with minor modifications (Garelick, Mackay et al. 2013). Briefly, the lower half of the ventricle was cut to ensure no atrial tissue was excised, then flash frozen in liquid nitrogen and pulverized while on dry ice with a sterile razor blade. The tissue was then homogenized with lysis buffer (1.5mM KCl, 2.5mM MgCl₂, 5mM Tris, pH 7.5; 50 mg tissue/ml buffer) using a Dounce homogenizer with 20 strokes on ice. Samples were incubated on ice for 5 min and incubated an additional 5 min with intermittent mixing by inversion following the addition of 0.27% deoxycholate and 0.56% Tween-20. Samples were then centrifuge at 6,000 g for 15 min at 4 °C. Seven and a half milligrams of protein (~ 600ul) of supernatant was layered onto a pre-chilled 20-50% linear sucrose gradient and centrifuged at 40,000 g for 3 hrs at 4 °C in a Beckman SW40Ti rotor. Gradients were fractionated while monitoring absorbance at 254nm with Gradient Station System (BioComp Instruments, Fredericton, NB, Canada).

2.2.6 RNA-sequencing and Bioinformatics

Samples from polysome fractionation containing ≥ 2 ribosomes were combined, and RNA isolated using Trizol reagent (ThermoFisher Scientific, Waltham, MA USA) and

QuickRNA mini-prep kit plus (Zymo Research, Irvine, CA USA) according to the manufacturer's protocol. Library preparation and RNA-Seq was performed by Novogene Co. Ltd (Beijing, China). Samples of 150 bp paired end reads with >20M reads were checked for quality and filtered based on read quality to eliminate low quality, low complexity reads (Phred <30, GC content ~50%). We also filtered and discarded rRNA, tRNA and mtRNA contaminants with adaptor sequences removed. Reads were then aligned with STAR RNA aligner allowing for 2 mismatches (Dobin et al. 2013). Reads that did not map uniquely were discarded and uniquely mapped reads were quantified to annotation model (mm10) and then normalized to sequence depth using transcripts per million (TPM). To account for technical variability across samples within a group, transcript abundance was normalized to the geometric mean of four mRNAs (*Vcp*, *Rps6*, *Rpl38* and *Gapdh* whose expression was show to not be different between WT and KO in RT-PCR experiments (data not shown). To minimize the influence that transcript abundance can have on translation, we removed any mRNAs that showed a significant difference between WT and KO as assessed by RNA-seq of whole-cell lysate RNA. To determine fold- enrichment for each mRNA in polysomes, the KO ratio of translation/transcription was divided by WT ratio of translation/transcription for each mRNA.

2.2.7 Cardiomyocyte dispersal

Single ventricular cardiomyocytes were enzymatically isolated following a modified AfCS protocol PP00000125 as previously described (O'Connell 2002). In brief, mice were injected with 200U heprin 5 minutes before sacrifice to prevent blood

coagulation. Mice were anesthetized with Ketamine+Xylene (90+10mg/kg), and the hearts were rapidly excised and retrogradely perfused at 3ml/min and 37 °C for 4-8 minutes with a calcium free bicarbonate-based buffer (113mM NaCl, 4.7mM KCl, 0.6 mM KH₂PO₄, 1.2m MgSO₄, 0.6mM NaH₂PO₄, 5.5mM glucose, 12mM NaHCO₃, 10mM KHCO₃, 10mM HEPES, and 30mM taurine). The perfusion buffer was gassed with 95% O₂ and 5% CO₂ and warmed to 37 °C for at least 30 minutes before use. Enzymatic digestion buffer was made using the above buffer and adding 0.25mg/ml liberase Blendzyme (Roche) and 12.5uM CaCl₂, this buffer was then used to perfuse the heart for about 13-18 minutes on a Langendorff apparatus until the heart was swollen and pale in color. The heart was then cut from the cannula the ventricles were placed in a dish containing stop buffer (perfusion buffer supplemented with 10% FBS and 12.5ul CaCl₂) and gently dissociated large pieces of heart tissue using tweezers.

2.2.8 Transverse Tubules

Dispersed cardiomyocytes were incubated for 5 minutes with Di-8-ANEPPS (ThermoFisher D3167) for visualization of t-tubules. Imaging was performed on a Live 5 (Zeiss) live cells scanning microscope with a final magnification of 100x. Transverse tubule images were analyzed using the AutoTT software program in ImageJ (Guo and Song 2014).

2.2.9 Calcium Tolerance

Dispersed cardiomyocytes were incubated at increasing calcium concentrations and then imaged on a Nikon Eclipse 6000 microscope and at 40X magnification. Imaging was repeated one hour later. For analysis, the person who quantified live cells was blinded to genotype. Live cells were quantified based off of morphological characteristics with typical shaped cells (rectangular, ridged looking structure) considered live cardiomyocytes. Percent alive was calculated using initial live cells/final live cells for each condition.

2.2.10 Gene Ontology

mRNAs that were differentially translated or differentially spliced were uploaded from the gene list to DAVID Bioinformatics Resources 6.8, Functional Annotation. Using a *Mus Musculus* background, Up_Keywords was used for gene ontology classification.

2.2.11 Statistics

Unless stated otherwise, unpaired Student's t-test was performed to determine if significant ($p < 0.05$) difference existed between WT and KO genotypes for the dependent variable under consideration. Area under the curve analysis was used to determine if there were differences in polysome profiles.

2.3 Results

2.3.1 RPL3 and RPL3L Expression During Post-natal Development

In skeletal muscle, *Rpl3l* mRNA expression was reported to gradually increase during post-natal development (Cheng and Porter 2002). To determine if a similar pattern of expression occurs in the heart, we performed qPCR and Western blot analyses to measure *Rpl3l* mRNA and protein, respectively, during post-natal development. As shown in Fig. 1A, *Rpl3l* mRNA expression was undetectable at post-natal day 1 (P1) and then gradually increased throughout post-natal development to P21; alternatively, its paralog, *Rpl3*, had peak expression at P1 and then progressively decreased through post-natal development with the lowest expression at P21. Next, we performed Western blot analysis to determine if the changes in *Rpl3l* and *Rpl3* mRNA expression during post-natal development were reflected at the protein level. As shown in Fig. 1B, we observed the same general pattern of expression in RPL3L and RPL3 during post-natal development as we found with their respective mRNA. The expression of RPS6 expression was relatively stable throughout post-natal development indicating the

observed changes in RPL3L and RPL3 were not driven by changes in ribosome content of the muscle.

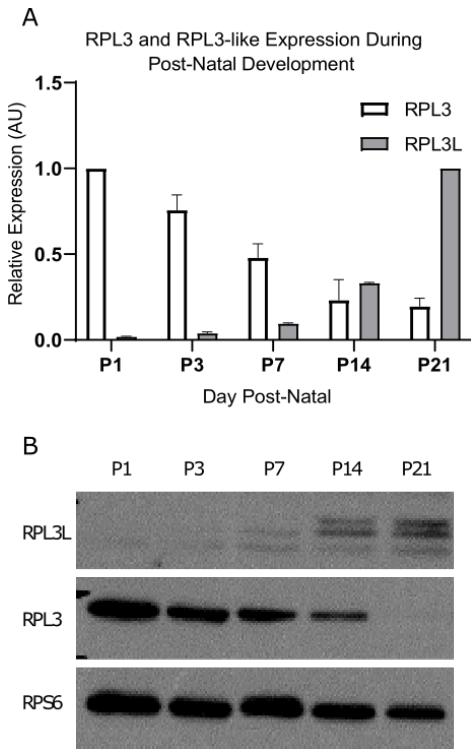


Figure 1: Up-regulation of *Rpl3l* in the heart during post-natal development. A, qPCR analysis showed progressive increase in *Rpl3l* mRNA starting post-natal day 1 (P1) with peak expression at P21; paralog *Rpl3* mRNA expression showed the opposite pattern with peak expression at P1 and lowest at P21. B, Western blot analysis showed quantitatively similar pattern of RPL3L and RPL3 expression as observed with respective mRNA. Data (n=3) are presented relative to P21 for *Rpl3l* and P1 for *Rpl3*.

2.3.2 RPL3L KO Strategy

A schematic of the targeting construct used to inactivate the *Rpl3l* gene is shown in Fig. 2A. A FAST cassette, containing a transcriptional “STOP” sequence, was inserted by homologous recombination upstream of the transcription start site of the *Rpl3l* gene.

Heterozygous *Rpl3l*^{+/-} breeding pairs were established to generate *Rpl3l*^{-/-} KO and *Rpl3l*^{+/+} WT littermates in roughly equal numbers indicating loss of *Rpl3l* expression was not embryonic lethal. qPCR confirmed *Rpl3l* mRNA expression was significantly reduced by 75% in the KO compared to WT while *Rpl3* mRNA expression was unchanged in the KO (Fig. 2B-C). As shown in Fig. 2D-E, Western blot analysis revealed at the protein level, RPL3L expression was significantly reduced by ~90% in the KO in comparison to WT.

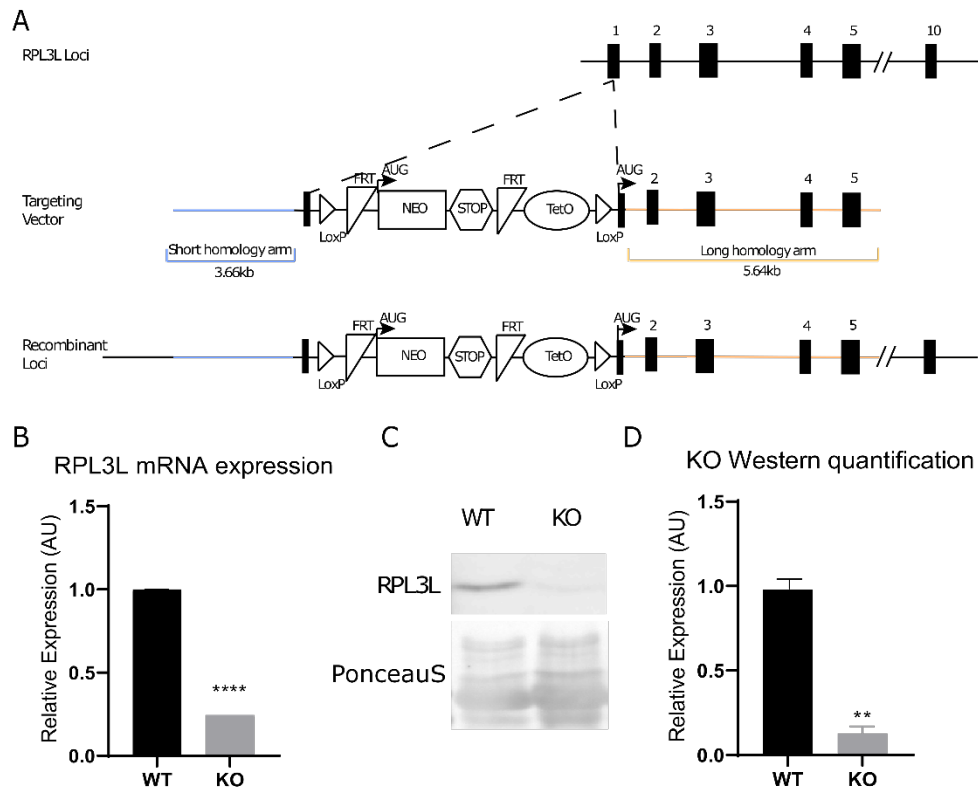


Figure 2: Effective knockdown of RPL3 expression in the heart. *Rpl3l* genetic KO model contains a stop cassette to interrupt expression of *rpl3l* mRNA production (A). rtPCR of the KO indicates that RPL3L is ~75% reduced when compared to the WT (B). Western blot analysis demonstrates that RPL3L is significantly reduced in the hearts of KO mice (C & D, $p < 0.01$). Student t-test were used to determine significance. N=3.

2.3.3 Translational Enrichment

To test our hypothesis that RPL3L-containing ribosomes would preferentially translate sarcomeric transcripts (in comparison to RPL3-containing ribosomes of KO mice), we performed RNA-seq of mRNA associated with polysomes isolated from WT

and KO whole-cell cardiac lysates. Prior to polysome fractionation, a portion of the whole-cell lysate was set aside for RNA-seq to determine the WT and KO cardiac transcriptome. As presented in Fig. 3A, polysome abundance was qualitatively similar between WT and KO groups. Providing confidence in the polysome isolation, the 25 most abundant polysome transcripts in cardiac muscle were either striated muscle-enriched mRNAs (*Myl2*, *Mb*, *Tnnc1*, *Tnnt2*) or mitochondrial mRNAs (*Cox7a1*, *Cox8b*, *Cox4i1*, *Atp5j2*); however, there was no significant difference in the polysome abundance of sarcomeric transcripts between WT and KO groups, contrary to our hypothesis (see Table 1). We did identify 216 transcripts whose polysome abundance was significantly different between WT and KO groups (see Supplemental Table 1 in the Appendices). Of these transcripts, 68 transcripts were significantly more abundant in WT whereas 148 transcripts were significantly more abundant in the KO. For the significantly different transcripts, Fig. 3B shows the 21 most abundant transcripts, presented as relative to WT; however, the abundance of these mRNAs was very low with the majority of the transcripts below 150 TPM. Gene ontology of those polysome transcripts more abundant in WT revealed enrichment for mRNAs involved with endoplasmic reticulum function. As shown in Fig. 3C, for polysome transcripts that were more abundant in the KO, gene ontology analysis showed the genes with the highest enrichment of ~3-fold were involved with RNA metabolism such as processing, splicing and RNA binding.

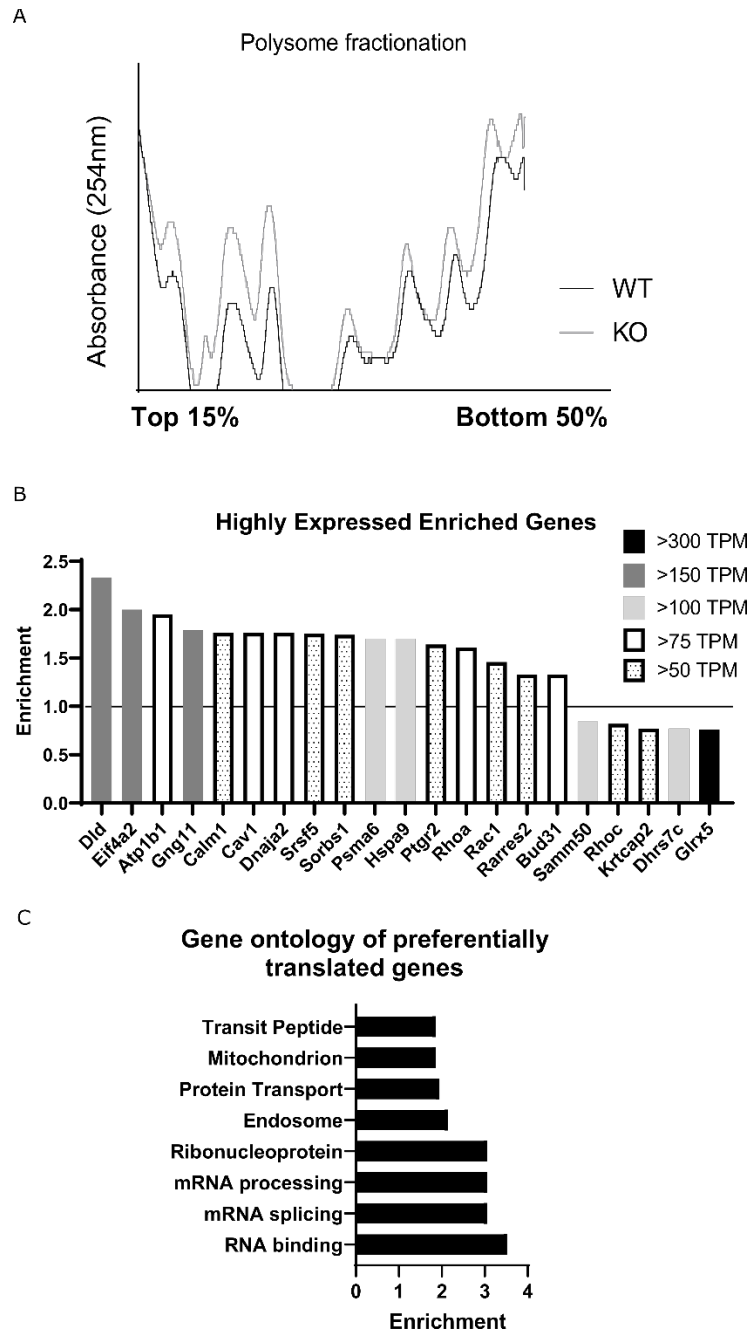


Figure 3 Modest differences in heart polysome composition between RPL3L KO and WT.

A, KO and WT heart polysome profiles were similar with no difference in polysome abundance as assessed by area under the curve analysis. B, mRNAs with highest polysome enrichment presented relative to WT have low level of expression. C, Gene ontology of genes with higher abundance in KO polysomes.

A primary determinant of whether or not a transcript is translated is the abundance of the transcript (Li, Bickel et al. 2014, Csardi, Franks et al. 2015). We performed whole-cell RNA-seq to identify and, subsequently remove, any transcripts that were differentially expressed between WT and KO groups (see Supplemental Table 2 of the Appendices), in an effort to minimize the chance that a difference in polysome transcript abundance was driven by a difference in transcript abundance between WT and KO. Having the whole-cell transcriptomic data, we next wanted to determine the relationship between the transcriptome and the translome for each mRNA that was not differentially expressed between WT and KO. As expected, transcript abundance and polysome transcript abundance were highly correlated; however, unexpectedly, KO showed a significantly higher correlation than WT (Fig 4). This finding suggests in WT cardiac muscle, there is some factor(s), or lack of mRNA selectivity influencing translation besides transcript abundance, though our findings indicate it is likely not RPL3L.

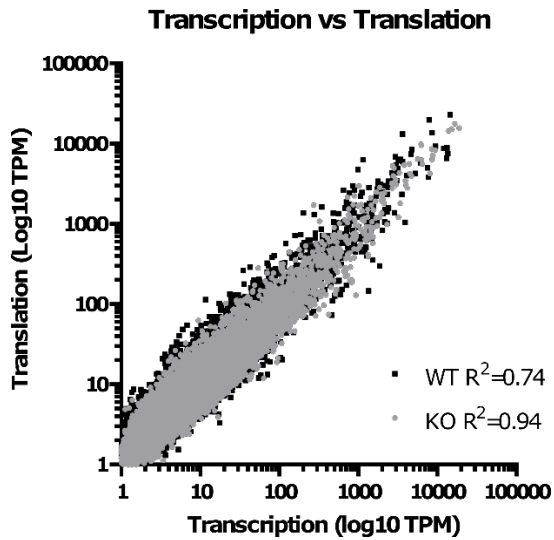


Figure 4: Transcript abundance is primary determinant of translation. The relationship between translation (polysome transcript abundance) and transcription (whole cell transcript abundance) is highly correlated (WT, $R^2=0.74$ vs KO, $R^2=0.94$). The higher correlation in KO suggests an inhibitory factor(s), or a lack of mRNA selectivity in WT affected translation other than RPL3L.

2.3.4 Differential Splicing

To investigate the possibility that alternative translation of mRNAs that are involved in mRNA splicing and RNA binding we utilized polysome RNA sequencing data and a software designed to detect splicing changes in replicate RNA sequencing. We found that there were 825 mRNAs exhibiting differential splicing events between WT and KO. Of those splicing events, 729 were alternative exon usage, and 96 were mutually exclusive exon usage. Gene ontology of differentially spliced mRNAs that exhibited differential splicing in KO showed an increase in mRNAs related to mitochondria, transit peptide, transport, protein transport, and oxidoreductase (Fig. 5). However, the top 3 mRNAs that showed reduced alternative splicing in KO were Neuronatin (Nnat), Aspartate beta-hydroxylase (Asph), and myotonic dystrophy protein kinase (Dmpk), all of which have known roles in calcium homeostasis.

Gene Ontology of differentially spliced mRNAs

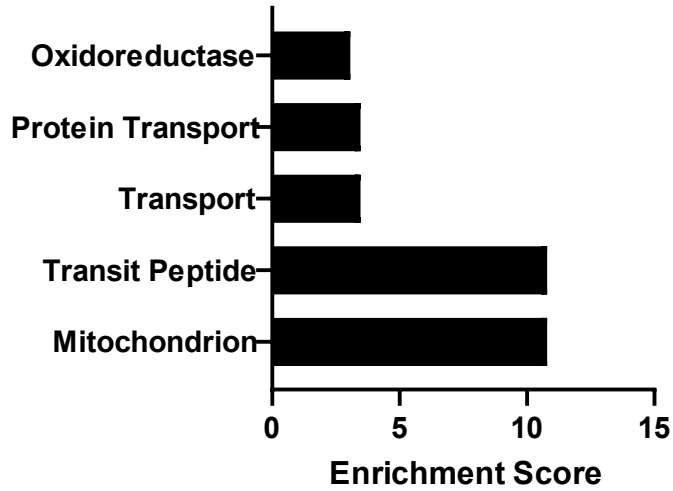


Figure 5: Gene ontology of differentially spliced mRNAs.

Gene ontology of differentially spliced mRNAs showed enrichment in mRNAs that are related to mitochondria, transit peptide, transport, protein transport, and oxidoreductase.

2.3.5 Calcium Handling

Because the top 3 most differentially spliced mRNAs were all involved in calcium homeostasis, we wanted to investigate calcium handling to see if these changes were sufficient to cause disruption in calcium homeostasis. We began by looking at calcium transients of dispersed cardiomyocytes before and after administration of isoproterenol. We found that while WT mice showed normal calcium transients before, and an appropriate response to isoproterenol cardiomyocytes from the KO all dying during or prior to data collection (n=5, data not shown). Given this unexpected finding, we wondered if the death of KO cardiomyocytes could be due to alterations in calcium handling. To investigate this possibility, we dispersed cardiomyocytes and titrated in varying levels of calcium. We found that while the WT mice had the highest level of survival at physiological levels of calcium, KO cardiomyocytes had the highest survival at very low levels of calcium and had increasing cell death as calcium concentration increased to physiological levels (Fig. 6).

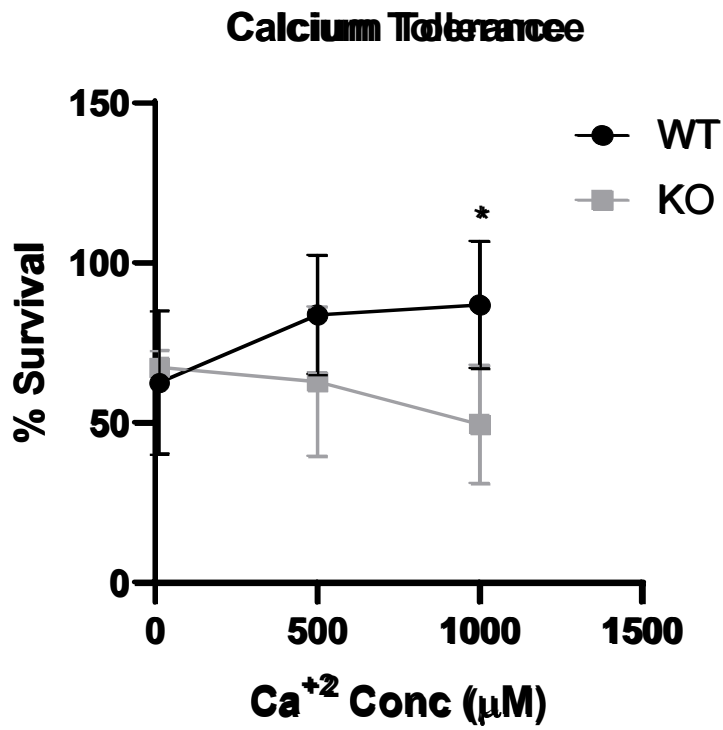


Figure 6: KO cardiomyocytes show an increase in calcium sensitivity. KO cardiomyocytes showed a decrease in survival with increasing amounts of calcium with the lowest level of survival at physiological levels of calcium. Data are presented as mean +/- SD (n=3) with asterisk denoting significance (p<0.05) between WT and KO using non-linear fit analysis.

2.3.6 Transverse Tubules

Transverse tubules (t-tubules) are invaginations of the sarcolemma that allows for concerted release of calcium from the sarcoplasmic reticulum in response to depolarization. During overload and in certain pathological conditions t-tubules can become disrupted due to ventricular remodeling. We wanted to know if altered calcium tolerance seen in KO mice could be due to disruption of t-tubules. To that end, we dispersed ventricular cardiomyocytes and imaged t-tubules. We found that t-tubules of KO mice were significantly disrupted when compared to WT (Fig. 7 A,B).

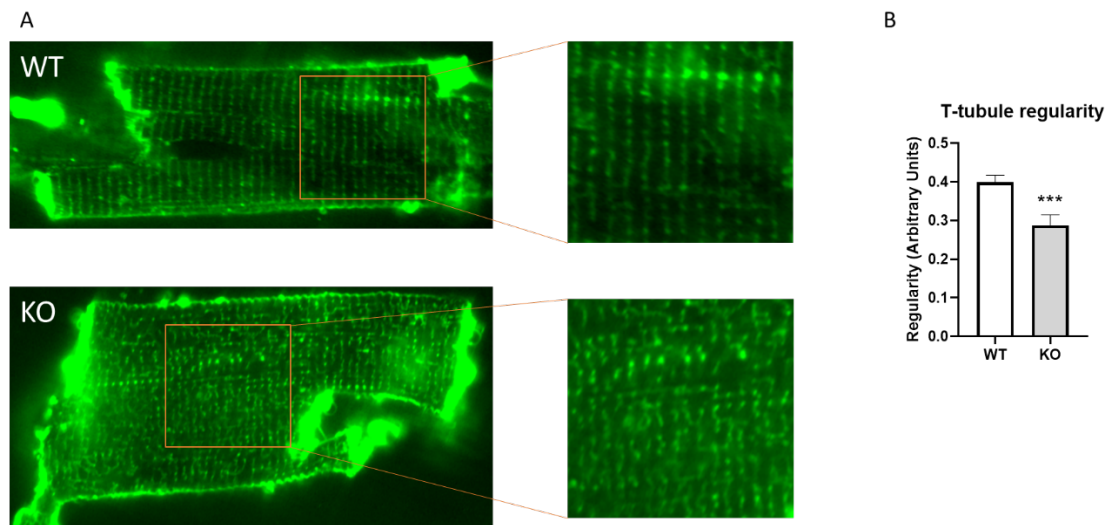


Figure 7: T-tubules of RPL3L mice show a decrease in regularity. Visual inspection of dispersed ventricular cardiomyocytes of KO mice exhibited lower t-tubule regularity than the WT. Quantification of t-tubule regularity via the program AutoTT revealed that the t-tubules were significantly more disrupted in the KO mice compared to WT. Data are presented as mean \pm SD (n=4) with asterisk denoting significance ($p < 0.05$) between WT and KO using Student's t-test.

2.4 Discussion

2.4.1 Summary of Findings

The major finding of the study is that the loss of *Rpl3l* had a minor effect on the cardiac translome, the abundance and/or composition of transcripts translated by the ribosome. While we did detect differences in the abundance of transcripts being actively translated between WT and KO, it represented only ~1% (216/16,643) of the translome which consisted of low abundant transcripts, being 150 TPM and less. Using gene ontology, we found that of the mRNAs that were differentially translated, many of them showed enrichment in splicing proteins. Despite the low level of translation of these proteins, we found that splicing was significantly different among WT and KO mice and that the top 3 most differentially spliced mRNAs all contribute to calcium homeostasis. Additionally, we found that dispersed ventricular cardiomyocytes show altered calcium homeostasis and disrupted t-tubules.

Most importantly, the results of the study do not support our hypothesis that RPL3L-containing ribosomes preferentially translate sarcomeric transcripts. In fact, we found no difference in the polysome abundance of any sarcomeric transcript between WT and KO.

2.4.2 Ribosome Specialization

The concept of ribosome specialization was formalized by Komili and coworkers in their proposal of a ribosome code in which specialized classes of ribosomes preferentially translated select sets of mRNAs (Komili, Farny et al. 2007). Support for the ribosome code came from a series of studies showing that RPL38-containing ribosomes

preferentially associated with Hox mRNAs through a 5'-UTR mediated mechanism (Kondrashov, Pusic et al. 2011, Xue and Barna 2012). Although additional evidence continues to accumulate supporting the concept of ribosome specialization based on ribosome heterogeneity, concerns have been raised regarding the use of artificial systems to manipulate RP levels and the possibility that the observed difference in the translation of distinct mRNA classes may be accounted for by a change in ribosome abundance (Genuth and Barna 2018, Ferretti and Karbstein 2019).

2.4.3 Translational Enrichment

A limitation of current study is we did not isolate ribosome-protected mRNA fragments as done with traditional Ribo-seq but rather isolated the full transcript, in theory, associated with the ribosome, i.e., actively being translated. As a result, we were unable to distinguish a transcript that was being highly translated, associated with 4-5 ribosomes, from a transcript having a lower level translation, associated with two ribosomes. So, while we did not detect a difference in the abundance of sarcomeric transcripts being actively translated in cardiac tissue between WT and KO mice, the possibility remains that the level of translation of a particular sarcomeric mRNA might in fact be different between WT and KO.

2.4.4 Calcium Homeostasis

Calcium homeostasis is imperative for proper cardiac functioning due to its central role in excitation-contraction coupling. Differential splicing of mRNAs that are involved in calcium homeostasis can have large effects on overall function and stress

response. Three of the most differentially spliced mRNAs are all implicated in calcium homeostasis: *Nnat*, *Asph*, and *Dmpk*. While the role of *Nnat* in cardiac tissue has not been elucidated, it has high sequence homology to phospholamban and overexpression of *Nnat* has been shown to increase intracellular calcium and cause endoplasmic reticulum stress in cultured adipocytes and neuronal cells (Suh, Kim et al. 2005, Sarkozy, Zvara et al. 2013, Sharma, Mukherjee et al. 2013). *Asph* undergoes extensive alternative splicing and gives rise to junctin and junctate, both of which play a role in calcium homeostasis (Gyorke, Hester et al. 2004, Hong, Kwon et al. 2008). In cardiomyocytes junctin forms a complex with triadin, calsequestrin and the ryanodine receptor (Zhang, Kelley et al. 1997). The association of this complex confers luminal calcium sensitivity to the ryanodine receptor (Gyorke, Hester et al. 2004). Junctate is also plays a role in calcium homeostasis by regulating agonist induced calcium entry into the cytoplasm and stabilizing the connection between the plasma membrane and the sarcoplasmic reticulum (Treves, Franzini-Armstrong et al. 2004). *Dmpk* is a gene that is associated with myotonic muscular dystrophy, a disease marked by progressive conduction defects and ventricular arrhythmias. *Dmpk* KO cardiomyocytes exhibited increased contractility and increase in intracellular calcium through an unknown mechanism (Pall, Johnson et al. 2003). While speculative at this time, the splicing differences observed in any of these three proteins could affect calcium handling and contribute to the t-tubule morphological changes seen in ventricular cardiomyocytes of *Rpl3l* KO mice.

2.4.5 Possible Roles of RPL3L and Future Directions

The findings from our study indicate that RPL3L has a modest impact on which transcripts are translated in the heart, leaving unanswered the question as why does

striated muscle have its own version of *Rpl3*? While the findings of the current study indicate no major preference for a distinct class of mRNAs, RPL3L-containing ribosomes might have altered function such that processivity and/or fidelity might be different compared to RPL3-containing ribosomes. Given that striated muscle transcripts, such as titin, nebulin and dystropin, are the largest proteins in the body, could it be that RPL3L slows ribosome processivity thereby increasing the fidelity of translation (Mordret, Dahan et al. 2019)? Evidence from Duchenne muscular dystrophy in which *Rpl3l* is replaced by *Rpl3*, mimicking our *Rpl3l* KO, reported enhanced translation in skeletal muscle of patients compared to control subjects (Ionasescu, Zellweger et al. 1971). One explanation for this curious finding is that RPL3L-containing ribosome (of control subjects) move more slowly during translation thereby increasing fidelity, though the difference in the rate of translation could also be accounted for by differences in the rate of initiation and/or termination. An important focus of future studies will be investigating if *Rpl3l* alters ribosome function (translation initiation, fidelity and termination) with the hope that a better understanding of *Rpl3l* function will reveal fundamental insight into striated muscle given the central role of the ribosome in cell biology.

CHAPTER 3. LOSS OF VENTRICULAR- SPECIFIC RIBOSOMAL PROTEIN RPL3L ENHANCES RESPONSE TO ACUTE ADRENERGIC STIMULATION

3.1 Introduction

3.1.1 Atrial Fibrillation

Atrial fibrillation (AF) is a condition in which chronic irregular electrical activity leads to inefficient filling of the ventricles. The sinoatrial node (SAN), a group of cells located in the wall of the right atrium, initiates and regulates the heartbeat. Under certain disease conditions the SAN may depolarize irregularly leading to aberrant electrical activity, which in turn can give rise to atrial fibrillation (Wijffels, Kirchhof et al. 1997, Fareh, Villemaire et al. 1998, Allessie, Ausma et al. 2002, Dobrev and Ravens 2003, Nattel, Maguy et al. 2007). AF has several co-morbid conditions including heart failure, stroke and myocardial infarction (Lin, Wolf et al. 1996, Soliman, Safford et al. 2014, Vermond, Geelhoed et al. 2015, Wijesurendra, Liu et al. 2018). The underlying conditions that can give rise to AF are multifactorial and may include contributions from genetics in about 30% of cases (Roberts 2006), or from other diseases (Fox, Parise et al. 2004, Abdulla and Nielsen 2009, Lubitz, Ozcan et al. 2010, Lubitz, Yin et al. 2010, Thorp, Owen et al. 2011).

3.1.2 RPL3L Tissue Specificity

The ribosome is the molecular machine responsible for translating mRNA into protein. The ribosome is composed of four strands of rRNA and ~80 ribosomal proteins.

There are a few instances in which a ribosomal protein has a paralog which often shows tissue-specific expression and appears to be functionally distinct (Rotenberg, Moritz et al. 1988, Popescu and Tumer 2004, Komili, Farny et al. 2007, Wong, Li et al. 2014, Guimaraes and Zavolan 2016). One such tissue-specific paralog is RPL3L which is only expressed in striated muscle, while the canonical paralog, *Rpl3* is expressed ubiquitously (Chaillou, Zhang et al. 2016). Recently, a genome-wide association study identified mutations in *Rpl3l* gene which were associated with a higher incidence of AF (Thorolfsdottir, Sveinbjornsson et al. 2018).

3.1.3 Knowledge Gap

The purpose of this study was to investigate the functional role of *Rpl3l* in the heart. Both echocardiography and electrocardiography showed no obvious differences in cardiac function or electrical activity, respectively, of *Rpl3l* KO mice compared to WT littermates. qPCR, Western blot, scRNA-seq and mass-spectrometry analyses confirmed *Rpl3l* was only expressed in the ventricles and not the atria or the SAN of WT mice. These findings show that *Rpl3l* is the first-known ventricular specific ribosomal protein and further suggest that the association of *Rpl3l* variants and AF maybe due to a ventricular pathology which promotes AF (Ehrlich, Nattel et al. 2002, Vermes, Tardif et al. 2003).

3.2 Materials and Methods

3.2.1 Animals

All experimental procedures involving animals were approved by the University of Kentucky Institutional Animal Care and Use Committee. Heterozygous *Rpl3l*^{+/-} mice (previously described in Chapter 2, Fig. 2A) were bred to generate KO and WT littermates and housed in a humidity- and temperature-controlled facility, maintained on a 14:10 hour light-dark cycle with food and water ad libitum. Male mice, 3-7 months of age were used in the described studies and euthanized by carbon dioxide asphyxiation followed by cervical dislocation.

3.2.2 RNA Isolation

Total RNA was isolated from atrial and ventricular tissues using Trizol reagent (ThermoFisher Scientific, Waltham, MA USA) and QuickRNA mini-prep kit plus (Zymo Research, Irvine, CA USA) according to the manufacturer's protocol. Ventricles and atria were isolated, minced with scissors, and homogenized using a Bullet Blender (Next Advance, Troy, NY USA) and 1 mm zirconia beads (BioSpec Products, Bartlesville, OK USA). Total RNA concentration and purity were assessed by measuring the optical density (230, 260, and 280nm) with a Nanodrop 1000 spectrophotometer (ThermoFisher Scientific, Waltham, MA USA).

3.2.3 RT-PCR Analysis

Complementary DNA was generated from 500 ng of total RNA using the SuperScript IV Reverse Transcriptase (ThermoFisher Scientific, Waltham, MA USA). TaqMan Fast Advanced Master Mix and TaqMan probes (*Rpl3* Mm02342628_g1, *Rpl3l* Mm00481336_g1, and *Gapdh* Mm99999915_g1) were used for real-time PCR (ThermoFisher Scientific, Waltham, MA USA). The $2^{(-\Delta\Delta CT)}$ was calculated using *Gapdh* as the control and normalized to *Rpl3l* or *Rpl3* for ventricle or atria analysis, respectively.

3.2.4 Western Blot Analysis

Frozen ventricle and atrium samples were homogenized in RIPA buffer (50m Tris HCl pH 7.4, 1% Triton X100, 0.5% Na deoxycholate, 0.1% SDS, 150 mM NaCl, 2 mM EDTA, 50 mM NaF) with Halt Protease Inhibitor Cocktail (ThermoFisher, Waltham, MA USA). Protein concentration was measured using DC Protein Assay (Bio-Rad, Hercules, CA USA). Thirty micrograms of protein homogenate samples were prepared for SDS-PAGE by boiling for 5 min in SDS sample buffer (50mM Tris-HCl pH 6.8, 10% glycerol, 2% SDS, 0.02% bromophenol blue, 1% beta-mercaptoethanol). Following SDS-PAGE, protein was transferred onto nitrocellulose membrane (Bio-Rad, Hercules, CA USA). Membranes were blocked with 5% milk in TBS-T (TBS, 0.1% TWEEN 20) for 1 hr and then incubated overnight at 4 °C with primary antibody. Primary antibody dilutions were as follows: RPL3 rabbit anti-mouse 1:2000 (Abcam ab228638, Cambridge, MA USA); RPL3L rabbit anti-mouse 1:2000 was generated by ThermoFisher Scientific using peptide sequence GPQKKHLEKEKPETLGNM. Following overnight incubation, membranes were washed in TBS-T and then incubated for 1 hr at room temperature with

a goat anti-rabbit secondary antibody conjugated to 680nm fluorophore (ThermoFisher, Waltham, MA USA). Fluorescent intensity was measured using ChemiDoc MP Imaging System (Hercules, CA USA) and band intensity was quantified using ImageJ. Fluorescence intensity of bands was normalized to Ponceau S staining (Biotium Inc, Fremont, CA, USA).

3.2.5 Single-cell RNA-Sequencing Analysis

Fastq files from single-cell RNA-sequencing (scRNA-seq) analysis of isolated mouse sinus atrial node (SAN) tissue, as reported by Linscheid and colleagues, were retrieved from NCBI Gene Expression Omnibus (accession number GSE130710, sample H4). Cell Ranger 3.1 pipeline (10X Genomics, USA) was used for read alignment using the mouse mm10 release 93 reference genome modified to include pre-mRNA. Cell calls were made using default parameters for Cell Ranger. Unique molecular identifier counts for all partitions identified as cells were greater than 2150. The re-analyze function in Cell Ranger was used to eliminate cell clusters enriched in mitochondrial reads as described on the 10x website (<https://kb.10xgenomics.com>). Only one cluster was eliminated because of enrichment in mitochondrial genes (the top most differentially expressed genes were mitochondrial genes indicating that these RNA seq reactions were from dead cells). The remaining 5,472 cells were used for analysis. K means clustering was used to define clusters. In Loupe Cell Browser, cells containing either *Rpl3* or *Rpl3l* were selected for further analysis to compare gene expression between the two cell populations. Genes with low average expression (<1 count on average) were discarded. For cell type determination, we used the genes that were found by Linscheid et al. to be the most differentially expressed in each cell type. To be defined as a specific cell type

cluster, the cluster had to have all or most of the following genes as their most differentially expressed genes: sinus node myocytes: *Myh6*, *Ctnna3*, *Ryr2*, *Rbm20*, *Dmd*, *Ttn*, and *Tbx5*; fibroblasts: *Coll1a1*, *Fbn1*, *Ddr2*, *Lama2*, *Lamc1*, *Pcsk6*, *Gpc6*, *Mecom*, *Rbms3*, and 4930578G10Rik; macrophages: *Maf*, *F13a1*, *Cd163*, *C3ar1*, *P2yr6*, *Mrc1*, *Mgl2*, *Adgre1*, and *Dab2*; vascular endothelial: *Ptprb*, *Icam1*, *Vwf*, *Ldb2*, *Pecam1* and *Cdh13*; adipocytes: *Ucp1*, *Cidea*, *Prdm16*, *Pparg*, *Lep*, *Ghr*, *Slc1a5*, *Pde3b*, *Sorbs1*, *Acs11*, and *Adopr2*; endocardial: *Npr3*, *Cdh13*, *Engm* *Hmcn1* and *Gmds* and epicardial cells: *Wt1*, *Rbfox1*, *Kcnd2*, *Grip1*, *Plxna4* and *Syne2*.

3.2.6 Quantitative Proteomics

The mass spectrometry proteomics data was downloaded from the ProteomeXchange Consortium via the PRIDE repository (<https://www.ebi.ac.uk/pride/>). Dataset for mouse SAN cells (PXD008736) include 6 samples with 12 fractions per sample performed in technical duplicate. Raw MS data were analyzed using MaxQuant v1.6.8.0 (Max-Planck Institute of Biochemistry, Department of Proteomics and Signal Transduction, Munich, Germany). Peptide search was performed using the UniProt reference proteome for *Mus musculus* (Proteome ID UP000000589). False-discovery rate (FDR) was set to 1% for peptide, protein, and side decoy identification with base FDR calculated on delta score. Unmodified, unique and razor peptides were used for protein quantification to address high amino acid sequence similarity between paralogous proteins. All other parameters were kept at default. To ensure that sensitivity was adequate and that the cells isolated were SAN, we quantified intensity of CTNNA3 and

HCN4 and eliminated any samples that did not exhibit a significant quantity for each of these proteins. The remaining samples were used to quantify RPL3 and RPL3L intensity.

3.2.7 Echocardiography

Transthoracic echocardiography was performed using the Visual Sonics 3300 imaging system equipped with 30-MHz probe. Mice underwent transthoracic echocardiography, under light anesthesia (inhaled isoflurane, 1-2%), with heart rate (350-500 beats per minute) and core temperature (37 °C) continuously monitored. The heart was visualized in 2D from modified parasternal long axis and short axis views. The left ventricular dimensions and calculated left ventricular ejection fraction (EF) were measured from the short axis M-mode display. All measurements were obtained in triplicate and averaged. The sonographer was blinded to animal genotype during imaging and analysis.

3.2.8 Electrocardiography

Mice were anesthetized by continuous isoflurane (2-4%) inhalation until unresponsive to paw pinch. A small abdominal incision was made and a telemetry probe (Data Science International, TA11ETA-F10) was implanted in the peritoneal cavity under aseptic conditions. The two ECG leads were secured near the apex of the heart and the right acromion. Mice were housed singly and given seven days to recover from the surgery before data collection. The implanted telemetry was used to measure core body temperature and electrocardiography (ECG). ECG data was collected for 24 h/day for 2

weeks and subsequently analyzed on Ponemah DSI telemetry software. Ventricular rate represents an average of three days' worth of data for each animal with a logging rate of fifteen minutes. For QRS and PR interval, a section of clean data was found during the inactive period and 150 individual beats were averaged for each animal. Heart rate during the isoproterenol challenge was obtained with a logging rate of one minute. Mice were monitored for one week and then were given a single injection of isoproterenol (ISO, 30 mg/kg, USP) and then monitored for another week post-injection. Representative traces were taken immediately after isoproterenol injection.

3.2.9 Statistics

Unless stated otherwise, unpaired Student's t-test was performed to determine if significant ($p < 0.05$) difference existed between WT and KO genotypes for the dependent variable under consideration. A two-way ANOVA was used to determine if there were significant differences between WT and KO genotype in heart rate in response to isoproterenol. A one-way ANOVA was used to determine if there was a significant difference in the rate of change in heart rate between WT and KO genotype following isoproterenol treatment and protein abundance relative to RPL3L abundance in the sinus atrial node as determined by quantitative proteomics.

3.3 Results

3.3.1 Atria and Ventricular Expression of RPL3L

We reported *Rpl3l* mRNA was approximately 2.5-fold higher than *Rpl3* mRNA in the heart (Chaillou, Zhang et al. 2016). In light of the findings reported by Thorolfsson and coworkers that Rpl3l coding variants increased risks for atrial fibrillation we wanted to determine the expression levels of *Rpl3l* and *Rpl3* in the atria and ventricles of the heart. qPCR analysis showed *Rpl3l* was significantly higher than *Rpl3* expression in the ventricles in WT mice (Fig. 8A). In the atria, the expression pattern was the opposite to the ventricles, where *Rpl3* expression was significantly higher than *Rpl3l* which was almost undetectable (Fig. 8B). In agreement with the mRNA expression pattern, Western blot analysis showed RPL3L was highly expressed in the ventricles, but almost undetectable in the atria (Fig. 8C).

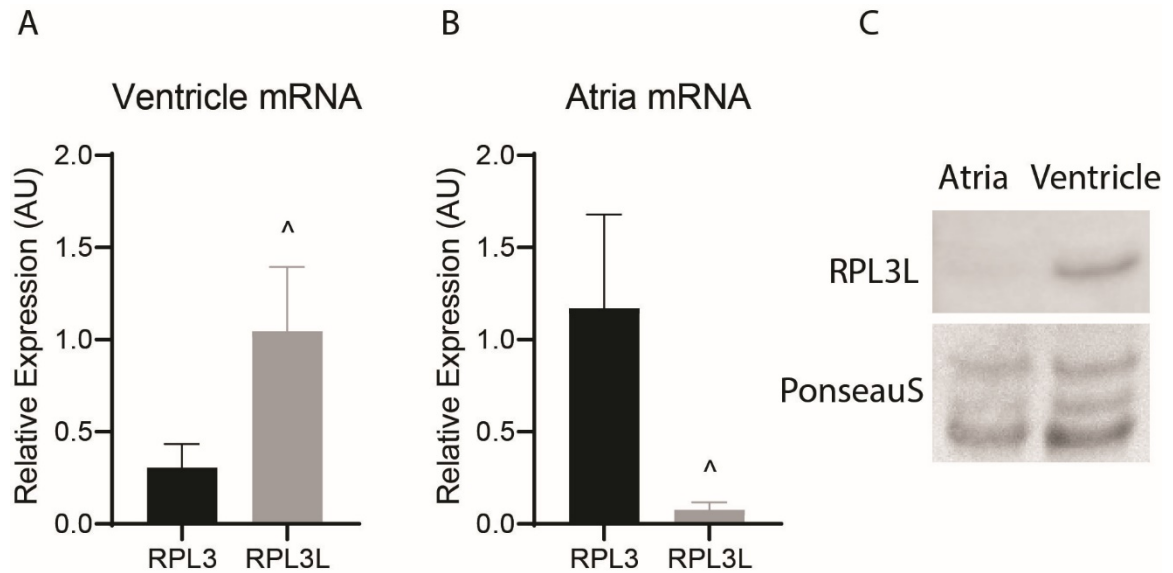


Figure 8. Ventricular specific expression of RPL3L.

A-B, qPCR analysis of ventricle samples showed *Rpl3l* mRNA expression was significantly higher than *Rpl3* expression whereas in the atria, *Rpl3l* mRNA expression was significantly lower than *Rpl3* expression (N=4). C, In agreement with mRNA results, Western blot analysis showed RPL3L expression was ventricular-specific. Data are expressed as mean \pm SE with significant difference designated by [^] ($p < 0.001$).

3.3.2 Echocardiography and Electrocardiography

To determine whether the loss of *Rpl3l* expression in the heart altered cardiac function, we performed echocardiography in WT and KO mice under anesthesia. We observed no significant difference on heart rate (Fig. 9A, $p > 0.05$), ejection fraction (Fig. 9B, $p > 0.05$), or left ventricular wall thicknesses (Fig. 9C, systole $p > 0.05$; Fig. 9D,

diastole $p > 0.05$) between the WT and KO mice. We also observed no difference in calculated cardiac output, fractional shortening, left ventricular mass, left ventricular volume during systole and diastole, and stroke volume between the two groups (Table 1). To determine if the electrical activity of the heart was altered in the KO, ECG probes were implanted to allow for continuous recording of electrical activity. There was no difference between WT and KO for ventricular rates ($p = > 0.05$, Fig. 10 A,D), QRS length ($p = > 0.05$, Fig. 10 B,D) or PR interval ($p = > 0.05$, Fig. 10 C,D). When treated with isoproterenol, both WT and KO mice showed a significant increase in heart rate (both $p = < 0.05$, Fig. 10 E-F), but the rate of response to isoproterenol in the KO was significantly higher in comparison to WT (Fig. 10 G).

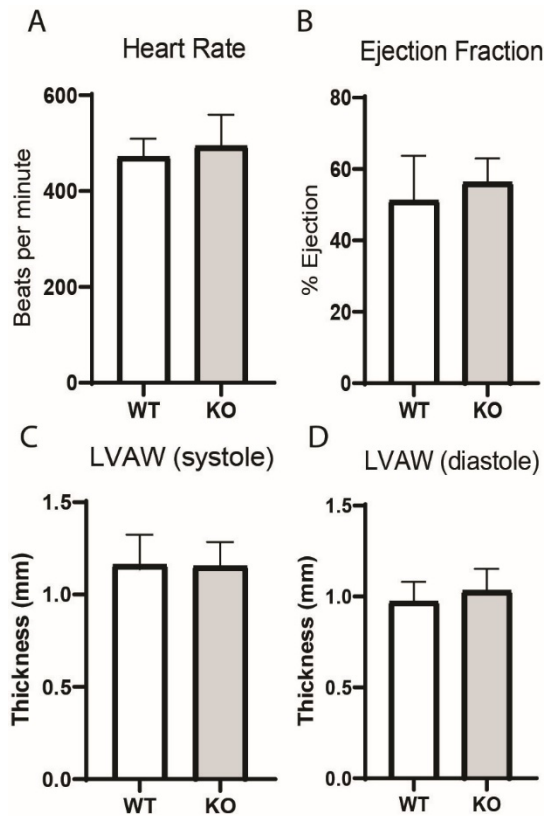


Figure 9: Loss of RPL3L does not affect cardiac function. Echocardiography revealed no difference in cardiac function between WT and KO mice. A, heart rate; B, ejection fraction; C-D, left ventricular wall thickness during systole or diastole. Data are expressed as mean \pm SE (n=10-17/genotype).

Table 1: Echocardiography.

<i>Metric</i>	<i>WT</i>	<i>KO</i>	<i>P value</i>
Cardiac output (mL/min)	22.00 \pm 4.40	24.42 \pm 4.58	>0.05
Fractional Shortening (%)	25.72 \pm 6.99	28.20 \pm 4.14	>0.05
Mass Anterior Wall (corrected, mg)	153.18 \pm 30.86	152.55 \pm 16.82	>0.05
Volume (systole, μ L)	48.67 \pm 17.47	42.16 \pm 9.90	>0.05
Volume (diastole, μ L)	95.39 \pm 18.33	91.27 \pm 12.57	>0.05
Stroke Volume (μ L)	46.72 \pm 9.51	49.11 \pm 4.52	>0.05

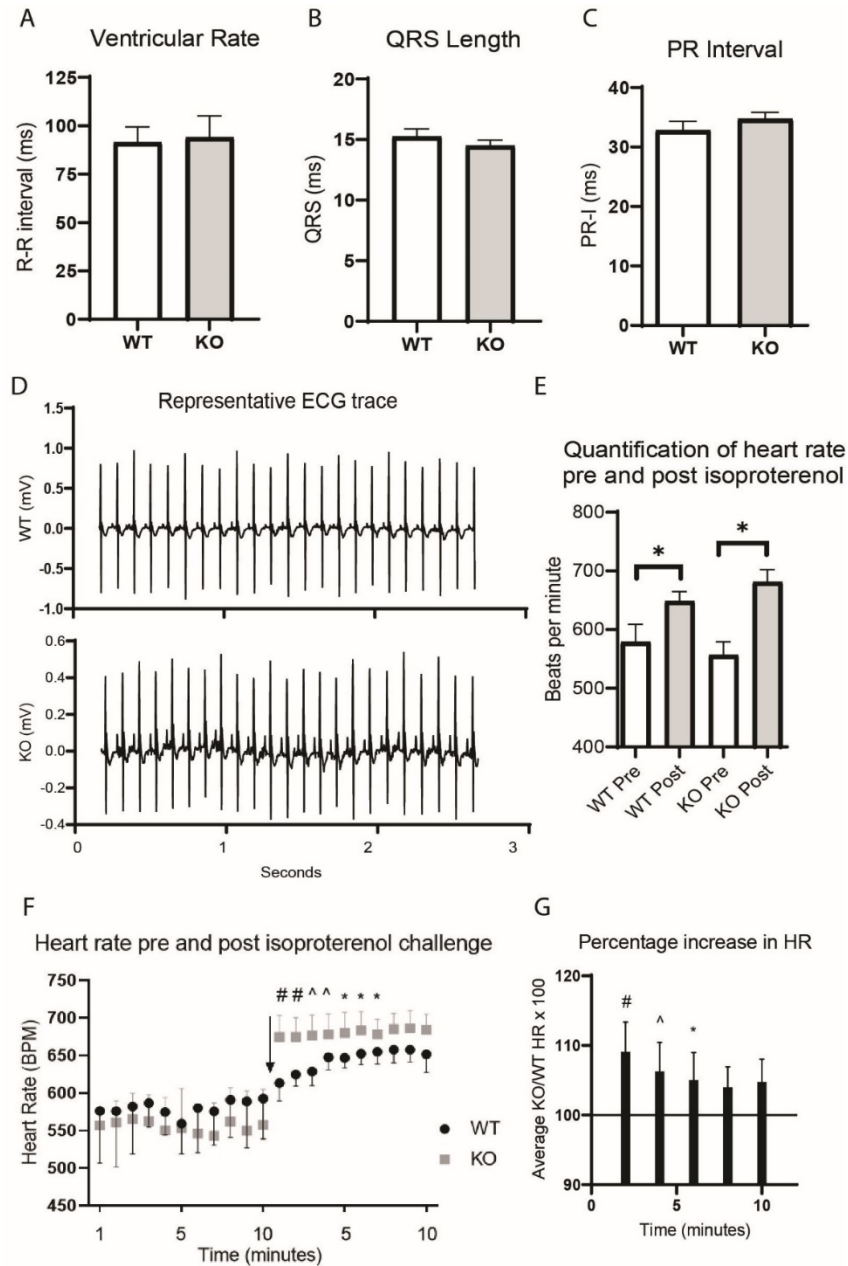


Figure 10: Electrical activity of the heart in WT and KO mice.

Electrocardiography showed no difference in A, ventricular rate; B, QRS length; and C, PR interval between WT and KO mice. D, representative ECG trace of WT and KO mice show minor variations which are typical of mouse ECGs. E, isoproterenol treatment significantly increased heart in both WT and KO mice. F, the rate at which heart rate increased was significantly greater in KO compared to WT; G, the rate of heart rate increase was determined by averaging the heart rate at two-minute intervals and then normalized to WT heart rate. Data are expressed as mean \pm SE (n=4-5/genotype) with significant difference designated as # $p < 0.0001$, ^ $p < 0.001$, * $p < 0.05$.

3.3.3 Single Cell RNA Sequencing of the SAN

Given the enhanced response to isoproterenol in the KO, and the reported association of AF and *Rpl3l* variants, we took advantage of a recently published scRNA-seq dataset from isolated SAN cells to determine the expression pattern of *Rpl3l* and *Rpl3* in the SAN (Zhang, Butters et al. 2012, Linscheid, Logantha et al. 2019). As shown in Fig. 11, t-distributed stochastic neighbor embedding (t-SNE) representation revealed that, of the 5,472 cells analyzed, only 203 were classified as sinus node myocytes based on the expression of *Myh6*, *Ctnna3*, *Ryr2*, *Rbm20*, *Dmd*, *Ttn* and *Tbx5*. In addition to these myocytes, five other distinct cell-types were identified including fibroblast, epicardial, endocardial, macrophage, adipocyte and an undefined cluster. *Rpl3l* transcript was only detected in approximately 1% (59/5472) of the cells and was not exclusive to one particular cell-type. Within sinus node myocytes, *Rpl3l* transcript was detected in ~10% (22/203) of the cells. However, with only ~10% of SAN cells expressing *Rpl3l*, its expression is similar to that seen in the atria but very low relative to the ventricles.

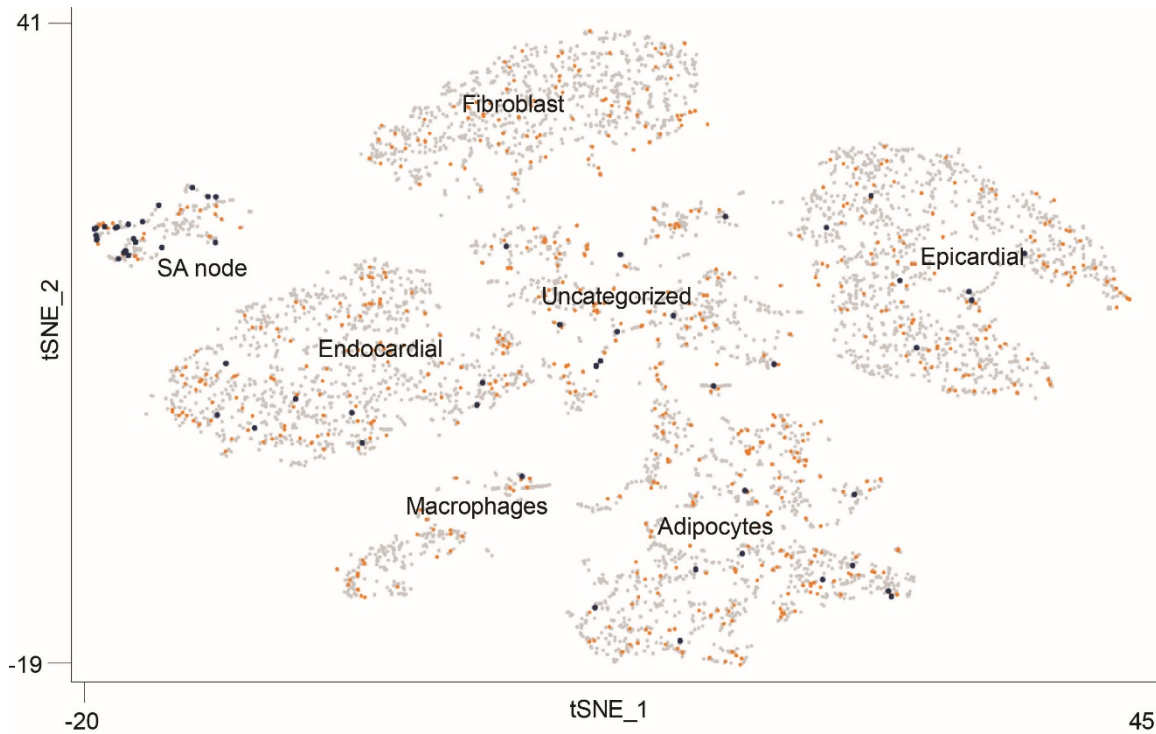


Figure 11: Low expression of *Rpl3l* in sinoatrial node.

t-distributed stochastic neighbor embedding (t-SNE) plot of single-cell nuclear RNA-seq data identified seven cell clusters including myocyte, fibroblast, epicardial, endocardial, macrophage, adipocyte and an undefined cluster. Cells expressing *Rpl3l* or *Rpl3* are indicated by blue or orange, respectively. *Rpl3l* transcript was detected in approximately 1% (59/5472) of the cells and was not exclusive to one particular cell-type. Within sinus node myocytes, *Rpl3l* transcript was detected in ~10% (22/203) of the cells.

3.3.4 Quantitative Proteomics

In addition to scRNA-seq analysis, Linscheid and colleagues also performed quantitative proteomics of the SAN (Linscheid, Logantha et al. 2019). Given RPL3L and RPL3 are 78% identical at the amino acid level, we re-analyzed the proteomic dataset paying particular attention to unaligned reads and using a less stringent cut-off for abundance. As shown in Fig. 12, RPL3L peptide abundance was 0.6% of RPL3 peptide

abundance in agreement with *Rpl3l* qPCR and scRNA-seq results demonstrating extremely low expression of *Rpl3l* transcript and protein in the atria. Despite SAN myocytes being ~3% of the cells (as shown by scRNA-seq) of the isolated tissue, proteomic analysis was sensitive enough to reliably detect the SAN specific proteins, HCN4 and CTNNA3, indicating low abundance of RPL3L peptides was not caused by a lack of sensitivity (Fig. 12).

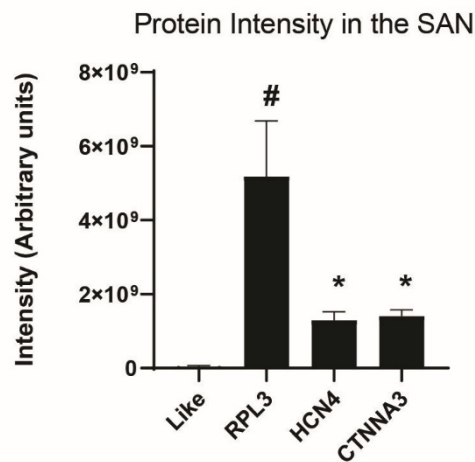


Figure 12: RPL3L barely detectable in sinoatrial node.

Quantitative proteomics showed RPL3L peptide abundance in the sinoatrial node was 0.6% of RPL3 peptide abundance in agreement with *Rpl3l* qPCR and scRNA-seq results demonstrating extremely low expression of *Rpl3l* transcript and protein in the atria. Despite sinus atrial node (SAN) myocytes being less than 3% of the cells (as shown by scRNA-seq) of the isolated tissue, proteomic analysis was sensitive enough to reliably detect the SAN specific proteins, HCN4 and CTNNA3, indicating low abundance of RPL3L peptides was not caused by a lack of sensitivity. Peptide intensity of RPL3, RPL3L, HCN4 and CTNNA3 from cells of the sinoatrial node. One-way ANOVA was used to determine significance of all genes compared to RPL3L with significant difference designated by # $p < 0.0001$, * $p < 0.05$.

3.4 Discussion

3.4.1 Summary of Findings

A major finding of this study was the ventricular-specific expression of RPL3-like (RPL3L) in the mouse heart - a finding that agrees with human expression data (Uhlen, Fagerberg et al. 2015). A second major finding of the study was that the loss of *Rpl3l* expression did not affect either the function or electrical activity of the heart in adult male mice. Repeat analysis (with modification) of previously published scRNA-seq and quantitative proteomics of mouse SAN tissue, with a focus on cells expressing *Rpl3l*, revealed that *Rpl3l* was only expressed in ~12% of the cells analyzed and that RPL3L was barely detectable in SAN tissue as determined by mass-spectrometry. We conclude that the atrial fibrillation phenotype observed in humans with a mutation in *Rpl3l* is not due to its expression in the atria or the sinoatrial node.

3.4.2 Tissue Specificity

During the course of characterizing the polycystic kidney disease gene region, Burn and coworkers identified *Rpl3l*, a gene with 74% nucleotide sequence identity to the *Rpl3* gene, which was subsequently shown to be exclusively expressed in skeletal muscle and the heart (Van Raay, Connors et al. 1996). More recent studies have confirmed the muscle-specific expression of *Rpl3l* mRNA in humans and found that of all the ribosomal proteins, *Rpl3l* showed the highest degree of tissue-specificity (Gupta and Warner 2014, Guimaraes and Zavolan 2016). Proteomic analysis of human fetal (17-23 weeks of age) heart revealed RPL3L was the most significantly enriched ventricular-

specific protein (relative to atria expression) which also included such other proteins as myosin light chain 5 (*Myl5*), monocarboxylate transporter 1 (*Slc16a1*) and calcineurin-like phosphoesterase domain-containing protein 1 (*Cpped1*) (Lu, Sinha et al. 2014). Similar to skeletal muscle during postnatal development, *Rpl3l* expression was significantly upregulated in the ventricle; in fact, from P1 thru P23, *Rpl3l* was second to *Hmcn2* as the most significantly upregulated gene in the ventricle (Cheng, Merriam et al. 2004, Talman, Teppo et al. 2018). In contrast, the expression of *Rpl3* during this time period was down-regulated by approximately 50%, similar to what is observed in skeletal muscle and, more broadly, reflects the often coordinated, inverse pattern of expression observed between ribosomal protein paralogs (Xue and Barna 2012).

3.4.3 Possible Roles of RPL3L

Besides our earlier study describing a possible role for *Rpl3l* in skeletal muscle hypertrophy, very little is known about the function of *Rpl3l*; however, in contrast, the function of *Rpl3* has been studied in great detail (Meskauskas, Petrov et al. 2005, Meskauskas and Dinman 2007, Russo, Esposito et al. 2013, Al-Hadid, Roy et al. 2016, Pagliara, Saide et al. 2016). As the first ribosomal protein predicted to interact with the ancestor of the large ribosomal subunit, it is not surprising then that RPL3 has a fundamental role in ribosome function, i.e., peptidyl transferase activity, and pre-rRNA processing (Meskauskas, Harger et al. 2003, Meskauskas and Dinman 2007, Poll, Braun et al. 2009, Caetano-Anolles and Caetano-Anolles 2015, Al-Hadid, Roy et al. 2016). These studies detailing the function of RPL3, raises several fundamental questions about RPL3L. Why has the ventricle and skeletal muscle evolved its own version of such an

ancient and fundamental ribosomal protein? What is so unique about the ventricles that requires them to have their own version of RPL3? Based on the high-degree of amino acid conservation (~80%) between RPL3 and RPL3L, it is reasonable to suggest that RPL3L performs similar, but distinct, functions as RPL3 (Van Raay, Connors et al. 1996). Early work on skeletal muscle ribosomes suggested the large size of myosin mRNA might require unique polyribosome structure to effectively translate such a large protein (Breuer, Davies et al. 1964). Could it be that RPL3L alters ribosome function in such a way that the ribosome is able to more effectively (e.g., initiation, fidelity, and/or processivity) translate large mRNAs? We now know that there are much larger sarcomeric proteins than myosin (223 kDa) found in the ventricles, including dystrophin (426 kDa), nebulin (801 kDa), obscurin (832 kDa) and the largest protein in the body, titin (3,906 kDa). While this idea remains to be rigorously tested, the evolution of a ventricular-specific version of such an important ribosomal protein suggests a better understanding of *Rpl3l* function will reveal novel insight regarding translation in striated muscle.

3.4.4 Phenotype of RPL3L KO Mice

If *Rpl3l* is so important, why did we not observe a more dramatic phenotype in the KO mouse? The lack of a cardiac phenotype was likely masked by compensation by *Rpl3*. RPL3 and RPL3L are ~80% identical at the amino acid level and hence it is reasonable to assume that these paralogs share some similar ribosomal functions, thus allowing RPL3 to functionally compensate for the loss of RPL3L in the KO. Although the upregulation of a paralog, or gene family member, in response to gene KO is well-

known in the literature, the compensation of *Rpl3* for *Rpl3l* further highlights the potential limitation of using a KO strategy to study gene function. Future studies will require using a knockin strategy to introduce mutations into the *Rpl3l* gene loci, such as those identified by Thorolfsson and coworkers, to study the connection between *Rpl3l* and AF (Thorolfsson, Sveinbjornsson et al. 2018). Finally, another possible factor as to why we did not observe a more robust cardiac phenotype in the KO is the resiliency of the mouse. For example, diseases which are life-threatening to humans, i.e, Alzheimer's disease and Duchenne Muscular Dystrophy do not dramatically affect longevity in the mouse.

3.4.5 Possible Roles of RPL3L in Atrial Fibrillation

The ventricular-specific expression of *Rpl3l* has important implications for the possible role that *Rpl3l* might have in the etiology of AF. The study by Thorolfsson and colleagues generated a great deal of interest because, unlike previous studies which had mostly identified non-coding sequence variants, these authors identify missense and splice-donor variants in *Rpl3l* which showed a significant association with AF (Thorolfsson, Sveinbjornsson et al. 2018). Given the ventricular-specific expression of *Rpl3l*, it is not readily apparent how mutations in *Rpl3l* might give rise to AF. AF can be caused by either an atrial pathology (like fibrosis, remodeling, or aberrant electrical dysfunction) or can originate via a ventricular pathology (Grogan, Smith et al. 1992, Burstein and Nattel 2008, Ling, Kistler et al. 2012, McGann, Akoum et al. 2014). Chronic heart failure is one such ventricular pathology that leads to increased incidence of AF (Ehrlich, Nattel et al. 2002, Santhanakrishnan, Wang et al. 2016). While some

argue that AF arises first and then leads to heart failure, Vermes et al., published a study which clearly showed AF often arose after ventricular dysfunction had been established (Vermes, Tardif et al. 2003). If left untreated, 24% of patients with ventricular dysfunction developed AF within 4 years (Vermes, Tardif et al. 2003). Patients with arrhythmogenic right ventricular pathologies also suffer high instances of abnormal electrical activity in the atria and atrial remodeling (Platonov, Christensen et al. 2011, Wu, Guo et al. 2016). Based on the findings from the current study, we speculate that the AF observed in patients with RPL3L mutations may reflect a ventricular pathology given that RPL3L protein is not detected in the atria or the SAN at physiologically relevant levels but is highly expressed in the ventricle. Determining how mutations in a ventricular-specific protein can promote AF will be an important focus for future research.

An alternative theory is that a subpopulation of the SAN expresses RPL3L but makes up such a small fraction of cells in the SAN that the signal is insufficient for detection. Although the SAN is spoken about as though it is a homogenous entity, there are 3 major morphological variations in cells that make up the node. There are short spindle cells that are primarily mononucleated, elongated spindle cells that extend up to 80um, and spider cells that are irregularly shaped (Verheijck, Wessels et al. 1998). Although these cell subtypes, show enrichment in regions of the SAN, they are not exclusive to any one area. There are also regional differences in the electrical activity of the SAN with cells near the periphery showing increase in upstroke velocity and overshoot verses the central cells show slower recovery of excitability (Kodama and Boyett 1985). It is possible that a subset of cells from any one of these categories

expresses RPL3L but that the protein level of that population was too low to detect when incorporated with the other populations of SAN cells and non-SAN cell types. Knowing if RPL3L and RPL3 are differentially expressed in the cells of the sinoatrial node would help to inform the relevance of RPL3L mutations causing atrial fibrillation and possibly help elucidate the role of RPL3L.

3.4.6 Genome Wide Association Studies

Genome-wide association studies are valuable because if a trait is known to be influenced by a gene, gene variant, or set of genes, this knowledge can be used to further research the trait. However, not all correlated genes or gene variants are causal for any particular trait. Quite often there can even be reverse causal effects or confounding effects that prevent researchers from truly discerning important genetic traits (Zhu, Zheng et al. 2018). While there are some models that allow researchers to better discriminate between correlation and causation, these methods are susceptible to a high rate of directional error (ie showing a causal effect rather than the loss of a gene or gene variant showing a causal effect) with increasing sample size (Hemani, Tilling et al. 2017). It is possible that variants in *Rpl3l* and atrial fibrillation are not causal and are mere correlations. To truly investigate this possibility a mouse model of the human *Rpl3l* variant would be necessary.

CHAPTER 4. REFLECTIONS AND LOOKING AHEAD TO FUTURE STUDIES

4.1 Reflections

Research efforts in this dissertation were designed to investigate the role of RPL3L in cardiac tissue. The specific objectives were to 1) determine the expression of RPL3L in the heart, 2) determine if there were functional cardiac abnormalities in its absence and 3) to determine if RPL3L associated ribosomes exhibited translational alterations.

Although cardiac tissue is one of few organs that expresses RPL3L, its function and exact expression pattern in the heart has not been well documented. Understanding the role that RPL3L plays in cardiac function may inform molecular aspects of pathological processes in the heart, such as cardiac hypertrophy or the possible role of translation in the development of cardiac fibrosis (Hannan, Stefanovsky et al. 1996, Chothani, Schafer et al. 2019). The importance of the ribosome and ribosomal composition in particular, have historically been understudied in the heart despite the role of translation in cardiac hypertrophy and fibrosis through the synthesis of proteins required for both of those pathological processes. In an effort to better understand the role of the ribosome and translational processes specific to the heart we must first understand how ribosomal composition affects translation in the heart under non-pathological conditions.

4.1.1 The Translatome

The focus of Chapter 2 was to determine if the loss of RPL3L affected cardiac translation as assessed by polysome composition. I found that out of 16,643 mRNAs that were detected, only 216 were differentially enriched in the translating fraction indicating that RPL3L had a modest effect on translation in the ventricles of the heart. Interestingly, I found that cardiac tissue of the RPL3L KO showed a higher correlation between polysome transcript abundance to whole-cell transcript abundance (translatome: transcriptome) than WT (Ch. 2, Fig. 3). This finding indicates there are likely alterations in translation in the KO that are not captured by the polysome fractionation. A limitation of polysome fractionation method I used was the inability to detect changes in translation with single ribosome resolution as is possible with Ribo-seq method. Traditional Ribo-seq is done by performing RNA sequencing on each individual, ribosome protected mRNA fragment. While Ribo-seq can be technically challenging, it does allow one to more precisely measure the level of translation for each detected mRNA. Although the technique I used cannot differentiate between mRNAs containing 2-4 ribosomes, from mRNAs containing 5+ ribosomes, it is the only way to assess the relationship between total mRNA and total translated mRNA. I hypothesize that if true Ribo-seq was done on the ventricles of KO mice, that the most differentially translated mRNAs would be transcripts that are enriched in striated muscle and that WT would show a relative depletion in those transcripts.

4.1.2 Calcium Handling and Cardiac Function

Investigation of the role that *Rpl3l* plays in calcium handling demonstrated that there were differences in calcium tolerance, and disrupted t-tubules in KO cardiomyocytes. Although we were not able to measure calcium directly we were able to demonstrate differences in response to increasing levels of calcium in dispersed cardiomyocytes (Ch. 2, Fig. 6). Interestingly, we found that the 3 mRNAs that were the most differentially spliced between WT and KO were involved in calcium handling: *Nnat*, *Asph*, and *Dmpk*. While these results do not definitively show a connection between splicing and calcium handling they point to a possible mechanism by which the WT transcriptome helps to regulate calcium homeostasis. We also looked at t-tubule morphology and found that KO mice had significantly more disrupted t-tubules than WT mice. Because t-tubule integrity is important for calcium homeostasis, this disruption in t-tubule morphology (and possibly t-tubule integrity) could account for alterations in calcium tolerance between WT and KO mice.

I also found that KO mice exhibit a heightened response to isoproterenol treatment. WT and KO mice showed no difference in cardiac function under resting conditions but when challenged with isoproterenol, KO mice had a more rapid response. Although no other data points to a possible mechanism by which RPL3L mice would be highly sensitized to isoproterenol, I speculate that calcium mishandling leads to this altered response through heightened intracellular calcium.

4.1.3 Atrial Fibrillation

As presented in Chapter 3, I explored the possibility that RPL3L has a role in atrial fibrillation; however, I found that RPL3L is not expressed in the atria and the RPL3L KO mouse showed no signs of atrial fibrillation or any overt cardiac abnormalities under resting conditions. Interestingly, RPL3L KO mice exhibited a heightened response to the beta-adrenergic agonist, isoproterenol. I reasoned that perhaps the alteration in responsiveness to adrenergic stimulation might be due to loss of RPL3L in the sinoatrial node. To test this hypothesis, I reanalyzed previously published single-cell RNA sequencing, and proteomic data from sinoatrial node (SAN) cells of mice. I found that although there were cells within the SAN that expressed RPL3L at the mRNA level, the same was not reflected at the protein level. Although nothing is known of RPL3L in the human SAN, human protein atlas confirmed that humans do not express RPL3L in the atria, suggesting that atrial fibrillation associated with variants of *Rpl3l* is likely due to a ventricular pathology.

To further investigate the possible role of *Rpl3l* variants in the development of atrial fibrillation, it would be valuable to generate RPL3L mutant mice which harbored the different *Rpl3l* mutations described in humans associated with a higher incidence of atrial fibrillation (Thorolfsdottir, Sveinbjornsson et al. 2018). Such a mouse model would help to circumvent a limitation of our RPL3L KO mouse – compensation by RPL3 which likely masked any possible cardiac phenotype resulting from loss of RPL3L expression. I speculate that if an RPL3L mutant model was made, aged mice would develop atrial fibrillation.

4.2 Future Directions

As with any research, answering questions only leads to more questions, and this project was no exception. While there is a lifetime of work that needs to be done to fully elucidate the role of RPL3L in striated tissue a few key experiments are listed below.

4.2.1 Ribo-seq

In the present work, I found that isolating the entire translational fraction to assess changes in polysome composition identified 216 mRNAs that were significantly different between WT and KO while accounting for differences in transcription. Ribo-seq, however, represents a more granular approach which would lead to a more robust list due to being able to quantify minute changes in translation. Using this technique would broaden our knowledge in three key ways. First, it would give us the ability to quantify exact number of ribosomes per mRNAs. This information would allow us to distinguish between high and low transcribed transcripts as well as determine if RPL3L has any role in initiation, elongation and processivity of translation.

4.2.1.1 Initiation

Some alterations in initiation can be due to 5'-UTR motifs, but changes in initiation can also indicate that the ribosome itself is not competent for normal rates of initiation due to structural changes. Depletion of a ribosomal protein such as RPL3L may cause changes in ribosome structure which affect translation initiation. I have preliminary data from a cell-free translation assay showing that skeletal muscle ribosomes isolated from KO mice have significantly reduced cap-dependent translation compared to WT

ribosomes. One explanation for this finding is the loss of RPL3L negatively affects the ability of the ribosome to effectively initiate translation.

4.2.1.2 Elongation

Using Ribo-seq elongation could also be assessed and possibly inform the function of RPL3L. For instance, ribosomes will often pause on unusual codons or misincorporate an amino acid. However, it is possible that having a specialized ribosome could mitigate pausing time and decrease the rate of mis-incorporation. Using Ribo-seq coupled to proteomics, it would be possible to inspect pause time of the ribosome on mRNA by statistical analysis of ribosome fragments found with a specific codon at the P site.

4.2.1.3 Processivity

In the context of translation, processivity refers to the ribosomes ability to continue translating without releasing from the transcript during translation of a single mRNA. By using Ribo-seq it would be possible to look at the location of ribosome protected fragments to learn about processivity rates of WT and RPL3L KO ribosomes. If ribosome protected fragments are found in the beginning of the message at high levels but then decrease along the length of the message, it is possible that the ribosome may have compromised processivity.

4.2.2 Muscle Function

In addition to the experiment described above a pivotal experiment would be to test the muscle function of WT and RPL3L KO mice. Although I did do grip strength testing in mice and found no significant difference between the genotypes, these results are confounded by 2 variables, the willingness of the mouse to hold on to the force transducer, and the experimenter's consistency in force and acceleration of pull. I would argue that the ideal muscle function test should be done *ex-vivo* in skeletal muscle and the heart, without the additional confounding variables of pinnation angles in muscle and tendon elasticity. By doing this experiment in WT and KO mice, especially coupled to Ribo-seq, we could determine if there are translational changes that leads to loss of contractility. I speculate that enhanced translation of sarcomeric transcripts would be reflected in functional muscle testing. This hypothesis is supported by preliminary data indicating that RPL3L KO mice have enhanced specific force in the extensor digitorum longus muscle.

4.2.3 Sinoatrial Node Subpopulations

Chapter 3 describes the expression pattern of RPL3L in the heart and shows some expression of *Rpl3l* mRNA in the SAN; however, the expression of the RPL3L protein was expressed just above the level of detection. Worthwhile experiments would include a more detailed examination of the SAN. Although the SAN is spoken about as though it is a homogenous entity, there are three morphologically distinct cell types within the node, and there are physiological differences in electrical function in cells at the center verses the periphery. Cells at the periphery show upstroke velocity, overshoot, and maximum

diastolic potential were increased relative to the centrally located SAN cells.

Alternatively, the centrally located cells of the SAN showed slower recovery of excitability. These electrical changes indicate that there could be some functionally significant, non-redundant role that both areas play and that those cells require RPL3L for optimal functioning. Although RPL3L protein was found in the SAN at extremely low, it is possible that this small amount of protein was specific to a certain cell type within the SAN. Such an expression pattern could explain both the connection between RPL3L mutations and atrial fibrillation, and the enhanced adrenergic response to isoproterenol observed in the RPL3L KO.

APPENDICES

Supplemental Table 1: Genes with significantly different cardiac polysome abundance between WT and KO mice.

Supplemental Table 1.			
Note: Values represent normalized expression to whole-cell transcript abundance (translatome/transcriptome) (n=3/genotype)			
Gene Symbol	WT	KO	p-value
Bzw1	2.92	6.16	0.047
Mrpl50	2.83	4.95	0.046
D330023K18Rik	2.65	1.5	0.023
Sms	2.52	4.46	0.041
Chmp5	2.2	4.59	0.046
Fbxo22	2.13	3.6	0.037
Rab5a	2.07	5.48	0.039
Sf3b1	2.07	4.01	0.029
Gbp6	2.05	4.05	0.018
Lin52	1.99	3.1	0.049
C1d	1.98	3.93	0.048
Spink4	1.86	1.01	0.036
Glr5	1.78	1.36	0.049
Eif4a2	1.76	3.82	0.026
Klf4	1.75	3.07	0.043
Ttc33	1.71	2.98	0.05
Pnkd	1.71	1.32	0.05
Atg10	1.69	3.84	0.024
Zfp715	1.68	3.24	0.025
Ifitm1	1.66	0.79	0.017

Supplemental Table 1 (continued)			
Gene Symbol	WT	KO	p-value
Bud31	1.65	2.29	0.04
Gpalpp1	1.61	1.33	0.037
Hnrnpu	1.61	2.96	0.045
Nampt	1.6	3.09	0.027
Atcayos	1.6	0.9	0.015
Uso1	1.55	2.9	0.042
Paip1	1.54	3.01	0.039
E130311K13Rik	1.51	3.15	0.033
Pnizr	1.5	2.38	0.045
Tex38	1.48	1	0.019
Nupr11	1.47	0.75	0.008
Rab9	1.46	4.27	0.045
Arglu1	1.46	2.17	0.05
Gipc2	1.45	2.29	0.018
Phkb	1.45	3.08	0.049
Stx12	1.44	2.29	0.048
Cav1	1.43	2.96	0.036
AI839979	1.4	2.22	0.04
Eif1a	1.4	2.46	0.047
Zfp830	1.39	2.13	0.022
Serbp1	1.38	2.45	0.042
Ptgr2	1.38	2.56	0.046
Adss	1.38	2.28	0.049
Sec62	1.37	2.96	0.043
Arhgef6	1.37	1.9	0.032

Supplemental Table 1 (continued)			
Gene Symbol	WT	KO	p-value
Appl2	1.37	1.85	0.048
Ranbp9	1.36	3.15	0.026
Ublcp1	1.32	2.68	0.049
Mrps10	1.31	1.1	0.004
Son	1.31	1.68	0.03
Ell2	1.3	2.63	0.037
Hist1h1e	1.29	0.84	0.045
Gng11	1.28	2.1	0.027
Dnaja2	1.27	2.39	0.032
Becn1	1.26	2.11	0.049
Tmed5	1.26	2.48	0.047
Tmem147	1.26	0.95	0.027
Trmt5	1.24	2.26	0.033
Srsf5	1.23	2.25	0.02
Gm16062	1.23	1.9	0.012
Ebi3	1.22	0.89	0.044
Mpeg1	1.21	1.7	0.046
Rab33a	1.21	0.87	0.049
Nol12	1.2	0.93	0.016
Psmb9	1.2	0.89	0.012
Cdca3	1.19	0.91	0.025
Chm	1.19	2.61	0.044
Frs2	1.19	1.77	0.05
Vrk3	1.18	0.81	0.013
Smad1	1.16	1.77	0.01

Supplemental Table 1 (continued)			
Gene Symbol	WT	KO	p-value
Slc38a2	1.15	2.02	0.041
Dbt	1.15	2.26	0.044
Ptprcap	1.15	0.71	0.011
Fas	1.15	2.4	0.039
Ikzf5	1.15	2.31	0.03
Igsf23	1.14	0.8	0.042
Rnf149	1.13	1.97	0.014
Copz2	1.13	0.83	0.047
Cox8a	1.11	0.87	0.031
Ipo8	1.11	1.51	0.042
Krtcap2	1.11	0.85	0.035
Hnrnpc	1.11	1.81	0.042
Vps29	1.11	2.21	0.035
Lat2	1.1	0.82	0.012
Nxpe5	1.09	0.78	0.043
Ddx21	1.09	1.53	0.047
Dnttip1	1.08	0.84	0.032
Ddx46	1.08	1.52	0.05
Ddx3y	1.07	2.45	0.017
Zfp326	1.06	1.98	0.039
Hgsnat	1.06	1.24	0.049
Nrbf2	1.05	2.2	0.004
Dhrs7c	1.05	0.8	0.015
Spry2	1.05	2.09	0.049
43718	1.04	2.26	0.041

Supplemental Table 1 (continued)			
Gene Symbol	WT	KO	p-value
Zpr1	1.03	0.82	0.045
Nelfe	1.02	0.72	0.007
Rac3	1.01	0.77	0.027
Slc22a5	1	1.49	0.035
Tsacc	1	1.68	0.048
Sorbs1	0.99	1.87	0.039
2900009J06Rik	0.99	2.21	0.016
Tcea1	0.99	1.84	0.039
Fam89b	0.98	0.69	0.032
Copb2	0.96	1.72	0.038
Sec23ip	0.96	1.53	0.042
Cobll1	0.96	1.72	0.04
Clec12a	0.95	1.35	0.018
Cdkn1b	0.95	2.29	0.031
Mmaa	0.94	1.34	0.045
Calm1	0.94	1.68	0.029
Sh3bp1	0.94	0.69	0.013
Hnrnp2	0.92	1.72	0.022
Mrpl55	0.92	1.08	0.04
Ccl8	0.92	2.42	0.034
Agpat2	0.91	0.69	0.044
Ecd	0.91	1.09	0.049
Fgf1	0.91	1.22	0.02
Ndufaf6	0.91	1.55	0.038
Epc2	0.9	1.52	0.045

Supplemental Table 1 (continued)			
Gene Symbol	WT	KO	p-value
Hrnnpa3	0.89	1.62	0.022
Otud1	0.89	2.04	0.04
Habp2	0.89	0.72	0.038
Decr2	0.88	1.3	0.034
Napsa	0.88	0.69	0.044
Fars2	0.88	0.77	0.035
Metap1d	0.88	1.27	0.026
Eva1b	0.87	0.72	0.042
Sos2	0.87	1.39	0.049
Med18	0.87	1.15	0.038
Cenpt	0.87	0.63	0.002
Atpaf2	0.87	0.71	0.044
Agrn	0.86	1.05	0.028
Relt	0.86	0.65	0.049
Dld	0.86	1.96	0.036
Adpgk	0.86	1.12	0.03
Npl	0.86	1.13	0.032
Slc39a7	0.85	0.66	0.006
Cers4	0.84	1.03	0.047
Cma1	0.84	1.13	0.044
Fbxo33	0.83	1.32	0.018
Eif5a	0.83	0.73	0.03
Fam98b	0.82	1.53	0.047
Tlcl1	0.82	0.59	0.026
Rnf126	0.82	0.66	0.042

Supplemental Table 1 (continued)			
Gene Symbol	WT	KO	p-value
Prpf4b	0.82	1.35	0.05
Ggnbp2os	0.81	1.02	0.028
Psmab6	0.79	1.39	0.014
Snrpa	0.78	0.6	0.003
Ramp3	0.78	0.69	0.015
Faf1	0.78	1.16	0.019
AA467197	0.78	1.43	0.016
Xpnpep1	0.77	0.68	0.032
Ino80e	0.77	0.61	0.005
Clybl	0.77	1.1	0.023
Cd59a	0.76	0.99	0.046
Nmnat3	0.76	1.07	0.034
Mgmt	0.74	0.92	0.037
Loxl1	0.74	0.59	0.036
Rhoa	0.74	1.22	0.018
Cfd	0.74	0.88	0.002
Myl6b	0.74	0.46	0.035
Tspsy11	0.74	1.45	0.023
Hamp	0.73	1.04	0.048
Spout1	0.72	0.97	0.042
Tob2	0.72	1.31	0.043
Rasa4	0.72	0.59	0.046
Tbrg1	0.71	1.15	0.047
Faap20	0.71	0.83	0.008
Trim63	0.7	0.94	0.049

Supplemental Table 1 (continued)			
Gene Symbol	WT	KO	p-value
Rpp25	0.7	0.92	0.026
Dhdds	0.7	0.56	0.048
Arap3	0.68	0.79	0.038
Il18bp	0.68	1.08	0.034
Stap2	0.68	0.9	0.032
Colq	0.67	0.47	0.043
Nploc4	0.65	0.57	0.02
Lamc1	0.65	0.85	0.047
Maf	0.65	1.12	0.003
Hmga1b	0.64	0.47	0.029
Anxa6	0.63	0.54	0.042
Hgs	0.63	0.54	0.005
Arhgap10	0.62	0.52	0.035
Rtfdc1	0.62	0.52	0.017
Arrb2	0.62	0.71	0.041
Gpi1	0.61	0.51	0.012
Stab1	0.59	0.69	0.028
Dpp3	0.59	0.52	0.019
Polg	0.59	0.71	0.03
Xrcc1	0.59	0.64	0.041
Tpi1	0.59	0.5	0.035
Tmem208	0.57	0.75	0.003
Gmppb	0.57	0.67	0.025
Ctdnep1	0.56	0.51	0.042
Vps51	0.56	0.4	0.004

Supplemental Table 1 (continued)			
Gene Symbol	WT	KO	p-value
Coq8b	0.55	0.44	0.038
Ifi30	0.54	0.67	0.026
Rhot2	0.54	0.43	0
Gm5643	0.53	1.66	0.038
Rps4l	0.52	0.84	0.017
Gstt2	0.52	0.66	0.002
Anapc2	0.51	0.4	0.029
Chpf2	0.51	0.69	0.021
Tbcc	0.51	0.64	0.011
Hdac11	0.51	0.72	0.009
Inf2	0.5	0.58	0.021
Oas1a	0.49	0.71	0.033
Jsrp1	0.47	0.68	0.034
Coro1a	0.46	0.54	0.037
Snrpb	0.46	0.36	0.016
Map3k10	0.46	0.62	0.046
Plcd3	0.45	0.6	0.042
Clec2d	0.44	0.77	0.04
Insl3	0.39	1.07	0.015
Gm1821	0.19	0.39	0.012

Supplemental Table 2: Differentially expressed mRNAs in cardiac tissue between WT and KO.

Supplemental Table 2.			
Note: Values represent normalized expression to the geometric mean of four genes (Vcp, Rps6, Rpl38 and Gapdh).			
Gene Symbol	WT	KO	p-value
Ptgds	371.5	248.8	0.026
Rpl3l	181.8	52	0.006
Ninj1	123.7	92.6	0.038
Eif4a2	103.6	50.1	0.014
Selenom	99.1	69.6	0.046
Eif4g2	81.4	47.1	0.046
Ppp1cb	65.1	31.1	0.012
Calm1	60	35.4	0.01
Hnrnpk	56.2	33.2	0.036
Srsf5	49.7	26.2	0.024
Qk	48.4	26.9	0.036
Zmat5	39.1	29.1	0.017
Tspyl1	39	19.8	0.018
Rbm42	36.9	28.2	0.046
Mgmt	34.7	24.5	0.034
Pdia3	29.5	15	0.017
Ssb	28.2	15.1	0.031
Chmp2b	27	11.2	0.036
Nampt	26.4	13.5	0.041
C1qtnf4	26.3	16.9	0.046
Fgf13	25.5	14.4	0.023

Supplemental Table 2 (continued)			
Gene Symbol	WT	KO	p-value
Tmem219	23.3	17.1	0.042
Snape5	23.3	10	0.024
2310009B15Rik	23	10.8	0.048
Ddx24	22.5	19.5	0.008
Tob1	22.2	10.9	0.041
Hnrnp2	22.2	13	0.013
Tnfaip8	21.9	12.6	0.027
Pex2	21.8	13.9	0.034
Osbp11a	21.6	14.1	0.03
Osgepl1	20.1	10.4	0.027
Cast	19.9	14.2	0.042
Polr1c	19.8	15.8	0.008
Dusp23	19.7	15.1	0.05
Mef2a	19.6	12.1	0.023
Mrm2	19.5	12	0.027
Copb2	19.5	10.7	0.02
Hnrnpa3	18.8	11.1	0.021
Ddx3y	18.6	8.6	0.007
Zfp358	18.6	23.5	0.045
Naprt	18.4	12.5	0.009
Myot	18.3	10.8	0.006
Gm5643	18.2	7.3	0.014
Tbrg1	18.1	12.1	0.019
Dnm1l	18.1	11.4	0.044
Cmpk1	17.8	10.5	0.033

Supplemental Table 2 (continued)			
Gene Symbol	WT	KO	p-value
Yae1d1	17.6	9.6	0.041
Pja2	17.6	9.7	0.04
Matr3	17.6	8.4	0.04
Slc17a7	17.5	13.9	0.04
Rab5a	17.1	8.3	0.016
Paip1	16.5	9.7	0.017
Rab9	16.3	6.7	0.039
Lrtm1	16.3	12.9	0.024
Dbt	16.2	8	0.011
Cdkn1b	15.6	7	0.034
Nabp1	15.5	8.7	0.026
Fgfr1op2	15.3	8.2	0.034
Ino80b	15.2	11.1	0.028
Nudt14	14.7	9.5	0.042
Aar2	14.5	10.8	0.048
Cobll1	14.4	7.9	0.025
Hdac2	14.3	7.3	0.043
Tfrc	14.3	7.1	0.021
Mreg	13.5	6.7	0.029
Fhl3	13.2	9.7	0.024
Aasdhppt	13.1	8.4	0.037
Ppox	13.1	7.3	0.049
Slc38a2	13	8.1	0.022
Med11	12.8	8	0.044
Abcd1	12.5	9.6	0.043

Supplemental Table 2 (continued)			
Gene Symbol	WT	KO	p-value
Eif2s3y	11.8	6	0.015
4921524J17Rik	11.6	6.1	0.03
Atg10	11.5	5.3	0.025
Tra2b	11.4	7.5	0.031
Decr2	11.3	6.5	0.04
Commd8	11.2	7.4	0.029
E130309D02Rik	11.1	7.7	0.013
Pcnp	10.9	7.4	0.039
Serfl	10.7	5.4	0.027
Mitf	10.7	6.7	0.034
Hdac11	10.6	6.4	0.038
Snap23	10.6	6.2	0.041
Lsm8	10.6	5.3	0.038
Ola1	10.2	6	0.036
Abhd14b	10.2	7	0.042
Crk	10.2	7	0.043
Otud1	10.1	5.3	0.032
Pdcd10	10	4.4	0.017
Nrbf2	10	4.2	0.014
Tomm70a	9.8	5.9	0.044
Sms	9.5	5.8	0.045
Nudt21	9.4	6.2	0.021
Uph	9.2	6.1	0.011
Pdss1	9	5.6	0.045
Mterf3	8.9	4.3	0.027

Supplemental Table 2 (continued)			
Gene Symbol	WT	KO	p-value
Asf1a	8.9	3.6	0.009
Mgea5	8.7	5.4	0.049
Klhl24	8.5	4.4	0.021
Btg3	8.4	5.6	0.049
Trmt5	8.3	4.7	0.05
Zfp639	8.2	5.5	0.042
Prrx1	8.2	5.6	0.046
Lym7	8.1	3.7	0.008
Dhx15	8	4.7	0.022
Lpgat1	8	4.8	0.032
Tmem37	7.9	5.7	0.013
Uso1	7.8	4.3	0.032
Reps1	7.8	6.1	0.04
Gal3st3	7.7	4.5	0.026
Ccdc58	7.5	4.5	0.042
Maf	7.5	4.9	0.028
Dcun1d1	7.4	4.6	0.03
Tmx4	7.4	4	0.009
Phkb	7.3	3.5	0.015
Fam45a	7.2	4.5	0.03
Faap100	7.2	6.1	0.046
Selenoo	7.2	5.7	0.041
Ube3a	7.1	5.3	0.04
Ip6k3	7	4.8	0.015
Tmem199	7	4.4	0.045

Supplemental Table 2 (continued)			
Gene Symbol	WT	KO	p-value
Ado	6.9	4.5	0.025
Shoc2	6.9	4.8	0.033
Lactb2	6.9	3.4	0.047
Thumpd3	6.8	4.4	0.011
Zfpm1	6.8	6	0.01
Fsd11	6.8	4.6	0.034
Nr3c1	6.7	3.3	0.02
Tmem38b	6.6	3.2	0.031
Map2k3os	6.6	3.2	0.022
Hspb11	6.5	4.2	0.036
BC028528	6.5	4.3	0.046
Lyar	6.4	3.9	0.049
Mob3a	6.4	4.6	0.021
Ikzf5	6.3	3.2	0.04
Rbfox1	6.2	3.5	0.024
Atxn711	6.2	3.6	0.016
Slc33a1	6.2	4	0.046
Polrmt	6.1	4.6	0.036
Ptpn	6	4.3	0.038
Pex13	6	3.1	0.033
Smarca5	6	3.5	0.041
Mtpap	5.7	3.7	0.019
Lactb	5.7	3.5	0.029
Rpl32l	5.7	4.1	0.011
Parp12	5.7	3.7	0.015

Supplemental Table 2 (continued)			
Gene Symbol	WT	KO	p-value
Ppp2r5e	5.6	3.6	0.048
Ddx41	5.6	4.2	0.029
Tdp2	5.6	3.2	0.012
Tfb1m	5.5	2.9	0.025
Cpne1	5.5	3.3	0.039
Ccdc43	5.4	3.7	0.01
Lrrc42	5.4	3.1	0.029
Mboat2	5.4	2.6	0.021
Rps6kb1	5.2	3.5	0.045
Usp15	5.2	3.6	0.033
Prpf4b	5.2	3.1	0.04
2610507I01Rik	5.2	1.7	0.024
Fgfr1op	5.2	3.6	0.038
Zfp326	5.2	2.9	0.024
Mtdh	5	3.1	0.046
Alg9	5	3.6	0.045
Kenn2	5	3.4	0.048
C8g	5	3.4	0.04
Evi2a	5	3.3	0.026
Yes1	4.9	3.2	0.047
Nmrk2	4.9	3	0.033
Arrdc3	4.9	2.8	0.04
Herc4	4.8	3.3	0.019
Gm17066	4.8	3.2	0.046
Ell2	4.8	2.6	0.008

Supplemental Table 2 (continued)			
Gene Symbol	WT	KO	p-value
Prg4	4.8	3.1	0.038
Nr2f2	4.6	3.1	0.045
BC003331	4.6	2.9	0.035
Mdfic	4.6	2.6	0.045
Wbp4	4.6	3	0.047
Zfp715	4.5	2.5	0.022
Lin52	4.5	2.7	0.025
Efemp1	4.4	2.2	0.029
Lingo3	4.4	3.7	0.046
Actr6	4.4	2.5	0.042
Far1	4.3	2.9	0.02
Ppp1r1a	4.3	2.4	0.018
Rnf149	4.2	2.3	0.041
Gca	4.2	2.1	0.032
Trmo	4.1	3.2	0.036
Dip2c	4	2.4	0.011
Mindy2	4	2.6	0.046
Esf1	3.8	2.3	0.021
Fam133b	3.8	2.2	0.017
Dnaaf3	3.8	3	0.032
Ufl1	3.8	2.5	0.034
Cd53	3.7	2.3	0.04
Intu	3.6	1.9	0.01
Taf2	3.6	2.3	0.022
Dbh	3.6	2.1	0.035

Supplemental Table 2 (continued)			
Gene Symbol	WT	KO	p-value
Oxsm	3.6	2.2	0.038
Smad1	3.6	2.4	0.01
5730455P16Rik	3.5	2.1	0.014
4930429F24Rik	3.5	2.2	0.05
Pnlsr	3.5	2.3	0.007
Hps6	3.5	2.4	0.021
E130311K13Rik	3.5	1.5	0.006
Cep19	3.4	2	0.011
Acdb3	3.4	1.9	0.036
Secisbp21	3.4	2.2	0.048
Rnf113a2	3.4	1.8	0.017
Pkn2	3.4	2.1	0.032
Gnai3	3.2	1.9	0.038
Armcx5	3.2	2	0.022
Chm	3.2	1.9	0.018
Zfp148	3.2	2	0.045
Nup54	3.1	2.1	0.029
Wdr75	3.1	1.9	0.049
Zfp317	3.1	2	0.022
Stk17b	3.1	2	0.036
Ssfa2	3	2	0.036
Ubxn2a	3	2	0.039
Ranbp6	2.9	1.7	0.01
Klhl2	2.9	1.9	0.025
Fam13a	2.8	1.6	0.021

Supplemental Table 2 (continued)			
Gene Symbol	WT	KO	p-value
Wif1	2.7	1.2	0.011
Ltn1	2.7	1.8	0.022
Gm6416	2.6	1.5	0.03
Clec11a	2.5	1.8	0.041
Qser1	2.5	1.7	0.024
Efnb2	2.5	1.8	0.014
Iqcb1	2.5	1.5	0.02
Ddx10	2.5	1.6	0.026
Thap6	2.4	1.4	0.025
Gm5	2.4	1.5	0.036
Tlr2	2.4	1.8	0.006
Fam76b	2.4	1.6	0.044
Morc3	2.3	1.7	0.039
Ep300	2.3	1.7	0.029
Nup11	2.3	1.4	0.031
Rspry1	2.3	1.6	0.048
Map10	2.3	1.3	0.016
Cyp2j6	2.3	1.5	0.041
Ccdc68	2.2	1.6	0.014
Donson	2.2	1.2	0.012
Zrsr1	2.1	1.4	0.035
Togaram1	2.1	1.5	0.034
Mpeg1	2.1	1.8	0.02
Pggt1b	2.1	1.4	0.049
Nepro	2.1	1.6	0.03

Supplemental Table 2 (continued)			
Gene Symbol	WT	KO	p-value
2610002M06Rik	2.1	1.3	0.05
Gipc2	2	1.4	0.032
Pid1	2	1.4	0.048
Zfp960	2	1.6	0.026
Ap5m1	2	1.4	0.048
6820431F20Rik	2	1.3	0.027
Btaf1	1.9	1.3	0.033
Pibf1	1.9	1.3	0.048
Man2c1os	1.8	1.1	0.024
Gm15441	1.8	1.2	0.039
Gm266	1.8	1.5	0.046
Wdpcp	1.7	1.2	0.049
Jchain	1.6	1.1	0.024

REFERENCES

- Abdulla, J. and J. R. Nielsen (2009). "Is the risk of atrial fibrillation higher in athletes than in the general population? A systematic review and meta-analysis." *Europace* **11**(9): 1156-1159.
- Al-Hadid, Q., K. Roy, G. Chanfreau and S. G. Clarke (2016). "Methylation of yeast ribosomal protein Rpl3 promotes translational elongation fidelity." *RNA* **22**(4): 489-498.
- Alkalaeva, E. Z., A. V. Pisarev, L. Y. Frolova, L. L. Kisselev and T. V. Pestova (2006). "In vitro reconstitution of eukaryotic translation reveals cooperativity between release factors eRF1 and eRF3." *Cell* **125**(6): 1125-1136.
- Allessie, M., J. Ausma and U. Schotten (2002). "Electrical, contractile and structural remodeling during atrial fibrillation." *Cardiovasc Res* **54**(2): 230-246.
- Avni, D., Y. Biberman and O. Meyuhas (1997). "The 5' terminal oligopyrimidine tract confers translational control on TOP mRNAs in a cell type- and sequence context-dependent manner." *Nucleic Acids Res* **25**(5): 995-1001.
- Badis, G., C. Saveanu, M. Fromont-Racine and A. Jacquier (2004). "Targeted mRNA degradation by deadenylation-independent decapping." *Mol Cell* **15**(1): 5-15.
- Baim, S. B. and F. Sherman (1988). "mRNA structures influencing translation in the yeast *Saccharomyces cerevisiae*." *Mol Cell Biol* **8**(4): 1591-1601.
- Ban, N., R. Beckmann, J. H. Cate, J. D. Dinman, F. Dragon, S. R. Ellis, D. L. Lafontaine, L. Lindahl, A. Liljas, J. M. Lipton, M. A. McAlear, P. B. Moore, H. F. Noller, J. Ortega, V. G. Panse, V. Ramakrishnan, C. M. Spahn, T. A. Steitz, M. Tchorzewski, D. Tollervey, A. J. Warren, J. R. Williamson, D. Wilson, A. Yonath and M. Yusupov (2014). "A new system for naming ribosomal proteins." *Curr Opin Struct Biol* **24**: 165-169.
- Ban, N., P. Nissen, J. Hansen, P. B. Moore and T. A. Steitz (2000). "The complete atomic structure of the large ribosomal subunit at 2.4 Å resolution." *Science* **289**(5481): 905-920.
- Barakat, A., K. Szick-Miranda, I. F. Chang, R. Guyot, G. Blanc, R. Cooke, M. Delseny and J. Bailey-Serres (2001). "The organization of cytoplasmic ribosomal protein genes in the Arabidopsis genome." *Plant Physiol* **127**(2): 398-415.
- Bell, S. P., R. M. Learned, H. M. Jantzen and R. Tjian (1988). "Functional cooperativity between transcription factors UBF1 and SL1 mediates human ribosomal RNA synthesis." *Science* **241**(4870): 1192-1197.
- Belsham, G. J., G. M. McInerney and N. Ross-Smith (2000). "Foot-and-mouth disease virus 3C protease induces cleavage of translation initiation factors eIF4A and eIF4G within infected cells." *J Virol* **74**(1): 272-280.
- Ben-Shem, A., N. Garreau de Loubresse, S. Melnikov, L. Jenner, G. Yusupova and M. Yusupov (2011). "The structure of the eukaryotic ribosome at 3.0 Å resolution." *Science* **334**(6062): 1524-1529.
- Beretta, L., A. C. Gingras, Y. V. Svitkin, M. N. Hall and N. Sonenberg (1996). "Rapamycin blocks the phosphorylation of 4E-BP1 and inhibits cap-dependent initiation of translation." *EMBO J* **15**(3): 658-664.
- Bolze, A., N. Mahlaoui, M. Byun, B. Turner, N. Trede, S. R. Ellis, A. Abhyankar, Y. Itan, E. Patin, S. Brebner, P. Sackstein, A. Puel, C. Picard, L. Abel, L. Quintana-Murci, S. N. Faust, A. P. Williams, R. Baretto, M. Duddridge, U. Kini, A. J. Pollard, C. Gaud, P. Frange, D. Orbach, J. F. Emile, J. L. Stephan, R. Sorensen, A. Plebani, L. Hammarstrom, M. E. Conley, L. Selleri and J. L. Casanova (2013). "Ribosomal protein SA haploinsufficiency in humans with isolated congenital asplenia." *Science* **340**(6135): 976-978.

Brenner, S., F. Jacob and M. Meselson (1961). "An unstable intermediate carrying information from genes to ribosomes for protein synthesis." *Nature* **190**: 576-581.

Breuer, C. B., M. C. Davies and J. R. Florini (1964). "Amino Acid Incorporation into Protein by Cell-Free Preparations from Rat Skeletal Muscle. II. Preparation and Properties of Muscle Ribosomes and Polyribosomes." *Biochemistry* **3**: 1713-1719.

Burstein, B. and S. Nattel (2008). "Atrial structural remodeling as an antiarrhythmic target." *J Cardiovasc Pharmacol* **52**(1): 4-10.

Buttgereit, D., G. Pflugfelder and I. Grummt (1985). "Growth-dependent regulation of rRNA synthesis is mediated by a transcription initiation factor (TIF-IA)." *Nucleic Acids Res* **13**(22): 8165-8180.

Caetano-Anolles, G. and D. Caetano-Anolles (2015). "Computing the origin and evolution of the ribosome from its structure - Uncovering processes of macromolecular accretion benefiting synthetic biology." *Comput Struct Biotechnol J* **13**: 427-447.

Chaillou, T., X. Zhang and J. J. McCarthy (2016). "Expression of Muscle-Specific Ribosomal Protein L3-Like Impairs Myotube Growth." *J Cell Physiol* **231**(9): 1894-1902.

Cheng, G., A. P. Merriam, B. Gong, P. Leahy, S. Khanna and J. D. Porter (2004). "Conserved and muscle-group-specific gene expression patterns shape postnatal development of the novel extraocular muscle phenotype." *Physiol Genomics* **18**(2): 184-195.

Cheng, G. and J. D. Porter (2002). "Transcriptional profile of rat extraocular muscle by serial analysis of gene expression." *Invest Ophthalmol Vis Sci* **43**(4): 1048-1058.

Chothani, S., S. Schafer, E. Adami, S. Viswanathan, A. A. Widjaja, S. R. Langley, J. Tan, M. Wang, N. M. Quaife, C. Jian Pua, G. D'Agostino, S. Guna Shekeran, B. L. George, S. Lim, E. Yiqun Cao, S. van Heesch, F. Witte, L. E. Felkin, E. G. Christodoulou, J. Dong, S. Blachut, G. Patone, P. J. R. Barton, N. Hubner, S. A. Cook and O. J. L. Rackham (2019). "Widespread Translational Control of Fibrosis in the Human Heart by RNA-Binding Proteins." *Circulation* **140**(11): 937-951.

Claude, A. (1940). "Particulate Components of Normal and Tumor Cells." *Science* **91**(2351): 77-78.

Couzin, J. (2002). "Breakthrough of the year. Small RNAs make big splash." *Science* **298**(5602): 2296-2297.

Csardi, G., A. Franks, D. S. Choi, E. M. Airoidi and D. A. Drummond (2015). "Accounting for experimental noise reveals that mRNA levels, amplified by post-transcriptional processes, largely determine steady-state protein levels in yeast." *PLoS Genet* **11**(5): e1005206.

Dechampsme, A. M., O. Koroleva, I. Leger-Silvestre, N. Gas and S. Camier (1999). "Assembly of 5S ribosomal RNA is required at a specific step of the pre-rRNA processing pathway." *J Cell Biol* **145**(7): 1369-1380.

Dobrev, D. and U. Ravens (2003). "Remodeling of cardiomyocyte ion channels in human atrial fibrillation." *Basic Res Cardiol* **98**(3): 137-148.

Drummond, M. J. and B. B. Rasmussen (2008). "Leucine-enriched nutrients and the regulation of mammalian target of rapamycin signalling and human skeletal muscle protein synthesis." *Curr Opin Clin Nutr Metab Care* **11**(3): 222-226.

Ehrlich, J. R., S. Nattel and S. H. Hohnloser (2002). "Atrial fibrillation and congestive heart failure: specific considerations at the intersection of two common and important cardiac disease sets." *J Cardiovasc Electrophysiol* **13**(4): 399-405.

Erales, J., V. Marchand, B. Panthu, S. Gillot, S. Belin, S. E. Ghayad, M. Garcia, F. Laforets, V. Marcel, A. Baudin-Baillieu, P. Bertin, Y. Coute, A. Adrait, M. Meyer, G. Therizols, M. Yusupov, O. Namy, T. Ohlmann, Y. Motorin, F. Catez and J. J. Diaz (2017). "Evidence for rRNA 2'-O-methylation plasticity: Control of intrinsic translational capabilities of human ribosomes." *Proc Natl Acad Sci U S A* **114**(49): 12934-12939.

Fareh, S., C. Villemaire and S. Nattel (1998). "Importance of refractoriness heterogeneity in the enhanced vulnerability to atrial fibrillation induction caused by tachycardia-induced atrial electrical remodeling." *Circulation* **98**(20): 2202-2209.

Fernandez-Tornero, C., M. Moreno-Morcillo, U. J. Rashid, N. M. Taylor, F. M. Ruiz, T. Gruene, P. Legrand, U. Steuerwald and C. W. Muller (2013). "Crystal structure of the 14-subunit RNA polymerase I." *Nature* **502**(7473): 644-649.

Ferretti, M. B. and K. Karbstein (2019). "Does functional specialization of ribosomes really exist?" *RNA* **25**(5): 521-538.

Fox, C. S., H. Parise, R. B. D'Agostino, Sr., D. M. Lloyd-Jones, R. S. Vasan, T. J. Wang, D. Levy, P. A. Wolf and E. J. Benjamin (2004). "Parental atrial fibrillation as a risk factor for atrial fibrillation in offspring." *JAMA* **291**(23): 2851-2855.

Fried, H. M. and J. R. Warner (1981). "Cloning of yeast gene for trichodermin resistance and ribosomal protein L3." *Proc Natl Acad Sci U S A* **78**(1): 238-242.

Friedrich, J. K., K. I. Panov, P. Cabart, J. Russell and J. C. Zomerdijk (2005). "TBP-TAF complex SL1 directs RNA polymerase I pre-initiation complex formation and stabilizes upstream binding factor at the rDNA promoter." *J Biol Chem* **280**(33): 29551-29558.

Gaba, A., A. Jacobson and M. S. Sachs (2005). "Ribosome occupancy of the yeast CPA1 upstream open reading frame termination codon modulates nonsense-mediated mRNA decay." *Mol Cell* **20**(3): 449-460.

Gamalinda, M. and J. L. Woolford, Jr. (2014). "Deletion of L4 domains reveals insights into the importance of ribosomal protein extensions in eukaryotic ribosome assembly." *RNA* **20**(11): 1725-1731.

Garcia-Gomez, J. J., A. Fernandez-Pevida, S. Lebaron, I. V. Rosado, D. Tollervey, D. Kressler and J. de la Cruz (2014). "Final pre-40S maturation depends on the functional integrity of the 60S subunit ribosomal protein L3." *PLoS Genet* **10**(3): e1004205.

Garelick, M. G., V. L. Mackay, A. Yanagida, E. C. Academia, K. H. Schreiber, W. C. Ladiges and B. K. Kennedy (2013). "Chronic rapamycin treatment or lack of S6K1 does not reduce ribosome activity in vivo." *Cell Cycle* **12**(15): 2493-2504.

Genuth, N. R. and M. Barna (2018). "The Discovery of Ribosome Heterogeneity and Its Implications for Gene Regulation and Organismal Life." *Mol Cell* **71**(3): 364-374.

Gingras, A. C., S. G. Kennedy, M. A. O'Leary, N. Sonenberg and N. Hay (1998). "4E-BP1, a repressor of mRNA translation, is phosphorylated and inactivated by the Akt(PKB) signaling pathway." *Genes Dev* **12**(4): 502-513.

Golomb, L., S. Volarevic and M. Oren (2014). "p53 and ribosome biogenesis stress: the essentials." *FEBS Lett* **588**(16): 2571-2579.

Grandori, C., N. Gomez-Roman, Z. A. Felton-Edkins, C. Ngouenet, D. A. Galloway, R. N. Eisenman and R. J. White (2005). "c-Myc binds to human ribosomal DNA and stimulates transcription of rRNA genes by RNA polymerase I." *Nat Cell Biol* **7**(3): 311-318.

Grogan, M., H. C. Smith, B. J. Gersh and D. L. Wood (1992). "Left ventricular dysfunction due to atrial fibrillation in patients initially believed to have idiopathic dilated cardiomyopathy." *Am J Cardiol* **69**(19): 1570-1573.

Guimaraes, J. C. and M. Zavolan (2016). "Patterns of ribosomal protein expression specify normal and malignant human cells." *Genome Biol* **17**(1): 236.

Guo, A. and L. S. Song (2014). "AutoTT: automated detection and analysis of T-tubule architecture in cardiomyocytes." *Biophys J* **106**(12): 2729-2736.

Gupta, V. and J. R. Warner (2014). "Ribosome-omics of the human ribosome." *RNA* **20**(7): 1004-1013.

Gyorke, I., N. Hester, L. R. Jones and S. Gyorke (2004). "The role of calsequestrin, triadin, and junctin in conferring cardiac ryanodine receptor responsiveness to luminal calcium." *Biophys J* **86**(4): 2121-2128.

Hannan, R. D., V. Stefanovsky, L. Taylor, T. Moss and L. I. Rothblum (1996). "Overexpression of the transcription factor UBF1 is sufficient to increase ribosomal DNA transcription in neonatal cardiomyocytes: implications for cardiac hypertrophy." *Proc Natl Acad Sci U S A* **93**(16): 8750-8755.

Hemani, G., K. Tilling and G. Davey Smith (2017). "Orienting the causal relationship between imprecisely measured traits using GWAS summary data." *PLoS Genet* **13**(11): e1007081.

Hess, E. L. and D. F. Oberhauser (1966). "Effects of deoxycholate on the microsome fraction of thymus." *Biochemistry* **5**(2): 751-755.

Hinnebusch, A. G. (2006). "eIF3: a versatile scaffold for translation initiation complexes." *Trends Biochem Sci* **31**(10): 553-562.

Hong, C. S., S. J. Kwon, M. C. Cho, Y. G. Kwak, K. C. Ha, B. Hong, H. Li, S. W. Chae, O. H. Chai, C. H. Song, Y. Li, J. C. Kim, S. H. Woo, S. Y. Lee, C. O. Lee and D. H. Kim (2008). "Overexpression of junctate induces cardiac hypertrophy and arrhythmia via altered calcium handling." *J Mol Cell Cardiol* **44**(4): 672-682.

Hornstein, E., A. Git, I. Braunstein, D. Avni and O. Meyuhas (1999). "The expression of poly(A)-binding protein gene is translationally regulated in a growth-dependent fashion through a 5'-terminal oligopyrimidine tract motif." *J Biol Chem* **274**(3): 1708-1714.

Huang, X. P., C. X. Zhao, Q. J. Li, Y. Cai, F. X. Liu, H. Hu, X. Xu, Y. L. Han, M. Wu, Q. M. Zhan and M. R. Wang (2006). "Alteration of RPL14 in squamous cell carcinomas and preneoplastic lesions of the esophagus." *Gene* **366**(1): 161-168.

Ionasescu, V., H. Zellweger and T. W. Conway (1971). "Ribosomal protein synthesis in Duchenne muscular dystrophy." *Arch Biochem Biophys* **144**(1): 51-58.

Ivanov, A. V., N. M. Parakhnevich, A. A. Malygin and G. G. Karpova (2010). "[Human ribosomal protein S16 inhibites excision of the first intron from its own]." *Mol Biol (Mosk)* **44**(1): 90-97.

Jansa, P. and I. Grummt (1999). "Mechanism of transcription termination: PTRF interacts with the largest subunit of RNA polymerase I and dissociates paused transcription complexes from yeast and mouse." *Mol Gen Genet* **262**(3): 508-514.

Jastrzebski, K., K. M. Hannan, E. B. Tchoubrieva, R. D. Hannan and R. B. Pearson (2007). "Coordinate regulation of ribosome biogenesis and function by the ribosomal protein S6 kinase, a key mediator of mTOR function." *Growth Factors* **25**(4): 209-226.

Jefferies, H. B., C. Reinhard, S. C. Kozma and G. Thomas (1994). "Rapamycin selectively represses translation of the "polypyrimidine tract" mRNA family." *Proc Natl Acad Sci U S A* **91**(10): 4441-4445.

Kim, Y., H. Zhang and R. L. Scholl (1990). "Two evolutionarily divergent genes encode a cytoplasmic ribosomal protein of *Arabidopsis thaliana*." *Gene* **93**(2): 177-182.

Kirby, M. L., G. Cheng, H. Stadt and G. Hunter (1995). "Differential expression of the L10 ribosomal protein during heart development." *Biochem Biophys Res Commun* **212**(2): 461-465.

Kodama, I. and M. R. Boyett (1985). "Regional differences in the electrical activity of the rabbit sinus node." *Pflugers Arch* **404**(3): 214-226.

Komili, S., N. G. Farny, F. P. Roth and P. A. Silver (2007). "Functional specificity among ribosomal proteins regulates gene expression." *Cell* **131**(3): 557-571.

Kondrashov, N., A. Pusic, C. R. Stumpf, K. Shimizu, A. C. Hsieh, J. Ishijima, T. Shiroishi and M. Barna (2011). "Ribosome-mediated specificity in Hox mRNA translation and vertebrate tissue patterning." *Cell* **145**(3): 383-397.

Kruiswijk, T., R. J. Planta and J. M. Krop (1978). "The course of the assembly of ribosomal subunits in yeast." *Biochim Biophys Acta* **517**(2): 378-389.

Kuhn, A. and I. Grummt (1992). "Dual role of the nucleolar transcription factor UBF: trans-activator and antirepressor." *Proc Natl Acad Sci U S A* **89**(16): 7340-7344.

Lazdins, I. B., M. Delannoy and B. Sollner-Webb (1997). "Analysis of nucleolar transcription and processing domains and pre-rRNA movements by in situ hybridization." *Chromosoma* **105**(7-8): 481-495.

Leary, D. J. and S. Huang (2001). "Regulation of ribosome biogenesis within the nucleolus." *FEBS Lett* **509**(2): 145-150.

Levy, S., D. Avni, N. Hariharan, R. P. Perry and O. Meyuhav (1991). "Oligopyrimidine tract at the 5' end of mammalian ribosomal protein mRNAs is required for their translational control." *Proc Natl Acad Sci U S A* **88**(8): 3319-3323.

Lewis, Y. E., A. Moskovitz, M. Mutlak, J. Heineke, L. H. Caspi and I. Kehat (2018). "Localization of transcripts, translation, and degradation for spatiotemporal sarcomere maintenance." *J Mol Cell Cardiol* **116**: 16-28.

Li, J. J., P. J. Bickel and M. D. Biggin (2014). "System wide analyses have underestimated protein abundances and the importance of transcription in mammals." *PeerJ* **2**: e270.

Lin, H. J., P. A. Wolf, M. Kelly-Hayes, A. S. Beiser, C. S. Kase, E. J. Benjamin and R. B. D'Agostino (1996). "Stroke severity in atrial fibrillation. The Framingham Study." *Stroke* **27**(10): 1760-1764.

Ling, L. H., P. M. Kistler, A. H. Ellims, L. M. Iles, G. Lee, G. L. Hughes, J. M. Kalman, D. M. Kaye and A. J. Taylor (2012). "Diffuse ventricular fibrosis in atrial fibrillation: noninvasive evaluation and relationships with aging and systolic dysfunction." *J Am Coll Cardiol* **60**(23): 2402-2408.

Linscheid, N., S. Logantha, P. C. Poulsen, S. Zhang, M. Schrolkamp, K. L. Egerod, J. J. Thompson, A. Kitmitto, G. Galli, M. J. Humphries, H. Zhang, T. H. Pers, J. V. Olsen, M. Boyett and A. Lundby (2019). "Quantitative proteomics and single-nucleus transcriptomics of the sinus node elucidates the foundation of cardiac pacemaking." *Nat Commun* **10**(1): 2889.

Littlefield, J. W., E. B. Keller, J. Gross and P. C. Zamecnik (1955). "Studies on cytoplasmic ribonucleoprotein particles from the liver of the rat." *J Biol Chem* **217**(1): 111-123.

Lopes, A. M., R. N. Miguel, C. A. Sargent, P. J. Ellis, A. Amorim and N. A. Affara (2010). "The human RPS4 paralogue on Yq11.223 encodes a structurally conserved ribosomal protein and is preferentially expressed during spermatogenesis." *BMC Mol Biol* **11**: 33.

Lu, Z. Q., A. Sinha, P. Sharma, T. Kislinger and A. O. Gramolini (2014). "Proteomic analysis of human fetal atria and ventricle." *J Proteome Res* **13**(12): 5869-5878.

Lubitz, S. A., C. Ozcan, J. W. Magnani, S. Kaab, E. J. Benjamin and P. T. Ellinor (2010). "Genetics of atrial fibrillation: implications for future research directions and personalized medicine." *Circ Arrhythm Electrophysiol* **3**(3): 291-299.

Lubitz, S. A., X. Yin, J. D. Fontes, J. W. Magnani, M. Rienstra, M. Pai, M. L. Villalon, R. S. Vasan, M. J. Pencina, D. Levy, M. G. Larson, P. T. Ellinor and E. J. Benjamin (2010). "Association between familial atrial fibrillation and risk of new-onset atrial fibrillation." *JAMA* **304**(20): 2263-2269.

Luukkonen, B. G., W. Tan and S. Schwartz (1995). "Efficiency of reinitiation of translation on human immunodeficiency virus type 1 mRNAs is determined by the length of the upstream open reading frame and by intercistronic distance." *J Virol* **69**(7): 4086-4094.

Lynch, M. and J. S. Conery (2000). "The evolutionary fate and consequences of duplicate genes." *Science* **290**(5494): 1151-1155.

Mageeney, C. M. and V. C. Ware (2019). "Specialized eRpL22 paralogue-specific ribosomes regulate specific mRNA translation in spermatogenesis in *Drosophila melanogaster*." *Mol Biol Cell* **30**(17): 2240-2253.

Mariottini, P., C. Bagni, F. Annesi and F. Amaldi (1988). "Isolation and nucleotide sequences of cDNAs for *Xenopus laevis* ribosomal protein S8: similarities in the 5' and 3' untranslated regions of mRNAs for various r-proteins." Gene **67**(1): 69-74.

Martin-Marcos, P., A. G. Hinnebusch and M. Tamame (2007). "Ribosomal protein L33 is required for ribosome biogenesis, subunit joining, and repression of GCN4 translation." Mol Cell Biol **27**(17): 5968-5985.

Mason, S. W., E. E. Sander and I. Grummt (1997). "Identification of a transcript release activity acting on ternary transcription complexes containing murine RNA polymerase I." EMBO J **16**(1): 163-172.

Matsui, M., N. Yachie, Y. Okada, R. Saito and M. Tomita (2007). "Bioinformatic analysis of post-transcriptional regulation by uORF in human and mouse." FEBS Lett **581**(22): 4184-4188.

McGann, C., N. Akoum, A. Patel, E. Kholmovski, P. Revelo, K. Damal, B. Wilson, J. Cates, A. Harrison, R. Ranjan, N. S. Burgon, T. Greene, D. Kim, E. V. Dibella, D. Parker, R. S. Macleod and N. F. Marrouche (2014). "Atrial fibrillation ablation outcome is predicted by left atrial remodeling on MRI." Circ Arrhythm Electrophysiol **7**(1): 23-30.

Meijer, H. A. and A. A. Thomas (2003). "Ribosomes stalling on uORF1 in the *Xenopus* Cx41 5' UTR inhibit downstream translation initiation." Nucleic Acids Res **31**(12): 3174-3184.

Merrick, W. C. (1992). "Mechanism and regulation of eukaryotic protein synthesis." Microbiol Rev **56**(2): 291-315.

Meskauskas, A. and J. D. Dinman (2007). "Ribosomal protein L3: gatekeeper to the A site." Mol Cell **25**(6): 877-888.

Meskauskas, A., J. W. Harger, K. L. Jacobs and J. D. Dinman (2003). "Decreased peptidyltransferase activity correlates with increased programmed -1 ribosomal frameshifting and viral maintenance defects in the yeast *Saccharomyces cerevisiae*." RNA **9**(8): 982-992.

Meskauskas, A., A. N. Petrov and J. D. Dinman (2005). "Identification of functionally important amino acids of ribosomal protein L3 by saturation mutagenesis." Mol Cell Biol **25**(24): 10863-10874.

Meyer, A. E., N. J. Hung, P. Yang, A. W. Johnson and E. A. Craig (2007). "The specialized cytosolic J-protein, Jjj1, functions in 60S ribosomal subunit biogenesis." Proc Natl Acad Sci U S A **104**(5): 1558-1563.

Michael, W. M. and G. Dreyfuss (1996). "Distinct domains in ribosomal protein L5 mediate 5 S rRNA binding and nucleolar localization." J Biol Chem **271**(19): 11571-11574.

Miloslavski, R., E. Cohen, A. Avraham, Y. Iluz, Z. Hayouka, J. Kasir, R. Mudhasani, S. N. Jones, N. Cybulski, M. A. Ruegg, O. Larsson, V. Gandin, A. Rajakumar, I. Topisirovic and O. Meyuhas (2014). "Oxygen sufficiency controls TOP mRNA translation via the TSC-Rheb-mTOR pathway in a 4E-BP-independent manner." J Mol Cell Biol **6**(3): 255-266.

Mitterer, V., G. Murat, S. Rety, M. Blaud, L. Delbos, T. Stanborough, H. Bergler, N. Leulliot, D. Kressler and B. Pertschy (2016). "Sequential domain assembly of ribosomal protein S3 drives 40S subunit maturation." Nat Commun **7**: 10336.

Mordret, E., O. Dahan, O. Asraf, R. Rak, A. Yehonadav, G. D. Barnabas, J. Cox, T. Geiger, A. B. Lindner and Y. Pilpel (2019). "Systematic Detection of Amino Acid Substitutions in Proteomes Reveals Mechanistic Basis of Ribosome Errors and Selection for Translation Fidelity." Mol Cell **75**(3): 427-441 e425.

Moreland, R. B., H. G. Nam, L. M. Hereford and H. M. Fried (1985). "Identification of a nuclear localization signal of a yeast ribosomal protein." Proc Natl Acad Sci U S A **82**(19): 6561-6565.

Moss, E. G. and R. S. Poethig (2002). "MicroRNAs: something new under the sun." Curr Biol **12**(20): R688-690.

Nakanishi, T., K. Kohno, M. Ishiura, H. Ohashi and T. Uchida (1988). "Complete nucleotide sequence and characterization of the 5'-flanking region of mammalian elongation factor 2 gene." *J Biol Chem* **263**(13): 6384-6391.

Nattel, S., A. Maguy, S. Le Bouter and Y. H. Yeh (2007). "Arrhythmogenic ion-channel remodeling in the heart: heart failure, myocardial infarction, and atrial fibrillation." *Physiol Rev* **87**(2): 425-456.

Nishi, R., S. Kidou, H. Uchimiya and A. Kato (1993). "The primary structure of two proteins from the large ribosomal subunit of rice." *Biochim Biophys Acta* **1216**(1): 110-112.

Noriega, T. R., J. Chen, P. Walter and J. D. Puglisi (2014). "Real-time observation of signal recognition particle binding to actively translating ribosomes." *Elife* **3**.

O'Connell, T. N., Y (2002). "Isolation of Adult Mouse Cardiac Myocytes from One Heart".

O'Leary, M. N., K. H. Schreiber, Y. Zhang, A. C. Duc, S. Rao, J. S. Hale, E. C. Academia, S. R. Shah, J. F. Morton, C. A. Holstein, D. B. Martin, M. Kaerberlein, W. C. Ladiges, P. J. Fink, V. L. Mackay, D. L. Wiest and B. K. Kennedy (2013). "The ribosomal protein Rpl22 controls ribosome composition by directly repressing expression of its own paralog, Rpl22l1." *PLoS Genet* **9**(8): e1003708.

O'Mahony, D. J., S. D. Smith, W. Xie and L. I. Rothblum (1992). "Analysis of the phosphorylation, DNA-binding and dimerization properties of the RNA polymerase I transcription factors UBF1 and UBF2." *Nucleic Acids Res* **20**(6): 1301-1308.

Oliveira, C. C. and J. E. McCarthy (1995). "The relationship between eukaryotic translation and mRNA stability. A short upstream open reading frame strongly inhibits translational initiation and greatly accelerates mRNA degradation in the yeast *Saccharomyces cerevisiae*." *J Biol Chem* **270**(15): 8936-8943.

Oyama, M., C. Itagaki, H. Hata, Y. Suzuki, T. Izumi, T. Natsume, T. Isobe and S. Sugano (2004). "Analysis of small human proteins reveals the translation of upstream open reading frames of mRNAs." *Genome Res* **14**(10B): 2048-2052.

Pagliara, V., A. Saide, E. Mitidieri, R. d'Emmanuele di Villa Bianca, R. Sorrentino, G. Russo and A. Russo (2016). "5-FU targets rpl3 to induce mitochondrial apoptosis via cystathionine-beta-synthase in colon cancer cells lacking p53." *Oncotarget* **7**(31): 50333-50348.

Palade, G. E. (1955). "A small particulate component of the cytoplasm." *J Biophys Biochem Cytol* **1**(1): 59-68.

Pall, G. S., K. J. Johnson and G. L. Smith (2003). "Abnormal contractile activity and calcium cycling in cardiac myocytes isolated from DMPK knockout mice." *Physiol Genomics* **13**(2): 139-146.

Panic, L., S. Tamarut, M. Sticker-Jantscheff, M. Barkic, D. Solter, M. Uzelac, K. Grabusic and S. Volarevic (2006). "Ribosomal protein S6 gene haploinsufficiency is associated with activation of a p53-dependent checkpoint during gastrulation." *Mol Cell Biol* **26**(23): 8880-8891.

Parks, M. M., C. M. Kurylo, R. A. Dass, L. Bojmar, D. Lyden, C. T. Vincent and S. C. Blanchard (2018). "Variant ribosomal RNA alleles are conserved and exhibit tissue-specific expression." *Sci Adv* **4**(2): eaao0665.

Perry, R. P. (2005). "The architecture of mammalian ribosomal protein promoters." *BMC Evol Biol* **5**: 15.

Perry, R. P. and O. Meyuhas (1990). "Translational control of ribosomal protein production in mammalian cells." *Enzyme* **44**(1-4): 83-92.

Pestova, T. V. and C. U. Hellen (2003). "Translation elongation after assembly of ribosomes on the Cricket paralysis virus internal ribosomal entry site without initiation factors or initiator tRNA." *Genes Dev* **17**(2): 181-186.

Pestova, T. V., I. B. Lomakin, J. H. Lee, S. K. Choi, T. E. Dever and C. U. Hellen (2000). "The joining of ribosomal subunits in eukaryotes requires eIF5B." *Nature* **403**(6767): 332-335.

Pinkstaff, J. K., S. A. Chappell, V. P. Mauro, G. M. Edelman and L. A. Krushel (2001). "Internal initiation of translation of five dendritically localized neuronal mRNAs." Proc Natl Acad Sci U S A **98**(5): 2770-2775.

Platonov, P. G., A. H. Christensen, F. Holmqvist, J. Carlson, S. Haunso and J. H. Svendsen (2011). "Abnormal atrial activation is common in patients with arrhythmogenic right ventricular cardiomyopathy." J Electrocardiol **44**(2): 237-241.

Poll, G., T. Braun, J. Jakovljevic, A. Neueder, S. Jakob, J. L. Woolford, Jr., H. Tschochner and P. Milkereit (2009). "rRNA maturation in yeast cells depleted of large ribosomal subunit proteins." PLoS One **4**(12): e8249.

Popescu, S. C. and N. E. Tumer (2004). "Silencing of ribosomal protein L3 genes in *N. tabacum* reveals coordinate expression and significant alterations in plant growth, development and ribosome biogenesis." Plant J **39**(1): 29-44.

Quade, N., D. Boehringer, M. Leibundgut, J. van den Heuvel and N. Ban (2015). "Cryo-EM structure of Hepatitis C virus IRES bound to the human ribosome at 3.9-A resolution." Nat Commun **6**: 7646.

Raska, I., K. Koberna, J. Malinsky, H. Fidlerova and M. Masata (2004). "The nucleolus and transcription of ribosomal genes." Biol Cell **96**(8): 579-594.

Reeder, R. H. P., C.S. McStay, B. (1995). UBF an architectural element for RNA polymerase I promoters. Nucleic Acids and Molecular Biology, Springer. **9**: 251-263.

Rheinberger, H. J. (1995). "From microsomes to ribosomes: "strategies" of "representation"." J Hist Biol **28**(1): 49-89.

Riis, B., S. I. Rattan, B. F. Clark and W. C. Merrick (1990). "Eukaryotic protein elongation factors." Trends Biochem Sci **15**(11): 420-424.

Roberts, R. (2006). "Mechanisms of disease: Genetic mechanisms of atrial fibrillation." Nat Clin Pract Cardiovasc Med **3**(5): 276-282.

Roberts, R. B. (1958). "Microsomal Particles and Protein Synthesis." p viii.

Rosado, I. V., D. Kressler and J. de la Cruz (2007). "Functional analysis of *Saccharomyces cerevisiae* ribosomal protein Rpl3p in ribosome synthesis." Nucleic Acids Res **35**(12): 4203-4213.

Rosorius, O., B. Fries, R. H. Stauber, N. Hirschmann, D. Bevec and J. Hauber (2000). "Human ribosomal protein L5 contains defined nuclear localization and export signals." J Biol Chem **275**(16): 12061-12068.

Rotenberg, M. O., M. Moritz and J. L. Woolford, Jr. (1988). "Depletion of *Saccharomyces cerevisiae* ribosomal protein L16 causes a decrease in 60S ribosomal subunits and formation of half-mer polyribosomes." Genes Dev **2**(2): 160-172.

Russ, J. R. (2007). Characterization of ribosomal protein L2 and analysis of missense codon discrimination in the yeast *saccharomyces cereveisiae*. College Park, Md., University of Maryland.

Russo, A., D. Esposito, M. Catillo, C. Pietropaolo, E. Crescenzi and G. Russo (2013). "Human rpL3 induces G(1)/S arrest or apoptosis by modulating p21 (waf1/cip1) levels in a p53-independent manner." Cell Cycle **12**(1): 76-87.

Salas-Marco, J. and D. M. Bedwell (2004). "GTP hydrolysis by eRF3 facilitates stop codon decoding during eukaryotic translation termination." Mol Cell Biol **24**(17): 7769-7778.

Salas-Marco, J. and D. M. Bedwell (2005). "Discrimination between defects in elongation fidelity and termination efficiency provides mechanistic insights into translational readthrough." J Mol Biol **348**(4): 801-815.

Santhanakrishnan, R., N. Wang, M. G. Larson, J. W. Magnani, D. D. McManus, S. A. Lubitz, P. T. Ellinor, S. Cheng, R. S. Vasan, D. S. Lee, T. J. Wang, D. Levy, E. J. Benjamin and J. E. Ho (2016).

"Atrial Fibrillation Begets Heart Failure and Vice Versa: Temporal Associations and Differences in Preserved Versus Reduced Ejection Fraction." *Circulation* **133**(5): 484-492.

Sarkozy, M., A. Zvara, N. Gyemant, V. Fekete, G. F. Kocsis, J. Pipis, G. Szucs, C. Csonka, L. G. Puskas, P. Ferdinandy and T. Csont (2013). "Metabolic syndrome influences cardiac gene expression pattern at the transcript level in male ZDF rats." *Cardiovasc Diabetol* **12**: 16.

Sasikumar, A. N., W. B. Perez and T. G. Kinzy (2012). "The many roles of the eukaryotic elongation factor 1 complex." *Wiley Interdiscip Rev RNA* **3**(4): 543-555.

Schuler, M., S. R. Connell, A. Lescoute, J. Giesebrecht, M. Dabrowski, B. Schroer, T. Mielke, P. A. Penczek, E. Westhof and C. M. Spahn (2006). "Structure of the ribosome-bound cricket paralysis virus IRES RNA." *Nat Struct Mol Biol* **13**(12): 1092-1096.

Shahbazian, D., P. P. Roux, V. Mieulet, M. S. Cohen, B. Raught, J. Taunton, J. W. Hershey, J. Blenis, M. Pende and N. Sonenberg (2006). "The mTOR/PI3K and MAPK pathways converge on eIF4B to control its phosphorylation and activity." *EMBO J* **25**(12): 2781-2791.

Sharma, J., D. Mukherjee, S. N. Rao, S. Iyengar, S. K. Shankar, P. Satishchandra and N. R. Jana (2013). "Neuronatin-mediated aberrant calcium signaling and endoplasmic reticulum stress underlie neuropathology in Lafora disease." *J Biol Chem* **288**(13): 9482-9490.

Shi, Z., K. Fujii, K. M. Kovary, N. R. Genuth, H. L. Rost, M. N. Teruel and M. Barna (2017). "Heterogeneous Ribosomes Preferentially Translate Distinct Subpools of mRNAs Genome-wide." *Mol Cell* **67**(1): 71-83 e77.

Simillion, C., K. Vandepoele, M. C. Van Montagu, M. Zabeau and Y. Van de Peer (2002). "The hidden duplication past of Arabidopsis thaliana." *Proc Natl Acad Sci U S A* **99**(21): 13627-13632.

Sirri, V., P. Roussel and D. Hernandez-Verdun (1999). "The mitotically phosphorylated form of the transcription termination factor TTF-1 is associated with the repressed rDNA transcription machinery." *J Cell Sci* **112** (Pt 19): 3259-3268.

Slavov, N., S. Semrau, E. Airoidi, B. Budnik and A. van Oudenaarden (2015). "Differential Stoichiometry among Core Ribosomal Proteins." *Cell Rep* **13**(5): 865-873.

Smith, T. F., J. C. Lee, R. R. Gutell and H. Hartman (2008). "The origin and evolution of the ribosome." *Biol Direct* **3**: 16.

Soliman, E. Z., M. M. Safford, P. Muntner, Y. Khodneva, F. Z. Dawood, N. A. Zakai, E. L. Thacker, S. Judd, V. J. Howard, G. Howard, D. M. Herrington and M. Cushman (2014). "Atrial fibrillation and the risk of myocardial infarction." *JAMA Intern Med* **174**(1): 107-114.

Sugihara, Y., H. Honda, T. Iida, T. Morinaga, S. Hino, T. Okajima, T. Matsuda and D. Nadano (2010). "Proteomic analysis of rodent ribosomes revealed heterogeneity including ribosomal proteins L10-like, L22-like 1, and L39-like." *J Proteome Res* **9**(3): 1351-1366.

Suh, Y. H., W. H. Kim, C. Moon, Y. H. Hong, S. Y. Eun, J. H. Lim, J. S. Choi, J. Song and M. H. Jung (2005). "Ectopic expression of Neuronatin potentiates adipogenesis through enhanced phosphorylation of cAMP-response element-binding protein in 3T3-L1 cells." *Biochem Biophys Res Commun* **337**(2): 481-489.

Talman, V., J. Teppo, P. Poho, P. Movahedi, A. Vaikkinen, S. T. Karhu, K. Trost, T. Suvitaival, J. Heikkonen, T. Pahikkala, T. Kotiaho, R. Kostianen, M. Varjosalo and H. Ruskoaho (2018). "Molecular Atlas of Postnatal Mouse Heart Development." *J Am Heart Assoc* **7**(20): e010378.

Tanaka, K. F., S. E. Ahmari, E. D. Leonardo, J. W. Richardson-Jones, E. C. Budreck, P. Scheiffele, S. Sugio, N. Inamura, K. Ikenaka and R. Hen (2010). "Flexible Accelerated STOP Tetracycline Operator-knockin (FAST): a versatile and efficient new gene modulating system." *Biol Psychiatry* **67**(8): 770-773.

Tanaka, M., N. Sotta, Y. Yamazumi, Y. Yamashita, K. Miwa, K. Murota, Y. Chiba, M. Y. Hirai, T. Akiyama, H. Onouchi, S. Naito and T. Fujiwara (2016). "The Minimum Open Reading Frame,

AUG-Stop, Induces Boron-Dependent Ribosome Stalling and mRNA Degradation." Plant Cell **28**(11): 2830-2849.

Thoreen, C. C., L. Chantranupong, H. R. Keys, T. Wang, N. S. Gray and D. M. Sabatini (2012). "A unifying model for mTORC1-mediated regulation of mRNA translation." Nature **485**(7396): 109-113.

Thorolfsson, R. B., G. Sveinbjornsson, P. Sulem, J. B. Nielsen, S. Jonsson, G. H. Halldorsson, P. Melsted, E. V. Ivarsdottir, O. B. Davidsson, R. P. Kristjansson, G. Thorleifsson, A. Helgadóttir, S. Gretarsdottir, G. Norddahl, S. Rajamani, B. Torfason, A. S. Valgardsson, J. T. Sverrisson, V. Tragante, O. L. Holmen, F. W. Asselbergs, D. M. Roden, D. Darbar, T. R. Pedersen, M. S. Sabatine, C. J. Willer, M. L. Lochen, B. V. Halldorsson, I. Jonsdottir, K. Hveem, D. O. Arnar, U. Thorsteinsdottir, D. F. Gudbjartsson, H. Holm and K. Stefansson (2018). "Coding variants in RPL3L and MYZAP increase risk of atrial fibrillation." Commun Biol **1**: 68.

Thorp, A. A., N. Owen, M. Neuhaus and D. W. Dunstan (2011). "Sedentary behaviors and subsequent health outcomes in adults a systematic review of longitudinal studies, 1996-2011." Am J Prev Med **41**(2): 207-215.

Treves, S., C. Franzini-Armstrong, L. Moccagatta, C. Arnoult, C. Grasso, A. Schrum, S. Ducreux, M. X. Zhu, K. Mikoshiba, T. Girard, S. Smida-Rezgui, M. Ronjat and F. Zorzato (2004). "Junctate is a key element in calcium entry induced by activation of InsP3 receptors and/or calcium store depletion." J Cell Biol **166**(4): 537-548.

Tschochner, H. and E. Hurt (2003). "Pre-ribosomes on the road from the nucleolus to the cytoplasm." Trends Cell Biol **13**(5): 255-263.

Uhlen, M., L. Fagerberg, B. M. Hallstrom, C. Lindskog, P. Oksvold, A. Mardinoglu, A. Sivertsson, C. Kampf, E. Sjostedt, A. Asplund, I. Olsson, K. Edlund, E. Lundberg, S. Navani, C. A. Szgyarto, J. Odeberg, D. Djureinovic, J. O. Takanen, S. Hober, T. Alm, P. H. Edqvist, H. Berling, H. Tegel, J. Mulder, J. Rockberg, P. Nilsson, J. M. Schwenk, M. Hamsten, K. von Feilitzen, M. Forsberg, L. Persson, F. Johansson, M. Zwahlen, G. von Heijne, J. Nielsen and F. Ponten (2015). "Proteomics. Tissue-based map of the human proteome." Science **347**(6220): 1260419.

van den Heuvel, J. J., R. J. Bergkamp, R. J. Planta and H. A. Raue (1989). "Effect of deletions in the 5'-noncoding region on the translational efficiency of phosphoglycerate kinase mRNA in yeast." Gene **79**(1): 83-95.

Van Raay, T. J., T. D. Connors, K. W. Klinger, G. M. Landes and T. C. Burn (1996). "A novel ribosomal protein L3-like gene (RPL3L) maps to the autosomal dominant polycystic kidney disease gene region." Genomics **37**(2): 172-176.

Verheijck, E. E., A. Wessels, A. C. van Ginneken, J. Bourier, M. W. Markman, J. L. Vermeulen, J. M. de Bakker, W. H. Lamers, T. Ophhof and L. N. Bouman (1998). "Distribution of atrial and nodal cells within the rabbit sinoatrial node: models of sinoatrial transition." Circulation **97**(16): 1623-1631.

Vermes, E., J. C. Tardif, M. G. Bourassa, N. Racine, S. Levesque, M. White, P. G. Guerra and A. Ducharme (2003). "Enalapril decreases the incidence of atrial fibrillation in patients with left ventricular dysfunction: insight from the Studies Of Left Ventricular Dysfunction (SOLVD) trials." Circulation **107**(23): 2926-2931.

Vermond, R. A., B. Geelhoed, N. Verweij, R. G. Tieleman, P. Van der Harst, H. L. Hillege, W. H. Van Gilst, I. C. Van Gelder and M. Rienstra (2015). "Incidence of Atrial Fibrillation and Relationship With Cardiovascular Events, Heart Failure, and Mortality: A Community-Based Study From the Netherlands." J Am Coll Cardiol **66**(9): 1000-1007.

Voit, R., M. Hoffmann and I. Grummt (1999). "Phosphorylation by G1-specific cdk-cyclin complexes activates the nucleolar transcription factor UBF." EMBO J **18**(7): 1891-1899.

Walter, P. and G. Blobel (1981). "Translocation of proteins across the endoplasmic reticulum. II. Signal recognition protein (SRP) mediates the selective binding to microsomal membranes of in-vitro-assembled polysomes synthesizing secretory protein." *J Cell Biol* **91**(2 Pt 1): 551-556.

Wang, X., W. Li, M. Williams, N. Terada, D. R. Alessi and C. G. Proud (2001). "Regulation of elongation factor 2 kinase by p90(RSK1) and p70 S6 kinase." *EMBO J* **20**(16): 4370-4379.

Warner, J. R. (1999). "The economics of ribosome biosynthesis in yeast." *Trends Biochem Sci* **24**(11): 437-440.

Wijesurendra, R. S., A. Liu, F. Notaristefano, N. A. B. Ntusi, T. D. Karamitsos, Y. Bashir, M. Ginks, K. Rajappan, T. R. Betts, M. Jerosch-Herold, V. M. Ferreira, S. Neubauer and B. Casadei (2018). "Myocardial Perfusion Is Impaired and Relates to Cardiac Dysfunction in Patients With Atrial Fibrillation Both Before and After Successful Catheter Ablation." *J Am Heart Assoc* **7**(15): e009218.

Wijffels, M. C., C. J. Kirchhof, R. Dorland, J. Power and M. A. Allessie (1997). "Electrical remodeling due to atrial fibrillation in chronically instrumented conscious goats: roles of neurohumoral changes, ischemia, atrial stretch, and high rate of electrical activation." *Circulation* **96**(10): 3710-3720.

Williams, M. E. and I. M. Sussex (1995). "Developmental regulation of ribosomal protein L16 genes in *Arabidopsis thaliana*." *Plant J* **8**(1): 65-76.

Wittmann, H. G., G. Stofflet, I. Hindennach, C. G. Kurland, E. A. Birge, L. Randall-Hazelbauer, M. Nomura, E. Kaltschmidt, S. Mizushima, R. R. Traut and T. A. Bickle (1971). "Correlation of 30S ribosomal proteins of *Escherichia coli* isolated in different laboratories." *Mol Gen Genet* **111**(4): 327-333.

Wong, Q. W., J. Li, S. R. Ng, S. G. Lim, H. Yang and L. A. Vardy (2014). "RPL39L is an example of a recently evolved ribosomal protein paralog that shows highly specific tissue expression patterns and is upregulated in ESCs and HCC tumors." *RNA Biol* **11**(1): 33-41.

Wu, L., J. Guo, L. Zheng, G. Chen, L. Ding, Y. Qiao, W. Sun, Y. Yao and S. Zhang (2016). "Atrial Remodeling and Atrial Tachyarrhythmias in Arrhythmogenic Right Ventricular Cardiomyopathy." *Am J Cardiol* **118**(5): 750-753.

Xue, S. and M. Barna (2012). "Specialized ribosomes: a new frontier in gene regulation and organismal biology." *Nat Rev Mol Cell Biol* **13**(6): 355-369.

Xue, S., S. Tian, K. Fujii, W. Kladowang, R. Das and M. Barna (2015). "RNA regulons in Hox 5' UTRs confer ribosome specificity to gene regulation." *Nature* **517**(7532): 33-38.

Yamamoto, R. T., Y. Nogi, J. A. Dodd and M. Nomura (1996). "RRN3 gene of *Saccharomyces cerevisiae* encodes an essential RNA polymerase I transcription factor which interacts with the polymerase independently of DNA template." *EMBO J* **15**(15): 3964-3973.

Zhang, H., T. Butters, I. Adeniran, J. Higham, A. V. Holden, M. R. Boyett and J. C. Hancox (2012). "Modeling the chronotropic effect of isoprenaline on rabbit sinoatrial node." *Front Physiol* **3**: 241.

Zhang, L., J. Kelley, G. Schmeisser, Y. M. Kobayashi and L. R. Jones (1997). "Complex formation between junctin, triadin, calsequestrin, and the ryanodine receptor. Proteins of the cardiac junctional sarcoplasmic reticulum membrane." *J Biol Chem* **272**(37): 23389-23397.

Zheng, M., Y. Wang, X. Liu, J. Sun, Y. Wang, Y. Xu, J. Lv, W. Long, X. Zhu, X. Guo, L. Jiang, C. Wang and J. Wan (2016). "The RICE MINUTE-LIKE1 (RML1) gene, encoding a ribosomal large subunit protein L3B, regulates leaf morphology and plant architecture in rice." *J Exp Bot* **67**(11): 3457-3469.

Zhu, Z., Z. Zheng, F. Zhang, Y. Wu, M. Trzaskowski, R. Maier, M. R. Robinson, J. J. McGrath, P. M. Visscher, N. R. Wray and J. Yang (2018). "Causal associations between risk factors and common diseases inferred from GWAS summary data." *Nat Commun* **9**(1): 224.

VITA

Laura Peterson Brown

Education:

Somerset Community College, 2012 –AS

Eastern Kentucky University, 2015 – BS

Professional positions:

Adjunct Instructor: BCTCS 2018 and 2019

Graduate Research Assistant: UK 2015-2020

Research Assistant: ECU 2014 and 2015

Visiting Research Assistant: UNL 2014

Scholastic and professional honors:

Women in Medicine and Science Award – Finalist

National Science Foundation Graduate Student Fellowship

Arthur and Frieda Bingham Prize

Colonel Plus Scholarship

President's List

Dean's List

Dean's Award

Workforce Development Scholarship

Professional publications:

Brown et al. Loss of ventricular specific ribosomal protein RPL3L enhances response to adrenergic stimulus. (submitted)

Brown et al. Loss of cardiac specific ribosomal protein L3-like expression alters the cardiac transcriptome leading to altered calcium handling. (submitted)

Ahern et al. Radr1 contributes to heart rate via L-type calcium channel regulation. (in preparation)

Boychuck et al. A hindbrain inhibitory microcircuit mediates vagally-coordinated glucose regulation. *Sci Rep.* 2019.

Morales-Sanchez et al. A multidomain enzyme, with glycerol-3-phosphate dehydrogenase and phosphatase activities, is involved in chloroplastic pathway for glycerol synthesis in *Clamydomonas reinhardtii*. *The Plant Journal.* 2017.